DOCTORAL DISSERTATION

EFFECTS OF SHEAR DISPLACEMENT RATE AND ACCELERATION ON SHEAR STRENGTH OF VARIOUS CLAYS IN RING SHEARING

(リングせん断試験における種々の粘土のせん断強度に及ぼすせん断変位速度および加速度効果)

NGUYEN THANH DUONG

A dissertation submitted in partial fulfillment of the requirement for the degree of

Doctor of Engineering

in

Geotechnical Engineering

March, 2019

Department of Environmental Engineering,
Graduate School of Sciences and Technology for Innovation,
Yamaguchi University, Japan

ABSTRACT

This research consists of laboratory-based experiments conducted to investigate the effects of the shear rate and acceleration of a sliding block on the shear strength of various types of clay in ring shear tests. In landslides, a change in sliding velocity (i.e., shear displacement rate) affects not only the peak strength, but also the residual strength of the soil. The rate effect on the shear strength of soil has become one of the most important considerations in geotechnical engineering. A better understanding of the rate effect on the residual strength of certain soils would be beneficial for predicting and evaluating the behaviour of reactivated landslides. Hence, the rate effect on the residual strength of various soils has been extensively investigated. In addition, the rate effect on the residual interface strength along the bedding plane between two soil layers has recently been investigated. However, there is currently no consistent theory that can describe the rate effect on the residual strength, particularly that of high-plasticity, low-permeability clay. Furthermore, research on the residual interface strength has been limited and further studies should be made. Besides developing along bedding planes, many landslides also often occur in over-consolidated (OC) soil which is highly fissured and jointed. The rate effect on the shear strength of OC soil has been widely examined in triaxial tests. Nevertheless, it needs to be more closely studied in terms of ring shearing, especially for the residual strength. Regarding a change in velocity during sliding, the acceleration may affect the residual strength. This effect is still unknown and should be clarified. As for the application of the rate effect, the rate dependency of the residual strength will affect the estimation of the earthquake-induced velocity and displacement. However, this issue also needs to be examined further. To summarise, the main objective of this study is to investigate the rate effect on the residual strength of high-plasticity, low-permeability clay, on the residual interface strength between two different soil layers, and on the shear strength of OC clay in ring shear tests. In addition, the effect of the acceleration of a sliding block on the residual strength is clarified. Finally, the estimation of earthquake-induced velocity and displacement is investigated through the rate dependency of the residual strength using the Newmark method. In this research, a conventional Bishop-ring shear apparatus was employed. The specimens for the ring shear tests were cut from samples which were pre-consolidated in a large consolidation tank.

Kaolin and kaolin-bentonite mixture samples were used to investigate the rate dependency of the residual strength of high-plasticity, low-permeability clay. The samples were tested with shear rates of 0.02 to 20 mm/min under the normal stress of 98 kPa using the single-stage procedure. The test results showed that the bentonite content significantly affected the rate dependency of the shear strength. In particular, the rate dependency of the residual strength

appeared to have changed from positive to negative when bentonite was added to kaolin clay. Regarding the physical properties of the studied soil, the results revealed that the rate effect on the residual strength was related to the clay fraction and the plasticity index. The type of rate effect on the residual strength was found to be dependent on the test procedure, especially for very low-permeability clay.

Next, specimens consisting of two layers, one kaolin layer (upper layer of the specimen) and one kaolin-bentonite mixture layer (lower layer of the specimen), were used to investigate the rate dependency of the residual interface strength. The test results showed that the residual interface strength and its rate dependency depended significantly on the bentonite content in the lower layer.

Furthermore, in order to examine the rate effect on the shear strength of OC clay, kaolin clay with artificial overconsolidation ratios (OCRs), in the range of 1 to 6, was applied in ring shear tests at shear rates of 0.02 to 20 mm/min under effective normal stress levels of 98 kPa to 588 kPa. The test results indicated that the rate dependency of both the peak strength and the residual strength depended on the stress history (OCRs). In particular, the magnitude of the positive rate effect on the residual strength tended to decrease as the OCRs increased. In addition, the variations in cohesion and frictional angles of the OC kaolin clay at the peak and residual states were different at different shear rates. Regarding the test procedure and rate effect, the multi-stage procedure for decreasing normal stress can be used to determine the residual strength of OC clay at shear rates of less than or equal to 0.5 mm/min.

The average acceleration values of 50.4 mm/h^2 and 100.8 mm/h^2 were used to investigate the acceleration effect on the residual strength of the kaolin and the 90% kaolin-10% bentonite mixture samples. The multi-stage procedure was applied to increase the shear rates gradually from 0.002 to 20 mm/min at different shearing times. The test results showed that the effect of acceleration on the residual strength was negligible and that this effect could be ignored in slope stability analyses.

Finally, the rate dependency of the residual strength was employed using the Newmark method to estimate the earthquake-induced velocity and displacement of an infinite plane slope whose slip surface had reached the residual state. The results of the computation revealed that considering the positive rate effect of the slip zone soil, the estimated velocity and displacement decreased significantly as compared to the cases without the rate effect.

ACKNOWLEDGEMENTS

Research for this dissertation began in March 2016 in the Division of Environmental Engineering, Graduate School of Sciences and Technology for Innovation, Yamaguchi University, Japan. During my years of study in Japan, I have received much support and encouragement from professors, researchers, colleagues, friends, Yamaguchi University, and family members.

First of all, I will always be grateful to my respected professor, Professor Motoyuki SUZUKI, for his support, assistance, and valuable guidance throughout my time at Yamaguchi University. He has continuously directed and supported me from the very beginning of my studies. His knowledge and experience of ring shear tests have greatly contributed to my ability to complete this dissertation.

Special thanks are also given to the dissertation examination committee: Professor Norikazu SHIMIZU, Professor Yukio NAKATA, Associate Professor Norimasa YOSHIMOTO, and Associate Professor Hiroyuki HARA, for their valuable advice and comments on my dissertation. They were very helpful and beneficial to me.

I wish to express my gratitude to the members of my laboratory and my other friends at Ube City and Yamaguchi University. Special thanks are also given to Tomohiro Miyamae who helped me translate the abstract of my thesis into Japanese. I would also like to offer my sincere thanks to Dr. Tran Thanh Nhan who recommended that I study at Yamaguchi University.

I would also like to take this opportunity to thank the Vietnam Ministry of Education and Training (MOET), Vietnam International Education Development (VIED), Hanoi University of Mining and Geology (HUMG), and the Department of Engineering Geology for their financial and spiritual support to my research and life in Japan.

In addition, I would like to show my gratefulness to the Library and International Student Office of Yamaguchi University, Ube International Student House Office, and Navy House Office for their kindness and valuable help during my stay at Yamaguchi University. My great gratitude is also extended to Ms. Heather Griswold for proofreading and editing this dissertation.

Last but not least, I would like to express my deepest gratitude to my family: my mother, my father, my father-in-law, my mother-in-law, and all other family members for their support and encouragement. Especially, I would like to express my deepest appreciation to my beloved wife, Nguyen Thi Thao and our precious son, Nguyen Gia Bao for their unconditional love, encouragement, and support at all times.

TABLE OF CONTENTS

LIST OF FIGURES

LIST OF TABLES

LIST OF SYMBOLS AND ABBREVIATIONS

Symbols		Unit
a	Intercept of fitting line	–
a_c	Critical acceleration	m/s^2
a_g	Ground acceleration	m/s^2
b	Slope of fitting line	–
c_p	Peak cohesion intercept	kPa
c_r	Residual cohesion intercept	kPa
d	Earthquake-induced displacement	cm
e_0	Initial void ratio	–
e_1	Void ratio before shearing	–
e_2	Void ratio after shearing	–
F	Frictional force	kN
N	Initial normal force	kN
k	Coefficient of permeability	cm/s
K_y	Yield (Critical) seismic coefficient	-
p_c	Pre-consolidation pressure in consolidation tank	kPa
w_0	Initial water content	–
v	Earthquake-induced velocity	cm/s
α	Acceleration in ring shear test	mm/min^2
α'	Coefficient of rate effect on residual strength	–
w_P	Plastic limit	%
w_L	Liquid limit	%
ϕ_p	Peak internal friction angle	deg
ϕ_r	Residual internal friction angle	deg

δ	Shear displacement in ring shearing	mm
$\dot{\delta}$	Shear displacement rate in ring shearing	mm/min
δ'	Required shear displacement to reach the peak strength	mm
ν	Vertical displacement during shearing	mm
ρ_0	Initial wet density	g/cm^3
ρ_s	Specific density	g/cm^3
σ'_N	Effective normal stress	kPa
σ_c	Consolidation pressure	kPa
σ_{N0}	Initial normal stress	kPa
σ_N	Normal stress	kPa
θ	Angle shear displacement	deg
τ	Shear stress	kPa
τ_p	Peak shear stress	kPa
τ_r	Residual shear stress	kPa
$(\tau/\sigma_N)_p$	Peak shear stress ratio	–
$(\tau/\sigma_N)_r$	Residual shear stress ratio	–

Abbreviations

CF	Clay fraction
NC	Normally consolidated
OCR	Over consolidation ratio
OC	Over-consolidated
PI	Plasticity index
RDBS	Reversal Direct Box Shear Test
RS	Ring Shear Test
TS	Triaxial Shear Test
K	Kaolin
10B	10% bentonite– 90% kaolin sample
20B	20% bentonite– 80% kaolin sample
30B	30% bentonite– 70% kaolin sample

CHAPTER 1. INTRODUCTION

1.1. Statement of problem

In reality, the movement rate of landslides can vary significantly from extremely slow to extremely rapid (Table 1.1). From field observations, Skempton and Hutchinson (1969) showed that the average rate of movement of reactivated landslides and mud flows falls in the range of 4×10^{-5} mm/min to 0.35 mm/min. In the Vaiont landslide, the average velocity of the sliding movement was estimated to be up to 20–30 m/s (Tika and Hutchinson, 1999). For a landslide at the residual state, the velocity or the shear displacement rate of a landslide block is not always constant (Fig. 1.1(b)). The data in Fig. 1.1(b) were determined based on the original data from Glastonbury and Fell (2008) (Fig. 1.1(a)). Previous studies have shown that the velocity (shear rate) may affect not only the peak strength, but also the residual strength of the soil during sliding.

Table 1.1 Classification of movement rate of landslides (Varnes, 1978; Cruden and Varnes, 1996)

Description	Varnes (1978)		Cruden and Varnes (1996)	
	mm/s	mm/min	mm/s	mm/min
Extremely slow	$<1.9\times10^{-6}$	$<11\times10^{-5}$	$<0.5\times10^{-6}$	3×10^{-5}
Very slow	1.9×10^{-6}	11×10^{-5}	0.5×10^{-6}	3×10^{-5}
Slow	48×10^{-6}	29×10^{-4}	50×10^{-6}	3×10^{-3}
Moderate	0.6×10^{-3}	0.036	5×10^{-3}	0.3
Rapid	17×10^{-3}	1	0.5	30
Very rapid	5	300	50	3×10^{3}
Extremely rapid	3×10^{3}	18×10^{4}	50×10^{3}	3×10^{6}
	$>3\times10^{3}$	18×10^{4}	$>50\times10^{3}$	$>3\times10^{6}$

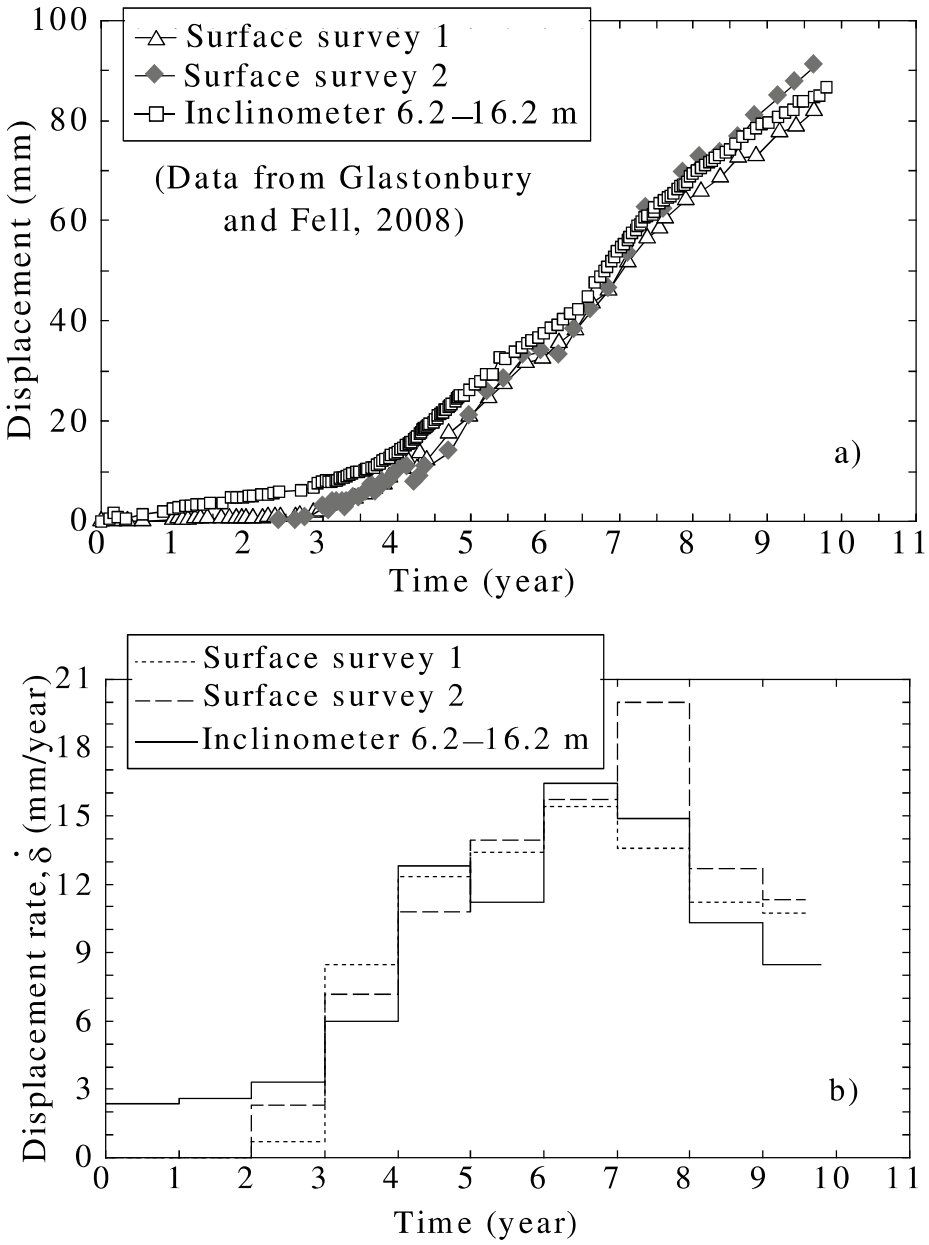

Figure 1.1 a) Surface and subsurface displacements at three positions for Slide 10 – Zone A (Original data from Glastonbury and Fell, 2008) and b) Surface and subsurface displacement rates for Slide 10 – Zone A.

The residual shear strength can decrease (negative effect), increase (positive effect), or remain constant (neutral effect) with an increasing shear displacement rate (Tika et al., 1996; Lemos, 2003). These phenomena indicate that the residual strength is a dynamic parameter that changes with the deformation process of landslides. In fact, the velocity or the movement rate of landslides can be very slow. However, during an earthquake or rainfall event, the velocity can increase significantly and reach a magnitude of velocity higher than that under normal conditions. A better understanding of the rate

effect on the residual strength of the soil would be beneficial for predicting and evaluating the behaviour of reactivated landslides. Tika and Hutchinson (1999) suggested that the catastrophic landslides at the Vaiont Dam might have been caused by the reduction in fast residual strength (negative rate effect) when the shear displacement rate exceeded 100 mm/min. In contrast, Leroueil (2001) and Wang et al. (2010) reported that a positive rate effect could prevent catastrophic landslides, even when a large shear displacement had occurred in a short period of time. This is because a positive rate effect leads to an increase in residual strength as the shear displacement rate increases, resulting in an increase in stability. Moreover, rate effects also play a significant role in the application of laboratory testing methods and in the test results. Therefore, studies on the shear rate effect on the residual strength of soil have a certain engineering significance. In fact, an earthquake can induce landslides in very gentle to gentle slopes ($\alpha=5^0$-10^0) (Fig. 1.2). Gentle slopes at the residual state often contain clay minerals, such as kaolinite and bentonite which have low residual strength. In this study, the behaviour of the shear strength mobilized along the failure surface of earthquake-induced shallow-to-moderate landslides (depths of 5 to 15 m) in gentle slopes will be investigated.

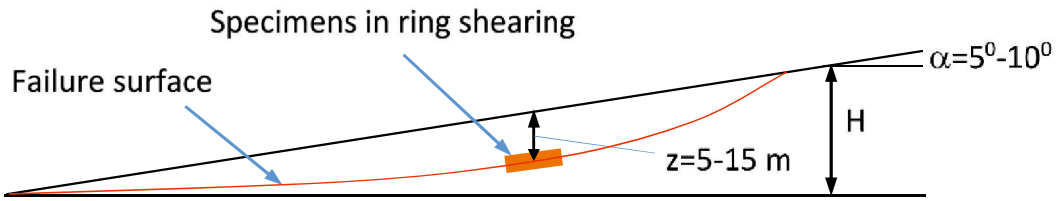

Figure 1.2 Earthquake-induced shallow-to-moderate landslides in gentle slopes

Although the factors related to the rate effect on the residual strength have been extensively studied, there is still no consistent theory that describes this rate effect on residual strength. This may be due to the differences in the test conditions, procedures, and types of soil used in the various studies. Some researchers have noted that the presence of smectite minerals (which are of high plasticity) in the soil can change the shear behaviour (Marui and Tiwari, 2004) and the rate effect on the residual strength of sand mixtures (Saito et al., 2006, 2007). In addition, these smectite minerals often play a key role in triggering landslides (Gibo, et al., 1987; Tiwari et al., 2005; Tiwari, 2007; Wang et al., 2010; Bhandary et al., 2005). Furthermore, Suzuki et al. (2001, 2009) stated that the rate dependency of the residual strength and the physical properties of soil (clay fraction, plasticity index, etc.) may have a linear relationship. However, the rate effect on

the residual strength of soil that contains smectite minerals with low permeability and high plasticity remains largely unknown and requires further examination.

Landslides often develop along discontinuous planes, bedding planes or the interface between two soil layers (e.g., Bromhead and Ibsen, 2004; Gratchev et al., 2005; Tiwari et al., 2005, 2007; Chigira and Yagi, 2006; Wang et al., 2007; Suzuki et al., 2012; Bromhead, 2013; Has and Nozaki, 2014). Recently, some investigations have been conducted to examine the residual strength at the interface between two soil layers (Suzuki et al., 2017; Scaringi et al., 2018). These investigations have partly reflected the behaviour of the residual strength on the boundary between two soil layers and the effect of some factors such as stiffness, normal stress, the shear displacement rate, and the stress history. However, the rate effect on the residual interface strength between two soil layers should be more closely examined. Tiwari et al. (2005) and Tiwari (2007) showed that the shear surfaces of all landslides in Niigata Prefecture are located at the interface between highly weathered and less weathered Tertiary mudstones. In addition, the smectite minerals in Tertiary mudstones play an important role in triggering landslides along the bedding plane in this area. Therefore, the presence of smectite minerals may affect the rate dependency of the residual interface strength between two soil layers.

In fact, over-consolidated (OC) soil is widely distributed in slopes and large-scale landslides. It can form due to the release of stress (erosion of soil on the slope), changes in the groundwater level, secondary consolidation (aging), chemical bonding, and desiccation stress (Hanzawa and Adachi, 1983). Many types of OC soil are fissured, jointed, contain slickensides, and are prone to instability (Skempton, 1964). In addition, the shear behaviour of OC soil differs from and is more complicated than that of normally consolidated (NC) soil (Skempton, 1970). Thus, the shear strength of OC soil has received much attention in the literature and in practice in terms of evaluating and predicting slope stability (e.g., Skempton, 1964, 1970, 1985; Stark, 1995; Stark and Eid, 1997). Hong et al. (2011) investigated the effect of cyclic loading on the residual strength of over-consolidated silty clay. The test results showed that the changes in the residual strength with the shear displacement rates after cyclic loading at low overconsolidation ratios (OCRs) were higher than those at higher OCRs. This indicates that the shear zone structure under different OCRs may affect the rate effect on the residual strength of the soil. Moreover, Vithana et al. (2012) revealed that the shear surface structure of OC soil may be disturbed by the dilation behaviour during shearing. The effect of the dilation process on the disturbance of the shear zone structure is exhibited differently at different

shear rates and it may affect the shear strength, especially at fast shear rates. Therefore, although the OCR seems to have no effect on the residual strength (Skempton, 1964; Lupini et al., 1981; Vithana et al., 2012; Li et al., 2017; Xu et al., 2018), it may affect the magnitude of the rate dependency of the residual strength and this effect should be examined. In addition, the ring shear apparatus has been widely used to determine not only the residual strength, but also the peak strength. In the ring shear test, although the drainage condition is allowed during shearing, the rate effect on the peak strength of OC soil may be different from that of NC soil, especially at fast shear rates. Therefore, the rate dependency of the peak strength of OC soil should be studied more in ring shearing.

Regarding the velocity, a change in velocity will lead to a change in acceleration which may affect the residual strength (this is known as the acceleration effect). In addition, changes in velocity and acceleration during movement have been used to establish the criteria for predicting slope stability and the time to slope failure (Picarelli et al., 2000; Dai et al., 2002; Xu et al., 2012). Thus, in addition to the rate effect, which is the basic factor affecting the stability of old landslides, changes in acceleration should be considered in analyses. However, reliable information on how the acceleration effect influences the residual strength is not available.

In seismic-slope stability analyses, the Newmark method (Newmark, 1965) has been widely used to estimate the seismically induced displacement of earth structures and natural slopes. This method assumes that the seismic coefficient (K_y) is constant during sliding. However, K_y may change during sliding due to the rate dependency of the shear strength and then affect the estimation of the earthquake-induced velocity and displacement. In this study, the rate effect on the residual strength will be taken into account using the Newmark method to estimate the earthquake-induced velocity and displacement.

In summary, this research will focus on the rate dependency of the shear strength of various types of soil containing smectite minerals, having low permeability and high plasticity, and OC clay. In addition, the rate effect on the residual interface strength between two different soil layers will be investigated. As for changes in the shear displacement rate, the acceleration effect on the residual strength will be clarified. Finally, the rate dependency of the residual strength will be applied to estimate the earthquake-induced displacement of a sliding block at the residual state using the Newmark method. All the experiments in this study were conducted with a ring shear apparatus (Bishop's type) (Bishop et al., 1971) using pre-consolidated samples.

1.2. Objectives of research

The specific objectives of this research are as follows:

– To investigate the effect of shear displacement rates on the residual strength of various types of clay having low permeability and high plasticity. In addition, to examine the rate effect on the residual interface strength between two different soil layers;

–To investigate the rate effect on the shear strength of OC clay in ring shearing. In addition, to elucidate the effect of the OCRs on the rate dependency of the residual strength and to examine the relationship between the OCRs and the rate dependency of the residual strength;

– To clarify the effect of acceleration on the residual strength;

– Finally, to apply the rate effect on the residual strength in order to estimate the earthquake-induced velocity and displacement of a sliding block using the Newmark method.

1.3. Scope of research

The Bishop-ring shear apparatus (Bishop et al., 1971) is employed in this study. The following steps are carried out to achieve the research objectives:

– A series of ring shear tests is conducted on pre-consolidated kaolin (K) and kaolin–bentonite mixture samples to investigate the rate dependency of the residual strength of soil having low permeability and high plasticity. Shear rates from 0.02 mm/min to 20 mm/min and an effective normal stress of 98 kPa are applied (equal to shallow landslides with a depth of about 5 m).

– The combined samples comprising one kaolin layer and one kaolin-bentonite mixture layer are used to investigate the rate dependency of the residual strength at the interface between the two soil layers. The multi-stage procedure, with an increase in the shear rate from 0.02 mm/min to 20 mm/min, is employed with normal stress levels ranging from 98 kPa to 294 kPa (depth of landslides from 5 to 15 m)

– Kaolin samples with artificial overconsolidation ratios (OCRs), in the range of 1 to 6, are created and then sheared to investigate the relationship between the rate dependency of the residual strength and the OCRs. Shear rates varying from 0.02 to 20 mm/min and normal stress levels varying from 98 kPa to 588 kPa are employed.

– Two average acceleration values of 0.014 mm/min^2 (50.4 mm/h^2) and 0.028 mm/min^2 (100.8 mm/h^2) are applied in the multi-stage procedure to gradually increase

the shear rates from 0.002 to 20 mm/min at the normal stress of 98 kPa to examine the acceleration effect. The acceleration effect on the residual strength is evaluated based on the results of tests conducted on kaolin and 10% kaolin-90% bentonite mixture samples.

– Finally, the rate dependency of the residual strength of kaolin clay is applied to estimate the earthquake-induced velocity and displacement of a block sliding along an infinite slope using the Newmark method.

1.4. Outline of dissertation

This research includes nine chapters; an outline for each is presented in Fig. 1.3.

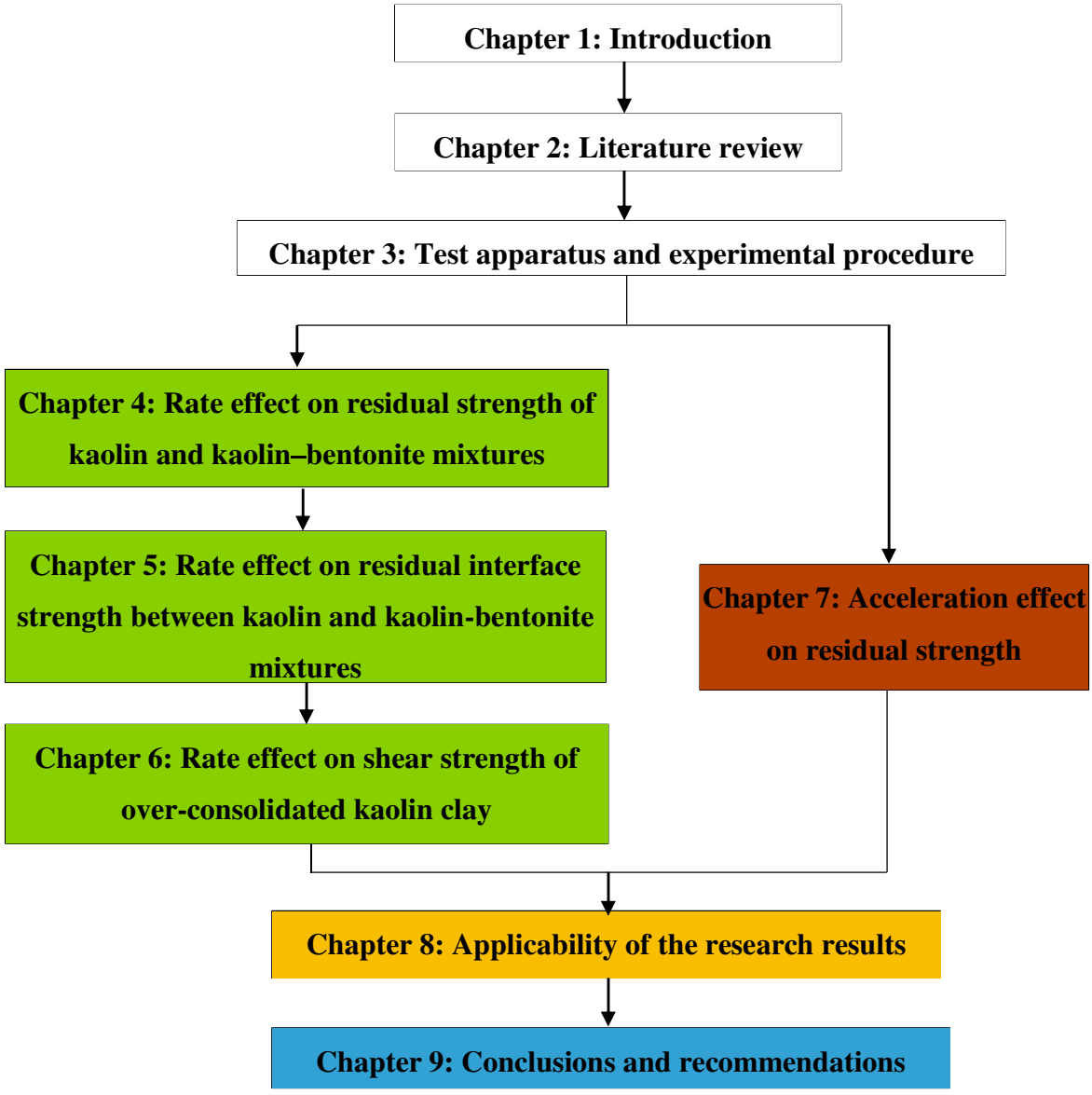

Figure 1.3 Flowchart of dissertation structure

The content of each chapter is described as follows:

Chapter 1 is an introductory chapter that gives the state of the problem regarding the effect of the shear rate and acceleration of a sliding block on the shear strength of clay. This chapter also introduces the objectives, the scope, and the organization of this dissertation.

Chapter 2 presents a literature review of the residual strength of soil, the determination of the residual strength, and the shear rate dependency of the residual strength and the peak shear strength. In addition, a review of the residual interface strength, and the application of the residual strength and acceleration are presented.

Chapter 3 summarises the test apparatus and the experimental procedure used in this study. The selection of samples and a description of the testing conditions are also provided.

Chapter 4 is one of the main chapters which evaluates the effect of shear displacement rates on the residual strength of kaolin and kaolin-bentonite mixture samples in ring shearing. A set of ring shear tests, conducted on kaolin and kaolin-bentonite mixture samples, will be presented in this chapter. In addition, the causes of the rate dependency of the residual strength and the relationship between the rate effect and the physical properties of the soil (e.g., clay fraction and plasticity index) are also included.

Chapter 5 investigates the rate dependency of the residual interface strength between the kaolin and the kaolin-bentonite mixtures. Ring shear tests were conducted on combined samples composed of one kaolin layer and one kaolin-bentonite mixture layer with the multi-stage procedure for increasing the shear rates.

Chapter 6 describes the shear displacement rate effect on the shear strength of over-consolidated kaolin clay (OC clay) in ring shearing. The relationship between the overconsolidation ratios (OCRs) and the rate dependency of the residual strength will also be presented.

Chapter 7 clarifies the effect of the acceleration of a sliding block on the residual strength of clay. In addition, the effect of the test procedure on the rate dependency of the residual strength is also given.

Chapter 8 shows the application of the rate dependency of the residual strength to a seismic slope stability analysis using the Newmark method. The earthquake-induced velocity and displacement of a block sliding at the residual state will be estimated based on the change in the seismic coefficient during sliding.

Chapter 9 presents the conclusions derived from the research results, the limitations, and recommendations for future works.

CHAPTER 2. LITERATURE REVIEW

2.1. Residual strength of clay

The residual shear strength of clay has been studied since the 1930s and the results have provided a better understanding of this parameter. The significance of the residual shear strength was considerably revealed after the 4th Rankine Lecture (Skempton, 1964). In this lecture, the residual shear strength was defined as the minimum drained shear strength at which a soil undergoes a large shear displacement under a given effective normal stress. For clay, the residual strength can be obtained at a shear displacement of about 300 mm (Skempton, 1985). The residual strength can be expressed by the Coulomb-Terzaghi law:

$\tau_r = c_r + \sigma'_N.\tan\phi_r$

where: τ_r: residual stress;

c_r: residual cohesion; ϕ_r: residual friction angle;

σ'_N: effective normal stress.

The value of c_r is small or almost equal to zero, thus the residual strength can be rewritten as $\tau_r = \sigma'_N.\tan\phi_r$

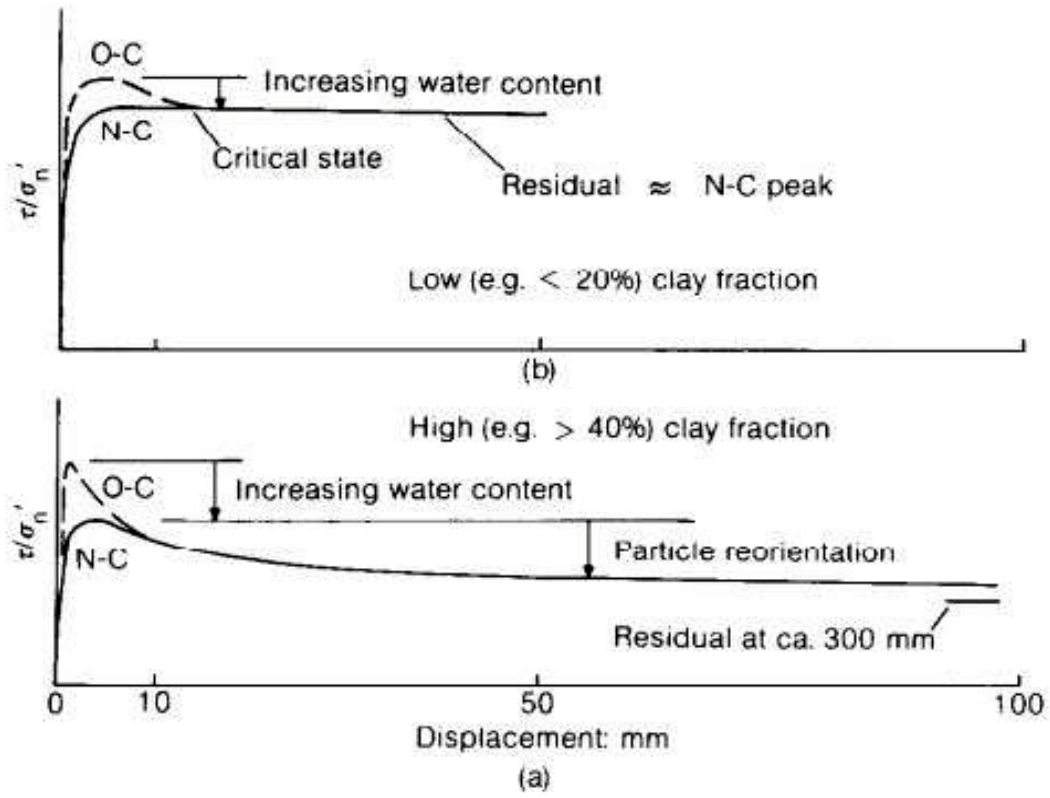

Figure 2.1 Shear behavior of OC and NC soils in ring shear tests (Skempton, 1985)

In general, when specimens are subjected to shear, the shear strength will increase and reach the peak value. After reaching the peak strength, the shear strength will decrease as the shear displacement increases (this is called shear strength loss). The loss of shear strength in over-consolidated (OC) soil is often higher than that in normally consolidated (NC) soil. For OC soil, the drained post-peak strength loss is due to two successive stages: 1) the dilatancy of the specimens and the increase in water content in the shear zone and 2) the orientation of the clay particles parallel to the shearing direction. For NC soil, the drained post-peak strength loss is only due to the orientation of the clay particles in parallel with the shear surface (Skempton, 1970, 1985). In some types of soil (NC soft clay and loose sand), the residual strength is almost equal to the peak strength and there is no shear strength loss. The shear behaviour of NC and OC soils is presented in Fig. 2.1 (Skempton, 1985).

The shear behaviour at the residual state can experience different shearing modes which depend on the dominance of the particles and the coefficient of inter-particle friction. Lupini et al. (1981) introduced the following three modes for the shearing mechanism:

Turbulent mode: this mode occurs when the soil is dominated by rotund particles, or possibly in soil that is dominated by platy particles which have a high coefficient of interparticle friction. In this mode, the residual friction angle is relatively high. It depends primarily on the shape and packing of the rotund particles and does not depend on the coefficient of interparticle friction. The orientation of the particles does not occur due to the dominance of round particles and the brittle behaviour is only due to the dilatancy.

Sliding mode: this mode occurs when the soil is mainly dominated by platy particles with low friction angles. In this mode, the residual friction angle is low due to the perfect orientation of the particles at the residual state. The residual friction angle mostly depends on the mineral components, the pore water chemistry, and the coefficient of interparticle friction.

Transitional mode: this mode occurs when neither round nor platy particles dominate the soil. This mechanism is a combination of the turbulent and the sliding modes. In this mode, the residual friction angle is sensitive to small changes in the grading of the soil

After further investigation of the residual shearing mechanism, Skempton (1985) divided the shearing mechanism, based specifically on the clay fraction (CF), into turbulent ($CF \leq 25\%$), transitional ($25\% < CF < 50\%$), and sliding ($CF \geq 50\%$) (Fig. 2.2)

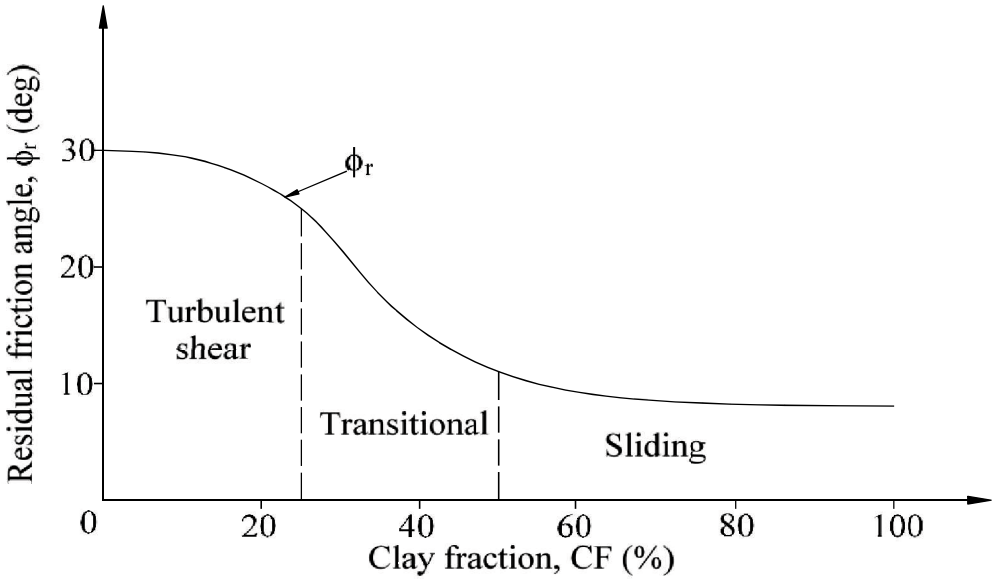

Figure 2.2 Shear modes at residual state (after Lupini et al., 1981; Skempton, 1985)

The residual strength can be obtained by various laboratory testing methods, including the triaxial shear (TS) test, the reversal direct box shear (RDBS) test, and the ring shear (RS) test. With each test method, a large shear displacement on the shear surface must be reached in order to obtain the residual state when subjected to shear stress. In the TS test, the amount of axial strain is limited to about 15% of the 100 mm-high sample. Although the orientation of the particles remains unchanged during shearing, this deformation cannot represent the true residual state. In the RDBS test, the amount of horizontal displacement in one cycle is about 6 to 7 mm, and the shear displacement can reach the residual state by a reverse in the direction of shearing (about five cycles or more). However, reversing the shear direction (forward and backward) may disturb the orientation of the particles on the shear surface. Different from the TS and RDBS tests, unlimited displacement can be obtained in one direction in the RS test so that the orientation of the grains on the shear surface is not changed during shearing, and a good preferred orientation of grains can be achieved. Therefore, the RS test can yield a residual strength that agrees well with the field value. Table 2.1 shows the test results for the residual strength of some types of clay obtained from different testing methods. It can be seen that the residual strength obtained from the RS test (expressed in terms of the friction angle) has the lowest value among them all.

The residual strength depends not only on the physical properties of the soil particles (mineralogical composition, size and shape of the particles, and plasticity characteristics), but also on the pore fluid chemistry (type and ion concentration) and the

testing conditions (shear displacement rate and effective normal stress). Although these factors have been comprehensively investigated, the effect of the shear rates on the residual strength remains a controversial issue.

Table 2.1 Residual friction angles of clays obtained by different testing methods

Soils	Physical properties	Test methods	Average, φ_r (deg), c_r=0	Reference
Blue London clay (Wraybury)	Undisturbed, w_L=70%; PI=29%; CF=58%.	RDBS test	13.5^0	Bishop et al. (1971)
	Undisturbed, w_L=72%; PI=29%; CF=57%.	Drained TS test, pre-sheared to large displacement	10.5^0	
		RS test (Bishop)	9.4^0	
	Remoulded, w_L=72%; PI=29%; CF=57%.	RS test (Bishop) (one sample)	9.5^0	
	Undisturbed, w_L=71.5%; PI=22.4%.	RS test (Bishop)	9.3^0	La Gatta (1970)
	Remoulded, w_L=71.5%; PI=22.4%.	RS test (Bishop)	8.3^0	
Brown London clay (Waltham-stow)	Slip surface, w_L=43–76%; PI=22–46%; CF=40–65%.	Drained, direct shear test	14.0^0	Bishop et al. (1971)
	Undisturbed, cut-plane w_L=70%; PI=26%; CF=50%.	Drained, direct shear test	14.2^0	
	Slip surface, w_L=71%; PI=26%; CF=63%.	Drained TS test.	13.7^0	
	Undisturbed, w_L=66%; PI=24%	RS test (Bishop)	10.0^0	
	Remoulded, w_L=66%; PI=24%	RS test (Bishop))	9.7^0	
Blue London clay (Herne Bay)	Undisturbed, w_L=81%; PI=33%; CF=61%.	RDBS test	13.5^0	
	Remoulded, w_L=85%; PI=34%; CF=59%.	RDBS test	12.5^0	
	Undisturbed, cut-plane w_L=81%; PI=33%; CF=61%	Drained TS test	14.7^0	
	Over-consolidated, w_L=95%; PI=61%; CF=59%	RS test (Bishop)	9.4^0	

2.2. Shear rate effect on residual strength

2.2.1. Types and causes of rate effect on residual strength

Many experiments have been conducted in the laboratory to investigate the rate dependency of the residual strength. It has been shown that the residual strength more or less depends on the shearing speed.

Tika (1989) introduced five types of variations in the residual strength with an increasing shear displacement rate:

Type I: the residual strength is unrelated to the shear displacement rate. Soil of this type shows a turbulent shear mechanism (e.g., sand and sandy silts) with a plasticity index (PI) less than 9, a sand fraction over 20%, and a clay fraction (CF) under 10%.

Type II: the residual strength either insignificantly to moderately increases, or slightly decreases, as the shear rate increases. This is followed by a drop in shear strength to lower than the slow residual value at higher shear rates. Soil of this type is often silty with $9 \leq PI \leq 21$ and usually shows the turbulent or transitional shear mode.

Type III: the residual strength decreases as the shear rate increases. This is followed by an increase and then a drop in shear strength to lower than the slow residual value at higher shear rates. Soil of this type has PI between 24 and 26 and exhibits the transitional or sliding shear mode.

Type IV: the residual strength decreases as the shear rate increases. This is followed by an increase in shear strength to above the slow residual value at higher shear rates. Soil of this type includes low plasticity and silty clays.

Type V: the residual strength increases as the shear rate increases. Soil of this type includes clay with PI between 36 and 51 and CF above 48%. It shows the sliding shear mode.

In the above five types of variations in residual strength, Types 2, 3, and 4 are not common; they are exhibited only in certain types of soil. Tika et al. (1996) proposed three general types of fast residual strength with the increase in shear displacement rates, namely, neutral, negative, and positive (Fig. 2.3).

+*Neutral rate effect*: the residual strength is unrelated to increases in the shear displacement rate.

+*Positive rate effect*: an increase in the fast residual strength greater than the slowly drained value is shown with increases in the shear displacement rate.

+*Negative rate effect*: a substantial drop in the fast residual strength less than the slow drained residual strength is shown when sheared at rates greater than the critical rate.

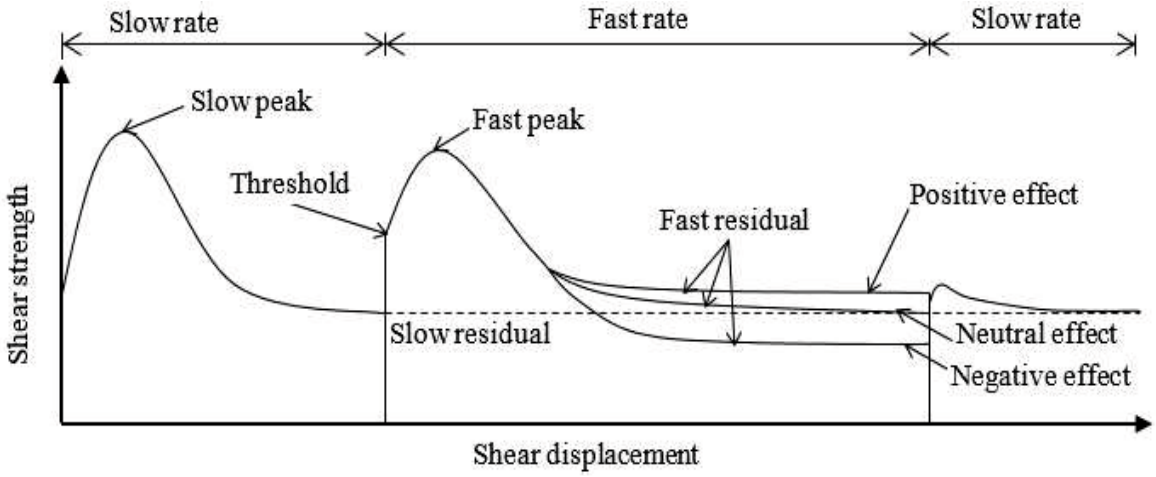

Figure 2.3 Summary of rate dependency of residual strength (Tika et al., 1996)

Tika et al. (1996) also showed that different shearing modes will have different types of rate effects. Soil with the turbulent shear mode (clay fraction, CF ≤25%) will exhibit a neutral or negative rate effect and will depend on the magnitude of normal stress. Soil with the sliding mechanism (CF ≥ 50%) will exhibit either a negative or positive rate effect. Lastly, soil with the transitional shear mode (25< CF <50%) will exhibit a negative rate effect (Fig. 2.4).

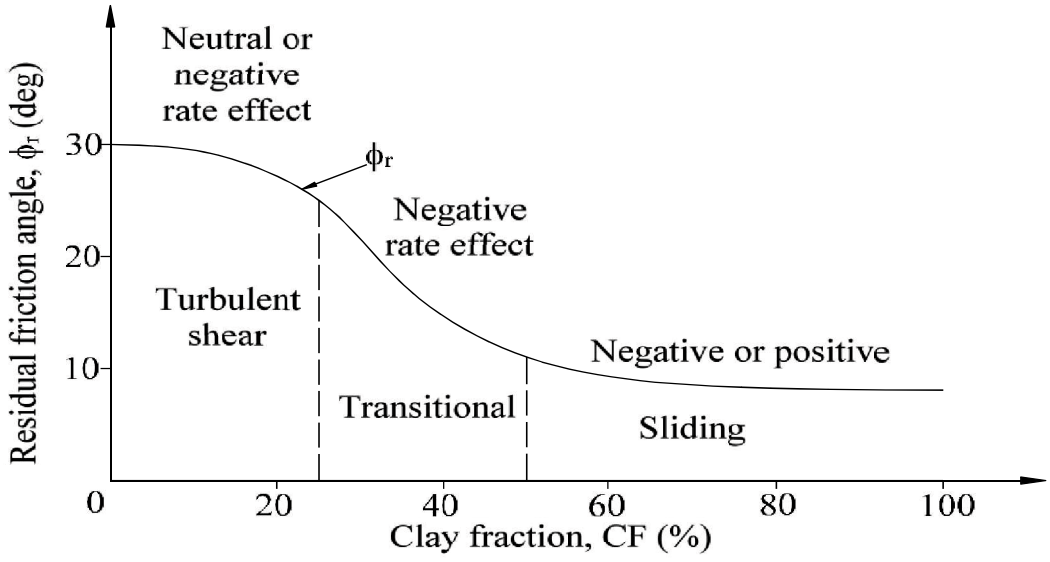

Figure 2.4 Relationship among clay fraction, shear mode, and shear rate effect (after Lupini et al., 1981; Skempton, 1985; Tika et al., 1996)

The rate effect on the residual strength of different soils has been extensively investigated. Fig. 2.5 shows the research results for the rate effect on the residual strength of different types of soil collected from previous studies. The figure shows that the three types of rate effect, namely, positive, negative, and neutral, have emerged from the literature. Differences in the types of soil used, the testing methods, the testing procedures, and the range in shear displacement rates will result in different types of rate effects. The range of shear rates used in these studies varies from very low to rapid. The data in Fig. 2.5 also indicates that the rate effect on the residual strength of high plasticity clay is still limited. In addition, most of these investigations were conducted on normally consolidated (NC) soil.

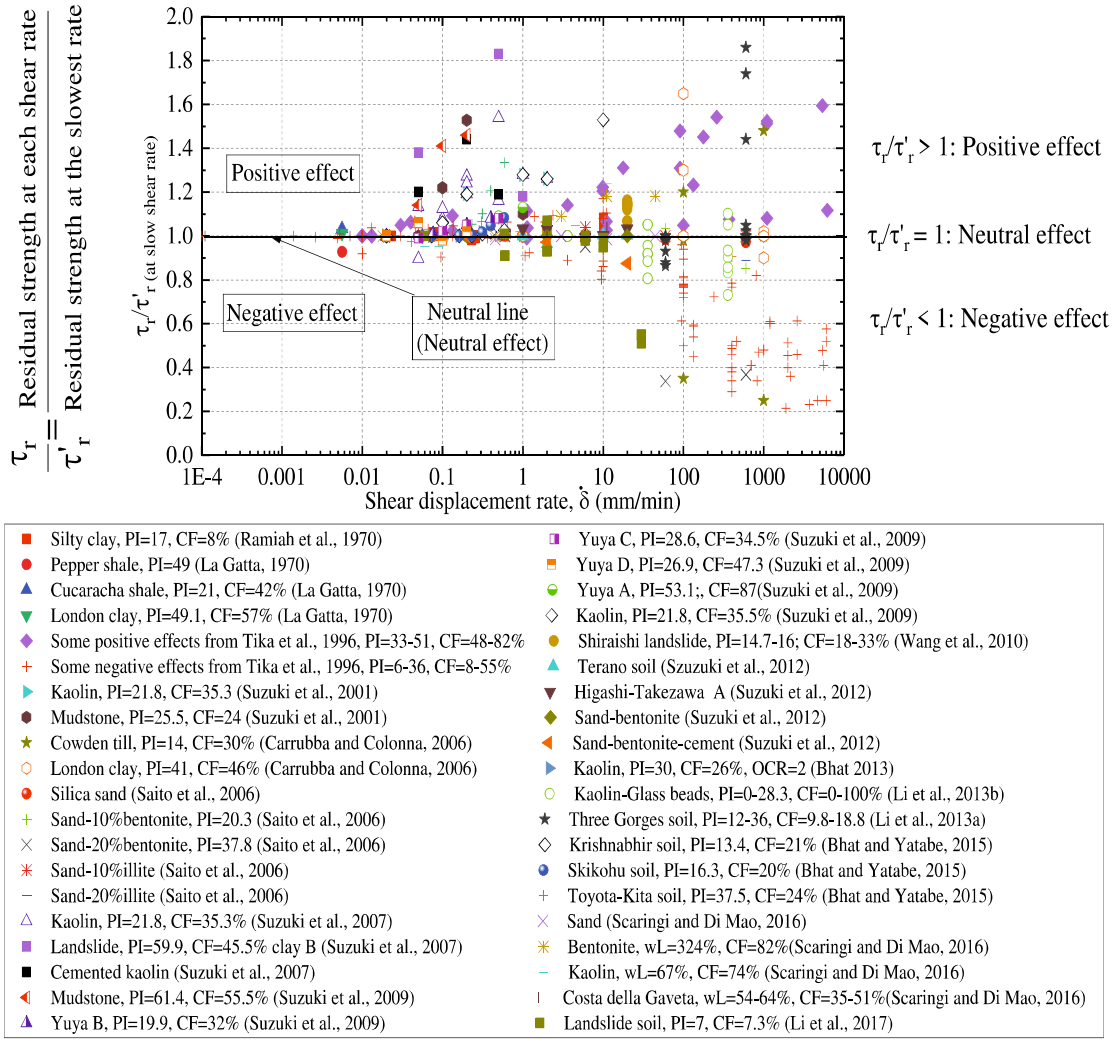

Figure 2.5 Rate effect on the residual strength of various soils

Through many investigations, some causes have been proposed to explain the rate dependency of the residual strength. The neutral rate effect was often exhibited in soil

when the shear rates increased in the slow ranges (Kenny, 1967; La Gatta, 1970; Raamiah et al, 1970; Skempton, 1985; Fukuoka and Sassa, 1991; Suzuki et al, 2012) and in granular soil (Hungr and Morgenstern, 1984; Skempton, 1985; Tika et al, 1996; Chen and Liu, 2013).

A positive rate effect can be attributed to a change from the sliding mode to the turbulent shear mode (e.g., Skempton, 1985; Tika et al., 1996; Lemos, 2003; Bhat, 2013). Skempton (1985) showed that the residual shear strength of Kalabagh Dam clay significantly increased when the shear rates exceeded 100 mm/min. This was probably due to the disturbance of the oriented surface structure at fast shear rates. This type of disturbance can lead to the development of the turbulent shear mode and result in an increase in residual strength. An increase in the fast residual strength can be associated with the shear viscosity effect (Tika et al., 1996; Lemos, 2003; Carrubba and Colonna, 2006) or the crushing of round particles (Fukuoka and Sassa, 1991). Fukuoka and Sassa (1991) supposed that the grinding of round particles would lead to an increase in the density and the interlocking between soil particles within the shear surface. This phenomenon will result in an increase in the internal friction angle of round Toyoura sand with shear displacement rates.

In contrast, a decrease in the fast residual strength can be caused by the delayed dissipation of excess pore water pressure (e.g., Skempton, 1985; Parathias, 1995a, b; Petley and Taylor, 1999; Li et al., 2013b). The delayed dissipation of excess pore water pressure can lead to a decrease in the effective normal stress, and consequently, a decrease in the shear strength. This is considered to be the main reason for the negative rate effect. However, excess pore water pressure may not affect the residual shear strength when shearing occurs at slow rates (e.g., Saito et al., 2006, 2007; Wang et al., 2010; Bhat, 2013; Kimura et al., 2013) or in sand or silty sand (Wang et al., 2010; Li et al., 2017). Moreover, an increase in the porosity (void ratio) and water content in the shear zone also reduces the fast residual strength (Tika et al., 1996; Li et al., 2017), as does an increase in the finer particles in the shear zone, as the larger particles are pushed out of the shear zone (Saito et al., 2007; Li et al., 2017) or the angular particles are crushed (Fukuoka and Sassa, 1991). Fukuoka and Sassa (1991) believed that the crushing of angular tennis court sand would lead to a decrease in the internal friction angle with an increase in the shear displacement rates. Furthermore, the negative rate effect can be attributed to the testing conditions. Tika et al. (1996) noted that the penetration of free water from the water bath into the shear zone can accelerate the reduction in the residual shear strength. More recently, Gratchev

and Sassa (2015) suggested that small rates of broken bond recovery and particle rebound at fast shear rates may reduce the fast residual strength. The causes of the rate dependency of the residual strength are summarised in Fig. 2.6.

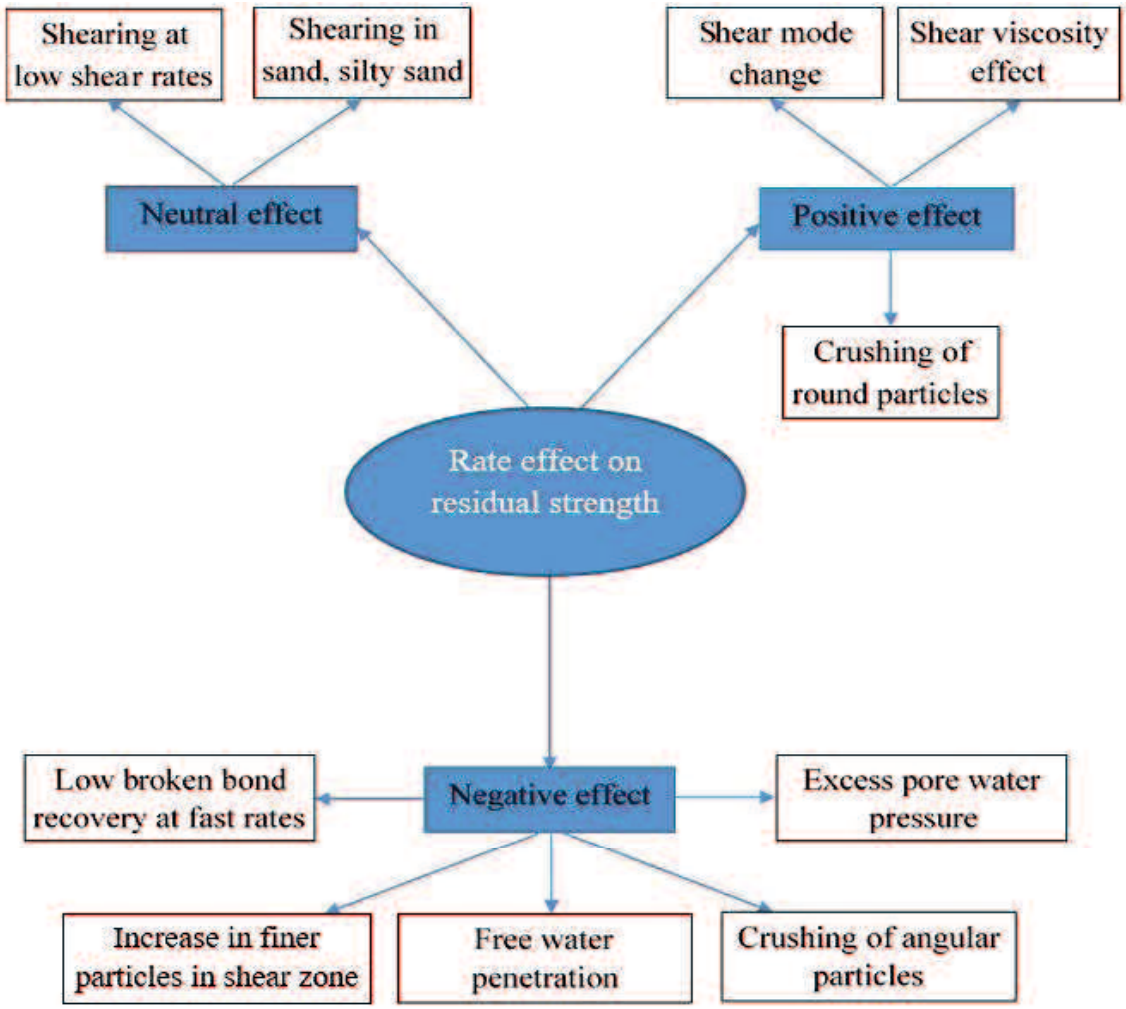

Figure 2.6 Causes of rate dependency of residual strength

2.2.2. Factors affecting rate dependency of residual strength

The magnitude of the rate effect on the residual strength may depend on the effective normal stress (Parathias, 1995a, b; Tika et al., 1996; Carrubba and Colonna, 2006). Some other investigations have also indicated that the magnitude of the rate effect decreased with the increasing effective normal stress (Petley and Taylor, 1999; Stark and Hussain, 2010; Kimura, 2013, Gratchev and Sassa, 2015). In particular, the rate effect on the residual strength is thought to be more evident at levels of effective normal stress below 100 kPa.

The rate dependency of the residual strength may also be related to some physical properties of the soil. To quantitatively evaluate the magnitude of the rate effect, Suzuki

et al. (2001) proposed parameter α′ (rate effect coefficient) for evaluating the effect of the shear displacement rates on the residual strength.

$$\alpha' = \frac{d(\tau/\sigma_N)_r}{d(\log\dot{\delta})} \tag{2.1}$$

Suzuki et al. (2001, 2009) showed that there was a linear relationship between the positive rate effect and the clay fraction, plasticity index, and activity. Accordingly, the magnitude of the positive rate effect is seen to increase as these parameters increase. This also confirms that the variation in residual strength with the shear displacement rate is relevant to the type and content of the clay minerals.

In terms of the physical properties of the soil, Li and Aydin (2013) also indicated that the magnitude of the positive rate dependency of the residual strength of soil may be decreased by the increasing coarse fraction and soil density. In addition, Scaringi and Di Maio (2016) believed that the rate dependency of the residual strength can be correlated with the pore water chemistry. The test results showed that the level of the positive rate effect might increase as the NaCl molarity in the pore fluid increases (Fig. 2.7).

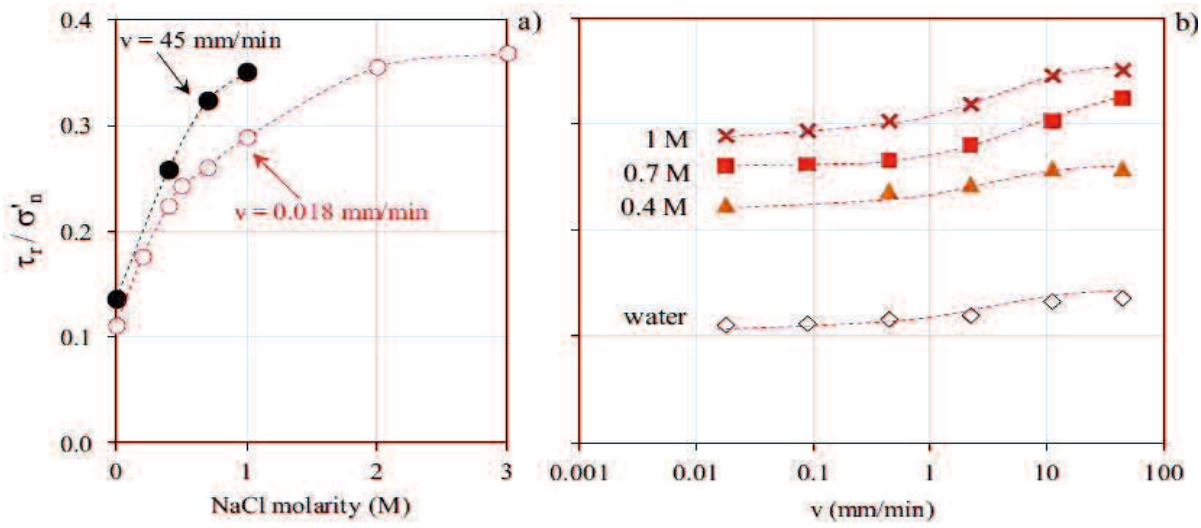

Figure 2.7 Rate dependency of residual strength of bentonite at different NaCl molarities in pore fluid (Scaringi and Di Maio, 2016)

2.2.3. Test procedure to evaluate rate effect on residual strength

There are two main procedures, single- and multi-stage procedures, which are often used to determine the residual strength of soil. In the single-stage procedure, each ring shear test will be conducted on an individual sample with different levels of effective normal stress. In contrast, in the multi-stage test procedure, a ring shear test will be

conducted on one sample, followed by a decrease or increase in the effective normal stress. The main advantage of the multi-stage procedure is that it saves time. The single- and multi-stage procedures were also used to evaluate the rate dependency of the residual strength. For evaluating the rate effect on the residual strength, the single-stage procedure was conducted on an individual specimen with different shear rates. This procedure will be used to evaluate the effect of the shear rates on the residual strength of the first-time slide. The main advantage of this procedure is that it limits the soil extrusion through the gap between the two halves of the shear box (Bishop's type) or the soil trap between the loading plate and the inner circumference of the shear box (Bromhead's type). However, the specimen preparation and testing in this procedure require a lot of time. In contrast, the multi-stage procedure saves time in terms of specimen preparation and testing. The multi-stage procedure is conducted on one specimen, followed by a decrease or increase in the shear displacement rate under a constant effective normal stress. This procedure should be used to investigate the rate effect on the residual strength of reactivated landslides. The first step of this procedure is to subject the specimens to shear in order to reach the residual state. This step corresponds to the first-time slide. At the residual state, the shear displacement rate will be gradually increased or decreased as the desired value under a constant effective normal stress. However, the test results may be affected by soil extrusion or a soil trap.

The single- and multi-stage procedure for increasing or decreasing the shear rate have been commonly used to evaluate the rate effect on the residual strength. However, in certain types of soil, different test procedures may affect the type of rate effect. For kaolin, the residual strength obtained from these procedures shows a positive rate effect (Suzuki et al, 2001, 2003, 2017; Bhat, 2013; Khosravi et al., 2013; Scaringi and Di Maio, 2016). In other words, the type of rate effect on the residual strength of kaolin is independent of the test procedure. However, in the case of bentonite, the test results from the single-stage and multi-stage shearing rate procedures are not consistent. Suzuki et al. (2003) investigated the rate dependency of the residual strength of Na-montmorillonite using the single-stage procedure. The test results showed that the residual strength decreased as the shear rates increased (negative rate effect). Scaringi and Di Maio (2016) examined the rate effect on the residual strength of bentonite using the multi-stage procedure. As opposed to the test results by Suzuki et al. (2003), their test results indicated a positive rate effect on the residual strength of bentonite. The test procedure and the rate effect on the residual strength of some previous studies are summarized in Table 2.2.

Table 2.2 Test procedure and rate effect on residual strength in some previous studies

Soil type	W_L	PI	CF	Test procedure	Rate effect	Reference
Kaolin	62	21.8	35.3	Single	Positive	Suzuki et al. (2001)
Mudstone	63	25.5	24	Single	Positive	
Kaolin	62	21.8	35.3	Single	Positive	Suzuki et al. (2017)
				Multistage	Positive	
Kaolin	52	30	26	Single	Positive	Bhat (2013)
Kaolin-glass beads	43.8	24	80	Single	Negative	Li et al. (2013b)
	33.8	17.5	60			
	27.2	12.3	50			
	22.8	9.3	40			
	13.4	2.3	20		Positive	
Sand+bentonite	50.8	20.3	20	Single	Negative	Saito et al. (2007)
	64.3	37.8	28		Negative	
Sand + illite	-	-	-		Negative	
Amber clay	96.3	62.5	66	Multistage*	Negative	Grachev and Sassa (2015)
Brown clay	88.2	54.5	19			
Black clay	38.6	19	11			
Landslide soil	86	21	-	Single	Negative	Nakamura and Shimizu (1978)
Kaolinite	53	24	-	Multistage	Positive	Khosravi et al. (2013)
Kaolinite	65.3	23.8	50.1	Single	Positive	Suzuki et al. (2003)
Montmorillonite	351.1	287	50.9	Single	Negative	
Kaolin	67	-	74	Multistage	Positive	Scaringi and Di Maio (2016)
Kaolin + 50% sand	-	-	37			
Kaolin + 40% sand	-	-	44.4			
Kaolin + 30% sand	-	-	51.8			
Kaolin + 20% sand	-	-	59.2			
Sand	-	-	-	Multistage	Neutral	
Kaolin+80% sand	-	-	14.8			
Bentonite	324	-	82	Multistage	Positive	Scaringi and Di Maio (2016)
Bentonite + 50 % sand	-	-	41			
Bentonite + 70 % sand	-	-	24.6		Neutral	
Bentonite + 80 % sand	-	-	16.4			
Bentonite + 90 % sand	-	-	8.2			
Sand	-	-				
Landslide soil	31	-	7.3	Single	Negative	Li et al. (2017)
Krishnabhir	34.1	13.4	21	Single	Positive	Bhat and Yatabe (2015)
Shikoku	47.5	16.3	20			
Toyooka-kita	96.5	37.5	24			

Note: *Multi-stage decreasing shear displacement rate procedure

2.3. Residual interface strength

The residual strength at the interface between bi-materials has received much attention in the literature. The residual interface strength between soils and solid materials, and solid materials and solid materials (steel, concrete, geotextiles, and geomembrane), related to the stability of friction piles, retaining walls, anchor rods, earth reinforcement, offshore pipelines, and landfill cover, has been extensively studied. In general, the residual interface strength is somewhat similar to the residual strength of the soil itself. It also depends on the properties of the soil, the size and shape of the particles, the applied normal stress, and the shear displacement rate. In addition, it depends on the interface characteristics and the surface roughness of the solid materials (Lemos and Vaughan, 2000).

In landslides, a shear zone often develops along the bedding plane, discontinuous plane or at the interface between two soil layers (e.g., Bromhead and Ibsen, 2004; Gratchev et al., 2005; Tiwari et al., 2005, 2007; Chigira and Yagi, 2006; Wang et al., 2007; Suzuki et al., 2012; Bromhead, 2013; Has and Nozaki, 2014). Bromhead and Ibsen (2004) described numerous landslides which had occurred in sedimentary rock along the coastline of Southeast Britain. These landslides are referred to as bedding-controlled landslides, they have rotational and transitional forms. Chigira and Yagi (2006), Wang et al. (2007), and Suzuki et al. (2012) also reported that most of the landslides triggered by the 2004 Mid-Niigata Prefecture earthquake (Japan) occurred along the planar bedding. Planar-bedding-parallel-sliding surfaces formed between sandstone and siltstone or between weathered and un-weathered rock (Fig. 2.8).

Figure 2.8 Sliding surface in sandstone in Niigata Prefecture (Suzuki et al., 2012)

Similarly, Has and Nozaki (2014) investigated the role of the geological structure in landslides triggered by the 2007 Mid-Niigata offshore earthquake. The authors

indicated that the bedding plane played an important role in the landslides. The slopes comprise sandstone and siltstone which are sheared off easily along the bedding planes. In Niigata Prefecture, the shearing surfaces of all the landslides are located at the contact between highly weathered and less weathered Tertiary black mudstone layers (Tiwari et al., 2005; Tiwari, 2007). These types of rock soften easily with the presence of water due to their smectite mineral content and are referred to as soft rocks. Therefore, the residual strength at the interface between two soil layers should be considered when evaluating and predicting the slope stability.

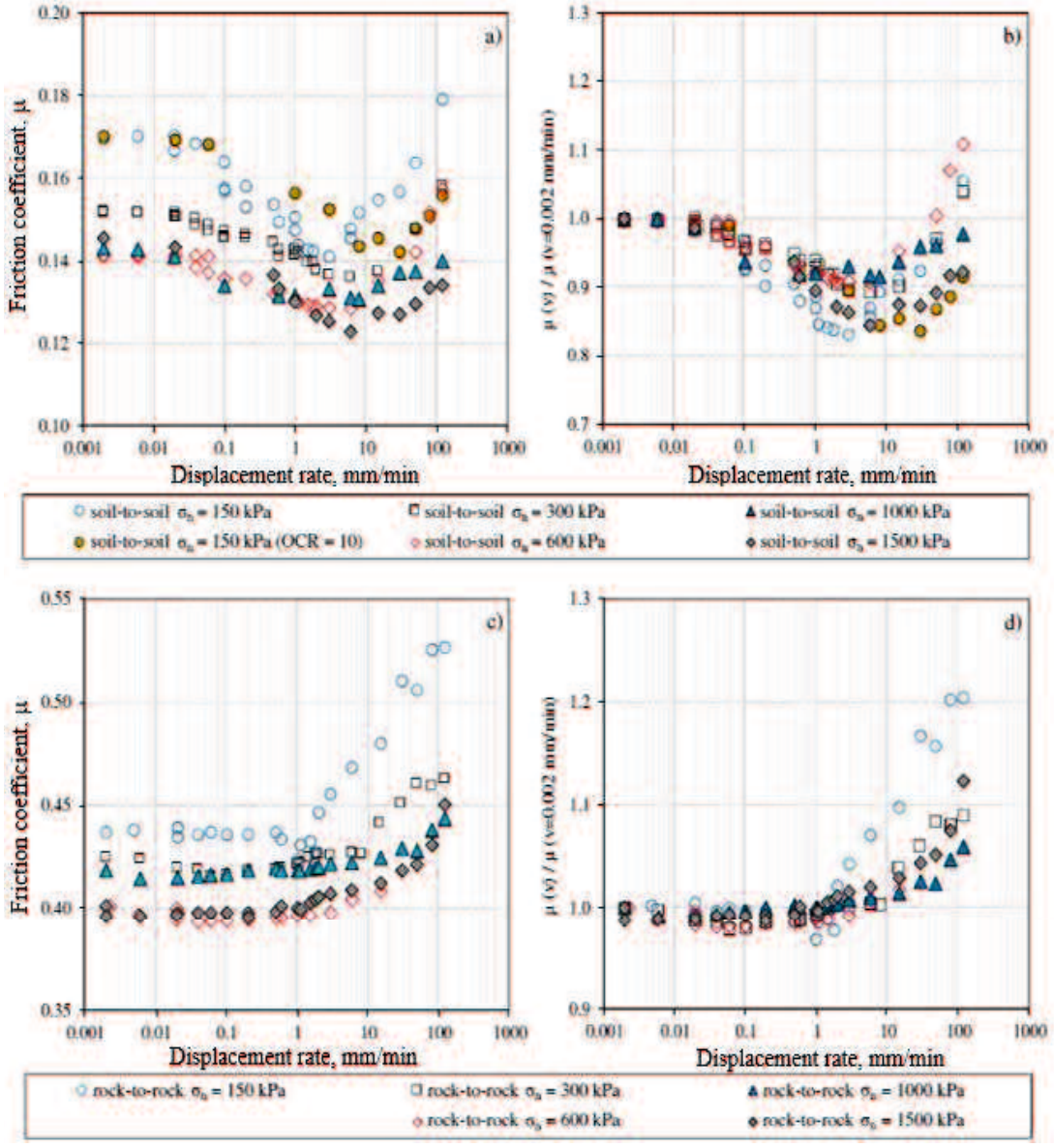

Figure 2.9 a) and b) Relationships between residual interface friction coefficient of soil-soil assembly samples and shear displacement rate, and c) and d) Relationships between residual interface friction coefficient or rock-rock assembly samples and shear displacement rate (Scaringi et al., 2018)

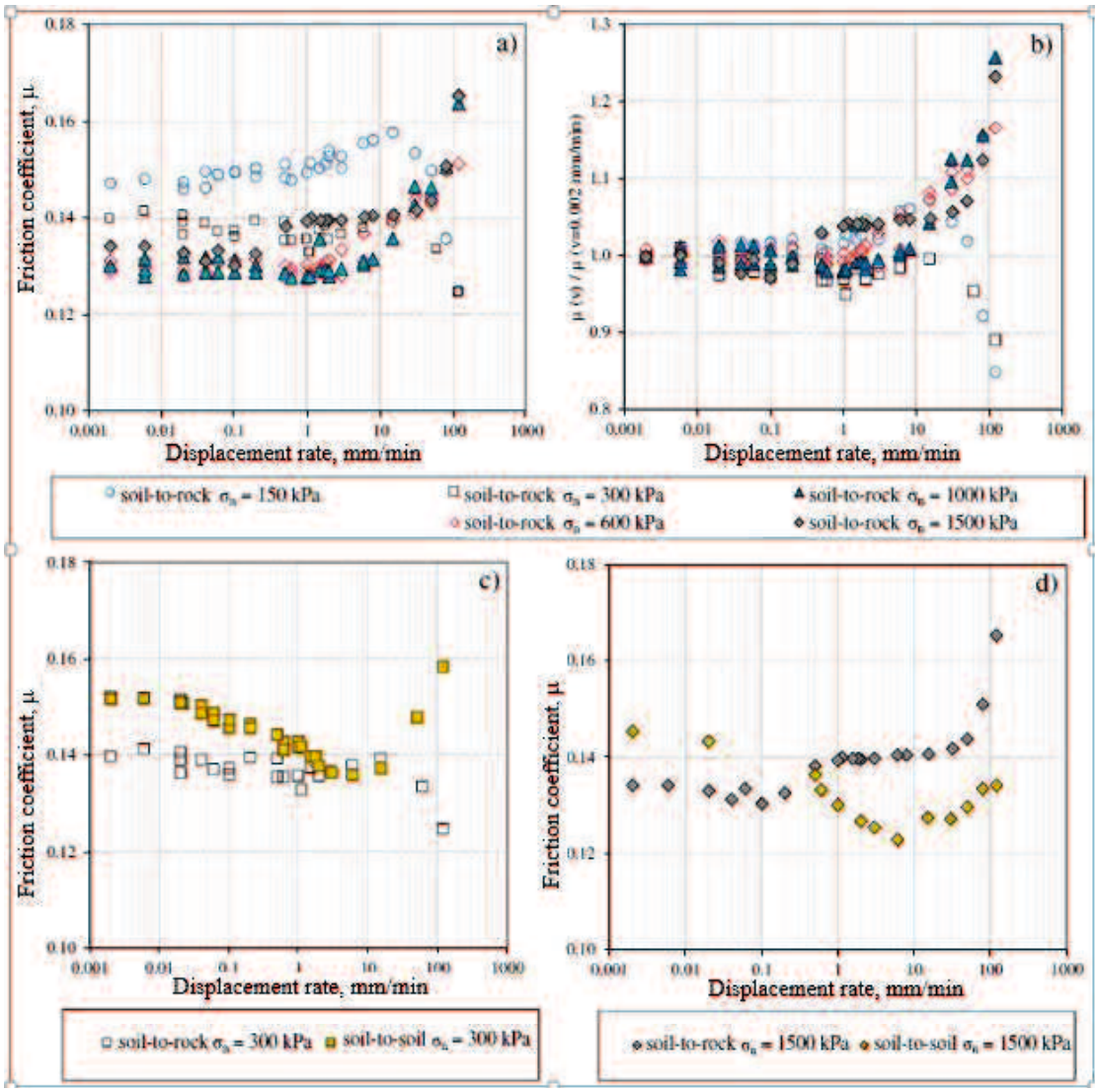

Figure 2.10 Relationships between residual interface friction coefficient of soil-rock assembly samples and shear displacement rate (Scaringi et al., 2018)

Recently, some investigations have been conducted to examine the residual strength at the interface between two soil layers. Suzuki et al. (2017) conducted ring shear tests on samples consisting of two halves to investigate the residual interface strength between two layers with different degrees of cementation (different cement contents). The test results showed that the rate effect on the residual strength was also exhibited in discontinuous planes. Scaringi et al. (2018) investigated the rate dependency of the residual strength at the interface of soil to soil, rock to rock, and soil to rock at the landslide stress level. The test results showed that all the sample assemblies exhibited positive rate dependency of the residual strength (Figs. 2.9 and 2.10). In addition, the rate dependency of the residual strength depended on the materials in contact, the normal

stress, and the stress history (OCR). The investigations of Suzuki et al. (2017) and Scaringi et al. (2018) partly reflected the behaviour of the residual strength on the boundary between two soil layers and the effect of some factors such as stiffness, normal stress, shear displacement rate, and stress history. However, the rate effect on the residual interface strength between two soil layers should be further investigated.

2.4. Shear rate (strain rate) effect on peak strength

The effect of the shear rate (or the strain rate) on the peak strength of soil is an important consideration in geotechnical engineering. It has been recognized and investigated for a long time by many researchers. Most of the researchers examined the relationship between the undrained shear strength and the strain rate in a triaxial apparatus (e.g., Casagrande and Wilson, 1951; Richardson and Whitman, 1963; Vaid and Campanella, 1977; Graham et al., 1983; Lefebvre and LeBoeuf, 1987; Asaoka et al., 1994; Sheahan et al., 1996; Zhu et al., 1999; Zhu and Yin, 2000; Diaz-Rodriguez et al., 2009; Mun et al., 2016).

Richardson and Whitman (1963) conducted triaxial compression tests to investigate the undrained strength behaviour of remoulded fat clay at different strain rates. The authors showed that the undrained peak strength significantly increased, especially at small strain levels, when strain rates increased from slow (1% strain in 500 minutes) to fast (1% strain in 1 minute). At small strain rates, the shear strength increased due to the increase in effective stress; at large strain rates, the increase in resistance was due to the decrease in pore water pressure.

Vaid and Campanella (1977) found that the undrained shear strength of Saint-Jean-Vianney clay increased by 5 to 10% for a ten-fold increase in the strain rate. For lightly over-consolidated natural soft clay, Graham et al. (1983) showed that the undrained strength rose by about 10 to 20% when the strain rate increased 10 times (Fig. 2.11). In addition, the authors suggested that the strain rate dependency of the undrained shear strength was independent of the soil plasticity, test type, and stress history (overconsolidation ratio, OCR $\leq$ 3).

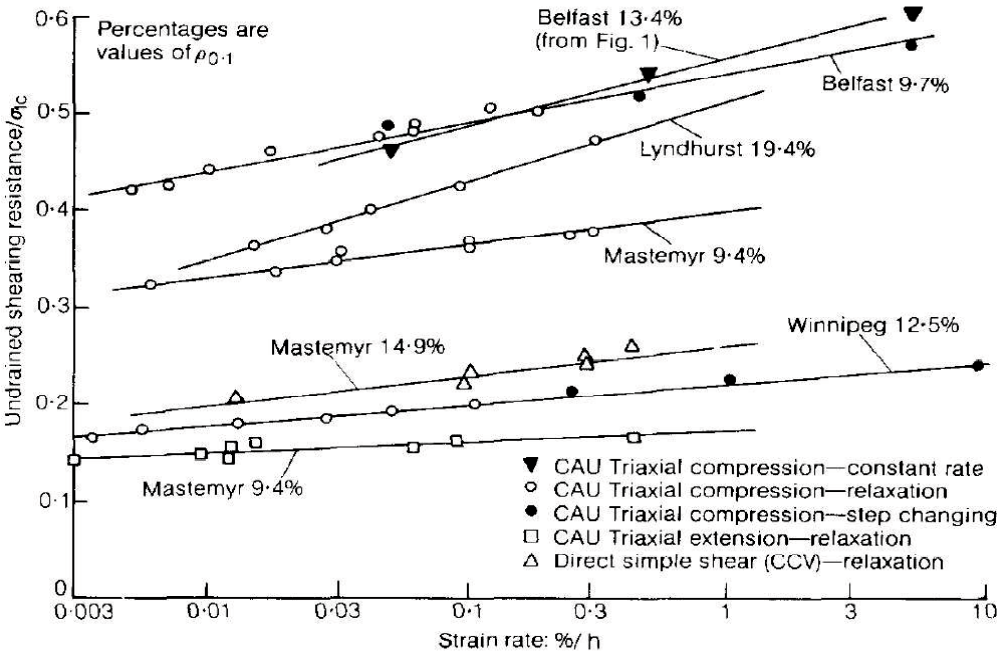

Figure 2.11 Variation in undrained shear strength with different strain rates (Graham et al., 1983)

Asaoka et al. (1994) investigated the behaviour of partially drained and undrained shear strength of Kawasaki clay at different strain rates using triaxial compression tests. For the partially drained condition, the drainage valve was kept open during the loading process, whereas it was closed for the undrained condition. The test results showed that, differently from the undrained shear strength, the partially drained strength tended to decrease with the increase in strain rate (Fig. 2.12).

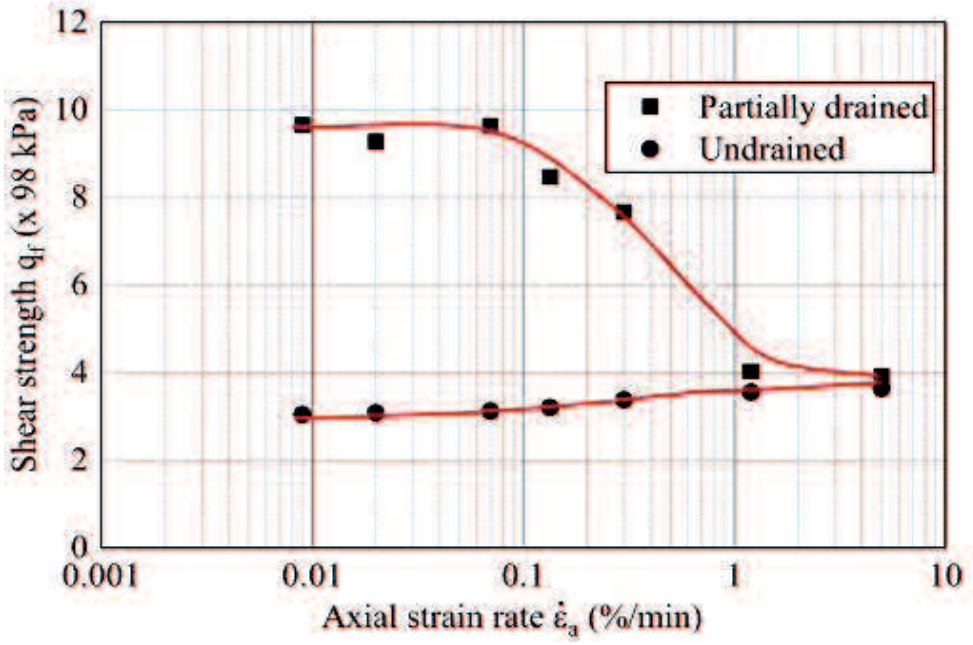

Figure 2.12 Variation in shear strength with axial strain rate (Asaoka et al., 1994)

Sheahan et al. (1996) investigated the strain rate dependency of the undrained strength of Boston blue clay at different overconsolidation ratios (OCRs) by using K_0 in consolidated-undrained triaxial compression tests. The test results revealed that the undrained strength increased as the strain rate increased. However, the strain rate dependency of the undrained strength (the strain rate parameter, $\rho_{0.5}$) tended to decrease with the increase in the OCR (Fig. 2.13). Here, $\rho_{0.5}$ is defined as the change in undrained shear strength caused by a 10-fold change in the strain rate with the reference strain rate at 0.5%/h. In other words, the increase in the undrained shear strength with an increase in the strain rate tended to decrease as the OCR increased.

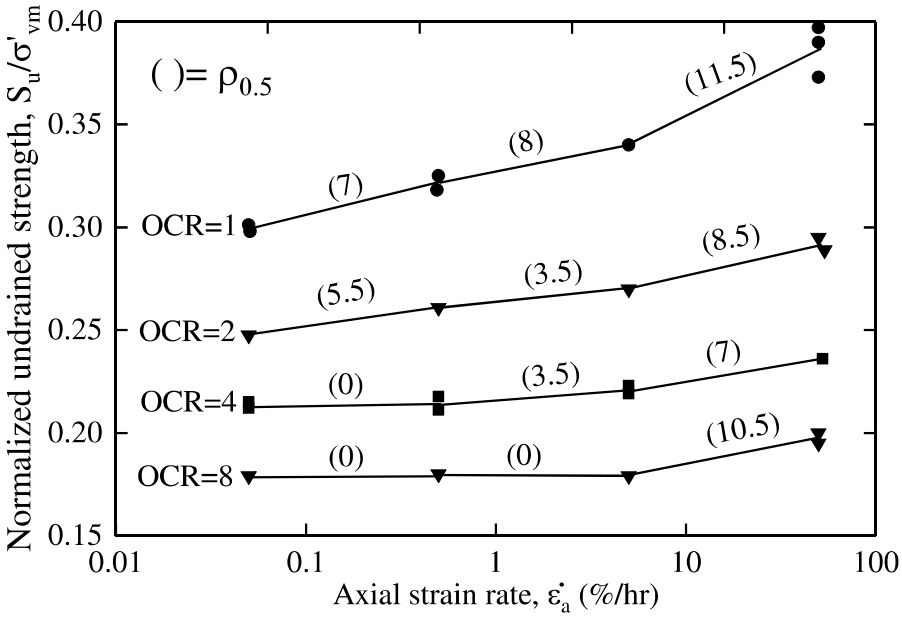

Figure 2.13 Normalized shear strength versus strain rate (Sheahan et al., 1996)

Zhu and Yin (2000) conducted consolidated-undrained triaxial tests on Hong Kong marine clay at different strain rates and OCRs. The test results indicated that higher strain rates result in higher undrained shear strength for OCRs ranging from 1 to 8 and strain rates ranging from 0.15%/h to 15%/h in both compression and extension triaxial tests (Fig. 2.14). However, the relationship between the strain-rate parameter ($\rho_{0.15}$) of the undrained strength and the OCRs is not clear (Fig. 2.15). Here, $\rho_{0.15}$ is defined as the change in undrained shear strength caused by a 10-fold change in the strain rate with the reference strain rate at 0.15%/h.

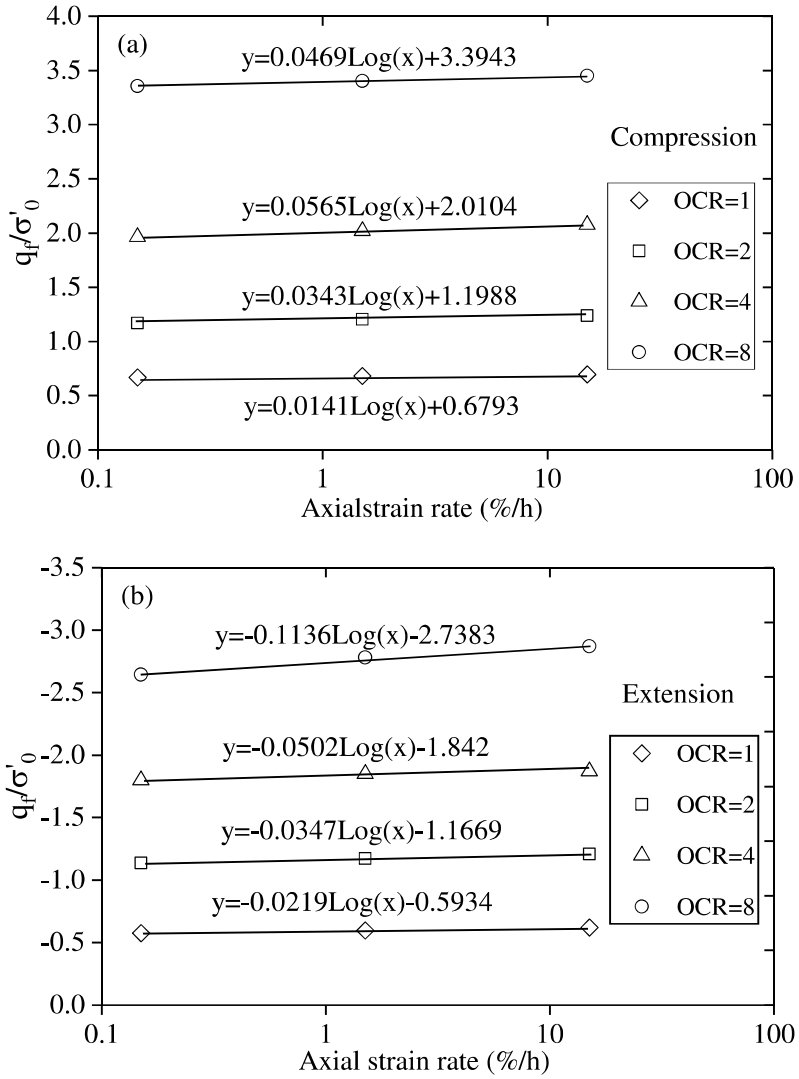

Figure 2.14 Relationship between normalized undrained shear strength and axial strain rate for (a) Compression tests and (b) Extension tests (Zhu and Yin, 2000)

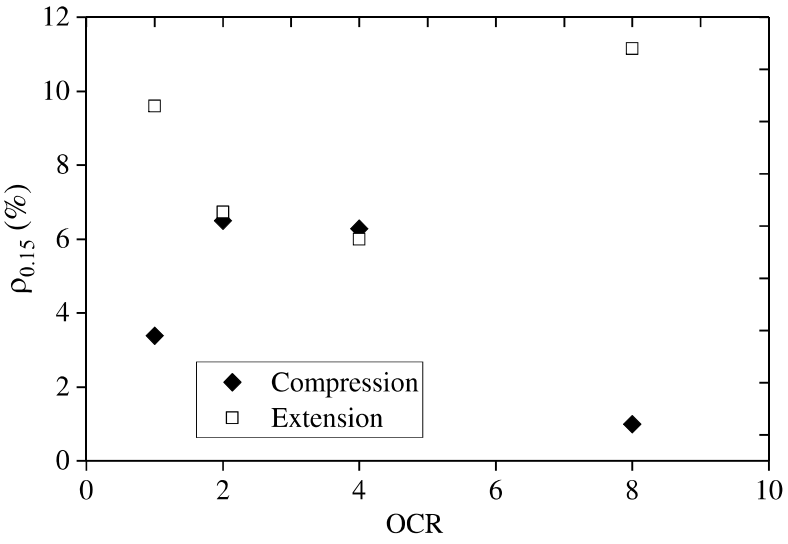

Figure 2.15 Relationship between OCRs and $\rho_{0.15}$ (Zhu and Yin, 2000)

The variation in peak shear strength at a wide range of strain rates or shear rates was also investigated (Thermann et al., 2006; Quinn and Brown, 2011; Robison and Brown, 2013). Quinn and Brown (2011) conducted triaxial tests under the drained condition to investigate the behaviour of the peak strength of kaolin at a wide range of strain rates ranging from 1%/h to 180000%/h. The test results revealed that, at the strain rate of 1%/h, the test was not fully drained and the soil behaviour was partially drained. When the strain rate was increased from 1%/h to 300%/h, the shear strength decreased with the strain rate. At this range in strain rates, the soil behaved as partially drained. When the strain rate exceeded 300%/h, the soil behaviour became fully undrained and the shear strength increased as the strain rate increased. Thermann et al. (2006) investigated the effect of the shear rate on the peak strength of till using direct shear tests. The shear rate was varied from 0.005 mm/min to 0.5mm/min. The test results revealed that at shear rates less than 0.05 mm/min, the soil behaviour was partially drained and the shear strength decreased as the shear rates increased. In contrast, at shear rates above 0.05 mm/min, the soil response became undrained and the shear strength increased with the shear rate.

The behaviour of undrained and partially drained peak shear strength is closely related to the shear-induced pore water pressure at different strain rates. In partially drained behaviour, the higher strain rates lead to an increase in the shear-induced pore water pressure and failure occurs. This phenomenon leads to a decrease in the partially drained peak strength as the strain rate increases. In contrast, in undrained behaviour, the higher strain rates lead to lower shear-induced pore water pressure. Many investigations, e.g., Casagrande and Wilson (1951), Richardson and Whitman (1963), Sheahan et al. (1996), Zhu et al. (1999), Zhu and Yin (2000), and Quinn and Brown (2011) have suggested that the lower shear-induced pore water pressure at fast strain rates is a major cause of the increase in undrained peak strength with increasing strain rates. Lefebvre and LeBoeuf (1987) revealed that, for destructured clay (normally consolidated), the effect of the strain rate on the pore water pressure generated during shearing was significant, whereas for structured clay (over-consolidated), the shear-induced pore water pressure was not substantially affected by the strain rate before failure occurred. At post-failure, the behaviour of the shear-induced pore water pressure of structured specimens was similar to that of destructured ones. For both structured and destructured clay, however, the magnitude of the strain rate effect on the undrained shear strength was similar. Diaz-Rodriguez et al. (2009) found that the increase in undrained strength of Mexico City clay,

with an increasing strain rate, might not be related to the pore water pressure generated during shearing. They suggested that the higher undrained strength at higher strain rates was due to experimental biases.

2.5. Reactivated landslides and application of residual shear strength

Reactivated landslides are active landslides which had been inactive (suspended). In other words, the reactivation of pre-existing landslides is a phenomenon in which part or all of a previous landslide mass moves along the pre-existing shear surfaces (Lee and Jones, 2004).

Fig. 2.16 shows the different stages of landslides: active (first-time slide), inactive, and reactivated (second-time slide). The inactive stage includes the suspended and dormant stages. The dormant stage shows that the inactive landslides can be reactivated. The reactivated stage (the reactivation of old landslides) is often related to heavy rainfall or earthquake occurrence (Cruden and Varnes, 1996).

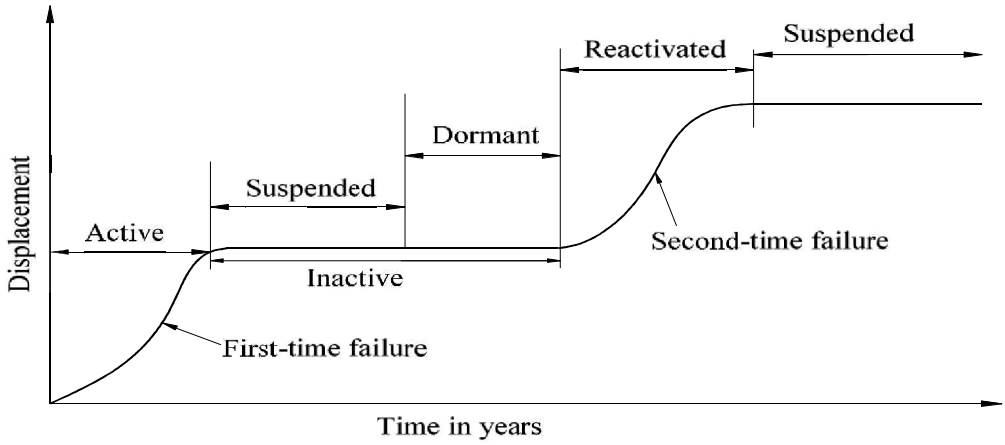

Figure 2.16 Activity of landslides in different stages (after Cruden and Varnes, 1996)

For reactivation, the materials along the pre-existing shear surfaces are at the residual state and residual shear strength will be seen at this state. This is how the residual strength can be used to predict the stability as well as to design countermeasures for reactivated landslides. This is also the most common application of residual strength to slope stability analyses.

In fact, there are some cases in which the slopes underwent a small shear displacement, but the shear strength sharply decreased to the residual value. These cases are related to the bedding shear in folded strata, sheared joints or faults, embankment failure or stratigraphic discontinuities (weathered and unweathered; soft and stiff layers) (Skempton, 1985; Mesri and Shahien, 2003). The failures in these cases can be considered

as first time slides. Therefore, the residual strength can be applied not only to pre-existing failures, but also to first-time slides. In addition, the residual state may exist in first-time slides in clay fills and cutting slopes in fissured clay or as a part of progressive failure (Mersi and Shahien, 2003).

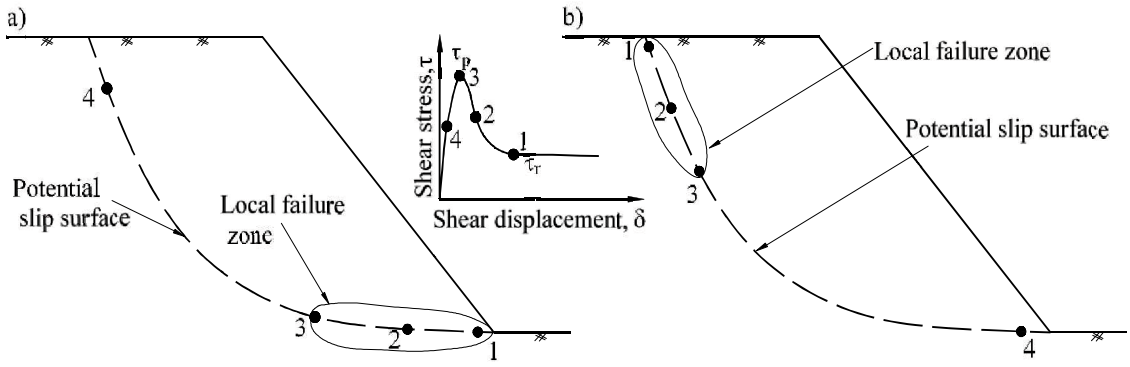

Figure 2.17 Progressive failure: a) Starting from toe of slope (Locat et al., 2011) and b) Starting from head of slope

Progressive failure can be simply defined as the phenomenon in which the mobilized shear stress and the shear deformation are non-uniform along the potential failure surface (Skempton, 1964). The shear stress along the failure surface may vary from the peak to the residual values. Fig. 2.17 shows the progressive failure along a circular failure surface. There is a local failure zone at which the soil has reached its peak strength (points 1 to 3). In the local failure, point 1 has reached the residual state.

The residual strength may not only be exhibited at the soil-soil contact, but also at the interface between the soil/solid materials and/or the solid materials/solid materials (steel, concrete, geotextiles, and geomembranes) (Lemos and Vaughan, 2000). This residual interface strength is related to the stability of friction piles, retaining walls, anchor rods, earth reinforcement, offshore pipelines, and landfill cover. For instance, for geosynthetic-reinforced soil, the residual strength is used to calculate the required geosynthetic strength, while the peak strength is used to determine the length and the spacing of the geosynthetic (Leshchinsky, 2001).

At the residual state, the experimental results show that the residual cohesion may be different from zero (Tiwari and Marui, 2005). However, this value is insignificant. In addition, Skempton (1985) also noted that the residual cohesion can be very low. Therefore, Stark et al. (2005) suggested that, related to the residual state, the cohesion value should be zero in stability analyses, except for the results of back-analyses which show value of cohesion greater than zero.

The rate dependency of the residual strength can be applied to slope stability analyses and the displacement of driven piles. In a slope stability analysis, if the soil shows a positive rate effect, the shear strength will increase with an increasing shear rate and the extra strength will resist movement. The rate of movement will then decelerate and the slide will come to a rest. In some cases, a reduction in the movement rate can lead to an increase in the shear strength of soil with transitional and/or sliding shear modes. On the other hand, if the soil shows a negative rate effect and if the velocity increases with an increasing shear displacement, the shear strength will drop below the slow residual strength. In this case, a catastrophic and large displacement will occur. The rate dependency of the residual strength was used to predict the displacement of reactivated landslides, in the static condition under heavy rainfall (Skempton et al., 1989), of the first-time slide in a dynamic condition (Lemos and Coelho, 1991).

In the case of driven pile installation, the application of the rate effect is related to the rate dependency of the residual interface strength between the soil and the pile materials (steel, concrete…). Some previous studies have shown that the coefficient friction and the texture of the contact surface between the soil and the pile surface depend significantly on the displacement rate of the piles during installation. In addition, there is a range in pile displacement rates over which the frictional resistance during construction is strongly sensitive to the installation rate. During pile loading, the frictional resistance drops to the slow residual value with further vertical displacement (Tika et al., 1996).

2.6. Acceleration of landslides and its application

The velocity of landslides is not always constant during sliding. It can vary from very slow to very fast. In terms of physics, the acceleration is defined as the rate of change in the shear rates with respect to the time of movement. Hence, the change in the shear rate (velocity) will lead to a change in the acceleration. The acceleration of a landslide can vary from a few mm/h^2 to hundreds of mm/h^2 (Mazzanti et al., 2015; Carlà et al., 2017; Xu et al., 2011).

The acceleration has been used to establish criteria for the prediction of slope stability and the time to slope failure (Picarelli et al., 2000; Dai et al., 2002; Xu et al., 2011). Picarelli et al. (2000) indicated that there was a linear relationship between the logarithm of the acceleration and the logarithm of the time to slope failure. Dai et al. (2002) showed that in the case of earthquakes, if the peak ground acceleration imposed

on the slopes exceeds the critical acceleration, then displacement or failure will occur. Xu et al. (2011) established a criterion for acceleration for an early warning system for creep slope failure. The authors indicated that the characteristics of changes in acceleration were totally different from those of cumulative displacement and the displacement rate in the whole process from the beginning to the slope failure. The acceleration often fluctuates around zero before reaching the critical phase, whereas it increases sharply in the critical failure stage (Figs. 2.18 and 2.19). Therefore, acceleration can be one of the main important parameters for establishing the criteria for an early warning system for landslide occurrence.

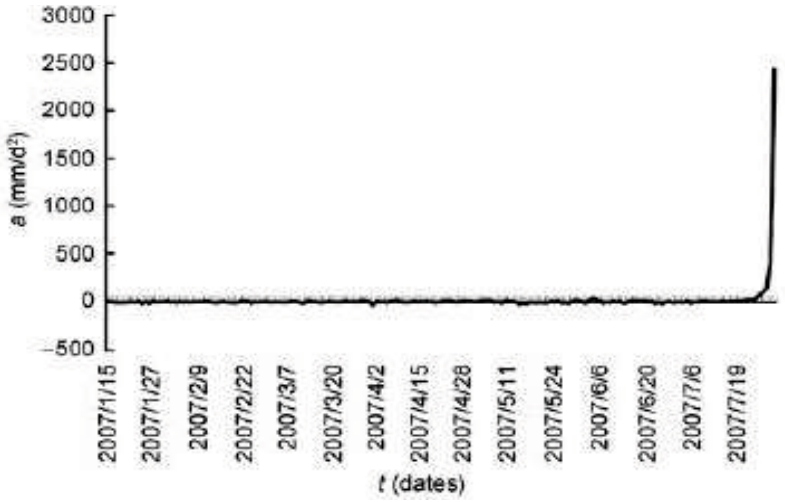

Figure 2.18 Acceleration-time curve of 2nd benchmark of Basshi landslide in 2017 (Xu et al., 2011)

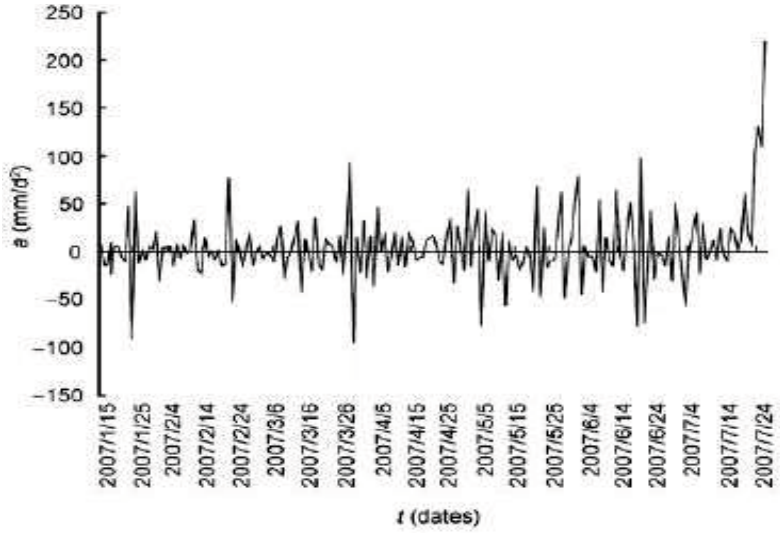

Figure 2.19 Acceleration-time curve of 2nd benchmark prior to July 26, 2007 (Xu et al., 2011)

Acceleration is a function of two variables: velocity and time. Changes in acceleration are related to changes in velocity and time or either velocity or time. As described above, the changes in the shear rate (velocity) more or less affect the residual strength. However, the effect of the changes in acceleration on the residual strength is still unknown.

2.7. Summary

1. The movement rate of landslides can vary from extremely slow to extremely fast and it is not always constant during sliding. Changes in the movement rate will affect the shear strength at both the peak and the residual states (rate effect). The rate effect on the shear strength has become one of the most important considerations in slope stability analyses.

2. The residual strength more or less depends on the shear displacement rate, especially at fast shear rates. Three types of rate effect, namely, positive, negative, and neutral, have emerged from the literature. Differences in the shear modes, the types of soil, and the range in shear rates will lead to different types of rate effect. In addition, the magnitude of the rate dependency of the residual strength may depend on the physical properties of the soil (clay fraction, plasticity index, and soil density), the effective normal stress, and the pore water pressure. Some causes have been proposed to interpret the rate effect on the residual strength. However, the rate dependency of the residual strength and its causes are still a controversial issue, especially in the cases of high-plasticity, low-permeability clay and over-consolidated (OC) clay.

3. The residual interface strength plays an important role in the stability of slopes having bedding planes or containing the interface between two soil layers. Recently, the rate effect on the residual interface strength between two soil layers has been investigated. However, this issue should be further examined.

4. The effect of the shear rate (the strain rate) on the peak strength of both NC and OC soils has been comprehensively investigated through triaxial shear tests which can measure the shear-induced pore water pressure. The strain rate effect on the peak strength is often closely related to the shear-induced pore water pressure at different strain rates. In fact, the ring shear apparatus has been widely used to determine not only the residual strength, but also the peak strength. In the ring shear test, although the drainage condition is allowed during shearing, the rate effect on the peak strength of OC soil may be different

from that of NC soil due to the dilation behaviour, especially at fast shear rates. Therefore, the rate dependency of the peak strength of OC soil should be further investigated by means of ring shear tests.

5. The rate dependency of the residual strength can be evaluated based on single- and multi-stage procedures with increasing/decreasing shear rates. However, these procedures may affect the rate dependency of the residual strength in some kinds of soil. This problem should also be given more attention.

6. The residual strength can be applied not only to old landslides, but also to the first-time slides in stiff and fissured clays, embankment failure, and slopes having bedding or discontinuous planes. The rate dependency of the residual strength can be applied to predict the displacement of a slope or to investigate the displacement of driven piles.

7. The changes in velocity and acceleration are important indicators for establishing an early warning system for landslide occurrences. However, the effect of acceleration on the residual strength is still unclear.

CHAPTER 3. TEST APPARATUS AND EXPERIMENTAL PROCEDURES

3.1. Introduction

The residual strength of soil can be determined through laboratory tests, including the triaxial shear (TS) test, the reversal direct box shear (RDBS) test, and the ring shear (RS) test. Among them, the ring shear test is considered to be the most suitable method for determining the residual strength. The main advantages of the ring shear test can be summarised as follows:

–In the RS test, the specimen can be sheared and the shear strength can be determined at any shear displacement. In contrast, in the TS and the RDBS tests, the shear displacement is limited;

–In the RS test, the specimen is sheared continuously in one direction. This is different from the procedure of the RDBS test. In the RDBS test, the shear direction is changed by the forward and backward processes. This leads to disturbing the particle orientation on the shear surface. The continuous shearing in one direction in the RS test allows for the formation of the perfect orientation of particles in parallel to the shear surface.

However, the ring shear test also has its own disadvantages. The main disadvantage of the RS test is soil leakage at the gap between the two parts of the shear box in Bishop's type of apparatus and at the boundary between the upper plate stone and the inner circumference of the shear box in Bromhead's type of apparatus. This leakage may cause a difference in normal stress at the edge and at the center of the specimen. In addition, the non-uniformity of the strain and shear stress levels during shearing is also a disadvantage of this test.

3.2. Test apparatus

There are two main types of ring shear apparatuses (as mentioned in sub-section 2.2). One is Bishop's type (Bishop et al., 1971) and the other is Bromhead's type (Bromhead, 1979). In this research, the conventional Bishop-type ring shear apparatus was employed. Details of this apparatus are shown in Fig. 3.1. The Bishop-type ring shear apparatus measures the shear force, shear displacement, vertical displacement, and frictional force automatically. The testing conditions can be either stress- or strain-controlled. With this apparatus, the strain-controlled method is employed, i.e., the

displacement rate and normal stress are separately controlled, and the shear stress is measured.

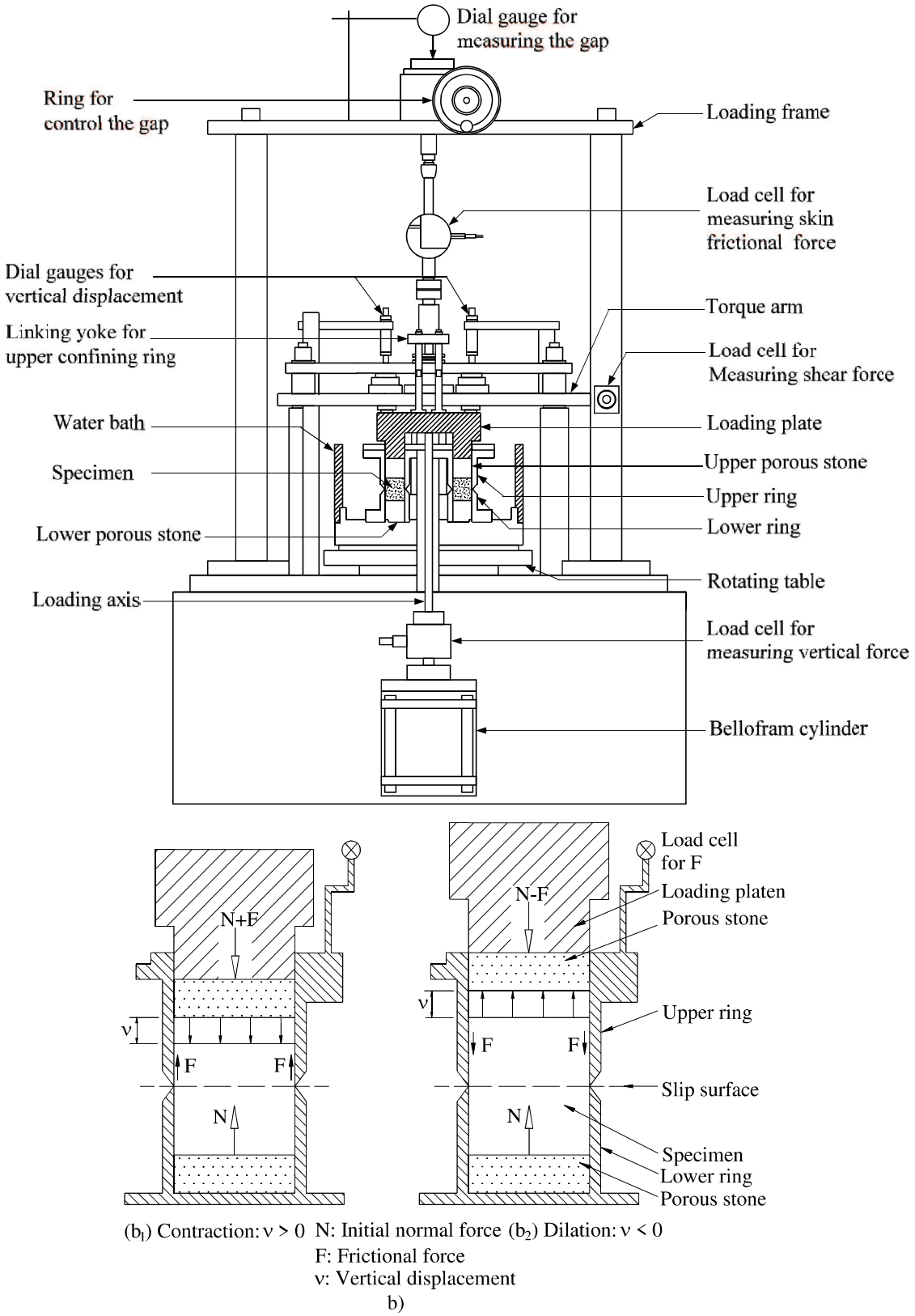

Figure 3.1 a) Cross section of ring shear device used in this study and b) System for measuring friction force and controlling normal force (Suzuki et al., 1997)

The frictional force originates from the displacement of the specimen relative to the shear box and exists between the specimen and the inner perimeter of the rings. It will act upward in the case of specimen contraction and downward in the case of specimen expansion (Fig. 3.1(b)). This force is measured during testing by a load cell attached to the loading frame via a linking yoke connected to the upper ring (Suzuki et al., 1997). The loading plate does not rotate during shearing, but rather is supported by a ball bearing to prevent any deviation in the normal stress. This apparatus uses an annular specimen with an inner diameter of 6 cm, an outer diameter of 10 cm, and a height of 2 cm.

In determining the residual strength of soil using a Bishop-type ring shear apparatus (Bishop et al., 1971), the normal stress, frictional force (F), and gap between the upper and lower rings will affect the test results. The testing conditions may be either stress or strain controlled. To obtain the residual strength in ring shearing, the strain-controlled method is often used, i.e., the displacement rate and normal stress are separately controlled, and the shear stress is measured. The measured frictional force (F) is shown in Fig. 3.1(b). The net normal stress is calculated based on the measured frictional force from the specimen and the inner circumference of the shear box. With regard to the gap, it is closed during consolidation to prevent soil leakage and open during shearing to mitigate the contact friction between the two halves of the shear box. The gap (d) between the upper and lower parts of shear box will affect the formation and thickness of the shear zone within the specimen. In other words, the thickness of the shear zone within the specimen in the RS test depends not only on the grain size (for granular soils) (Sadrekarimi and Olson, 2008) or the displacement rates (for clay) (e.g., Jostad et al., 2006; Gylland et al., 2014), but also on the gap between the upper and lower parts of the shear box. The thickness of the shear zone may affect the measured shear strength, the shear strength behaviour at different shear rates (especially for clay specimens), and then affect the application of shear strength to actual cases. Suzuki (2008) investigated the effect of the gap (d) on the measured shear strength of Ube Masado soil (weathered granite soil) and Toyoura sand in the RS test. The research results showed that an increase in size of the gap led to a decrease in the measured shear strength (Fig. 3.2). However, the gap is equal to 5 to 10 times the D_{50} ($d/D_{50} = 5 \div 10$) and has little effect on the test results (D_{50} is the mean diameter of the soil particle). This indicates that a suitable gap (d) also depends on the grain size. Therefore, it is important to measure the frictional force (F) and to set a suitable gap (d) in order to obtain an accurate value for the shear strength.

In this study, the gap between the upper and lower parts of the shear box will be open to 0.1 mm before shearing.

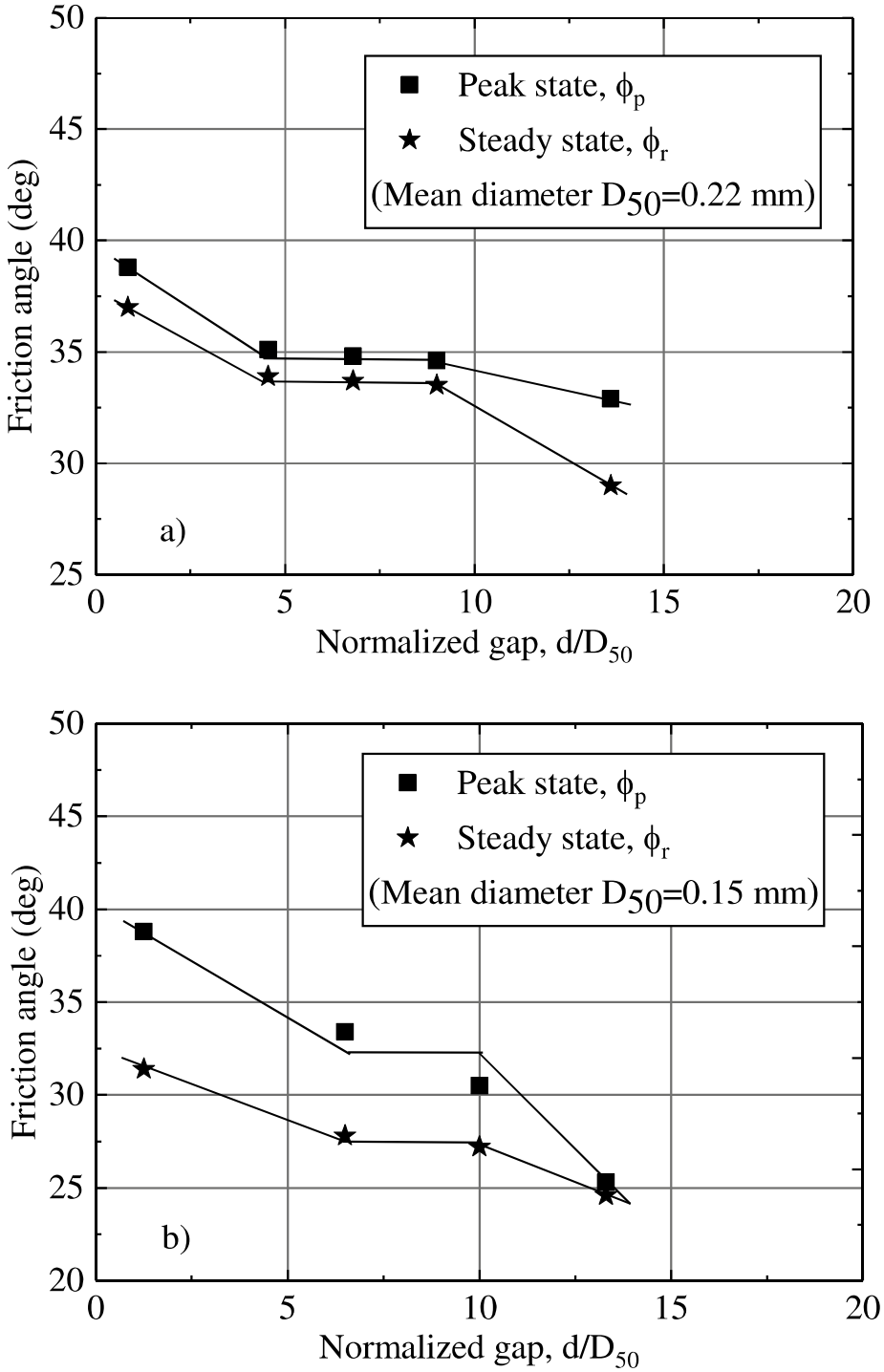

Figure 3.2 Relationship between normalized gap and internal friction angle for (a) Ube Masado soil and (b) Toyoura sand (Suzuki, 2008)

3.3. Materials and physical properties

Two commercial clays, kaolin and bentonite in the form of dry powder were used in this research. The grain size distribution curves of kaolin and bentonite are shown in Fig. 3.3.

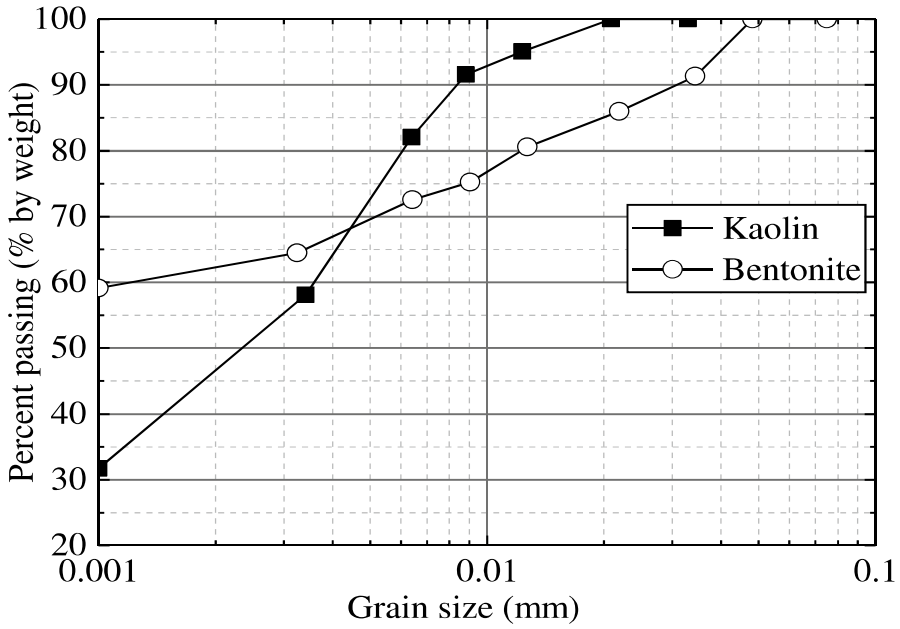

Figure 3.3 Grain size distribution curves of kaolin and bentonite

In this study, ring shear tests were conducted on reconstituted samples of kaolin (K) and kaolin–bentonite mixtures. For the mixture samples, 10%, 20%, and 30% bentonite (dry weight) were mixed with 90%, 80%, and 70% kaolin, respectively. These samples are referred to herein as 10B, 20B, and 30B, respectively. Some previous studies have investigated the residual shear strength of kaolin–bentonite mixtures and have reported that the residual strength decreases with the increasing bentonite content. However, with more than 30% bentonite, the residual shear strength of the mixture samples was almost unchanged and was similar to that of bentonite alone (Di Maio and Fenelli, 1994; Tiwari and Marui, 2003; Marui and Tiwari, 2004) (Fig. 3.4). Hattab et al. (2015) measured the internal friction angle of kaolin–bentonite mixtures by means of triaxial tests. Their results showed that the peak internal friction angle decreases with an increasing bentonite content up to 35%, with the peak friction angles being similar to those of pure bentonite samples at bentonite contents above 35%. Therefore, the maximum of 30% bentonite in the kaolin–bentonite mixtures used in this study was considered sufficient to reflect the behaviour of the residual strength of bentonite.

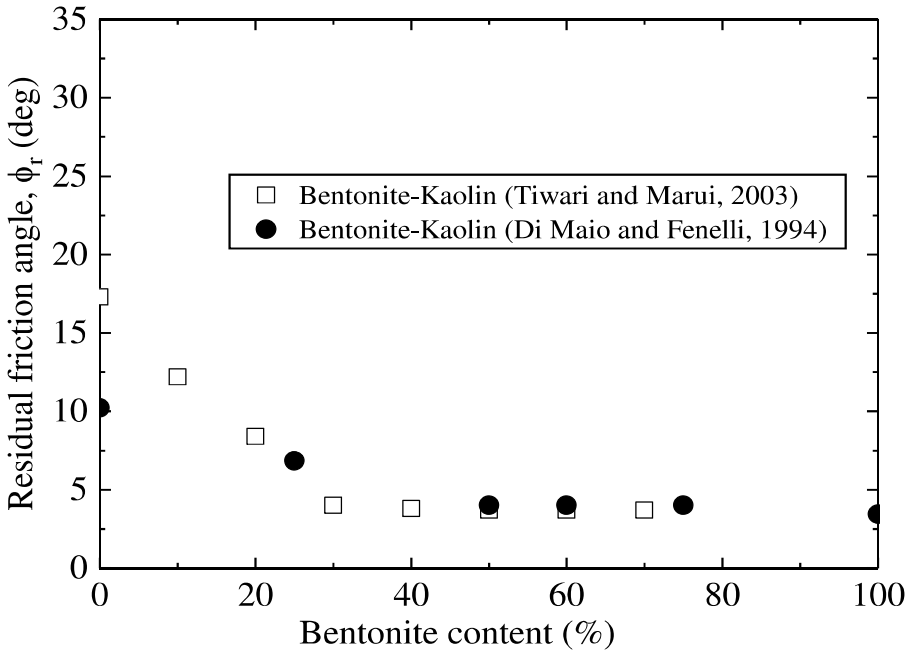

Figure 3.4 Residual strength of kaolin-bentonite mixtures

The physical properties of the samples are summarised in Table 3.1. The consistency limit is presented in Casagrande's plasticity chart (Fig 3.5). In Table 3.1, the permeability coefficient (k) was determined based on oedometer tests (Japanese Geotechnical Society, JGS 0411–2009) under a consolidation pressure of 78.4 kPa. The oedometer tests were carried out on reconstituted kaolin and kaolin-bentonite mixture samples prepared by the pre-consolidation process in a consolidation tank, under a consolidation pressure of 49 kPa. The initial water contents of all of the samples used in the oedometer tests were close to their respective liquid limits.

Table 3.1 Some physical properties of kaolin, bentonite, and their mixtures

Samples	ρ_s (g/cm^3)	CF (%)	w_L (%)	w_P (%)	PI	Oedometer test k (cm/s)
Kaolin (K)	2.645	46.0	77.5	35.4	42.1	3.3×10^{-7}
Bentonite (B)	2.759	62.0	405.0	53.7	351.3	-
10B	2.656	47.6	116.0	36.3	79.7	3.2×10^{-8}
20B	2.667	49.2	144.0	39.4	104.6	1.9×10^{-8}
30B	2.678	50.8	172.0	42.9	129.1	6.0×10^{-9}

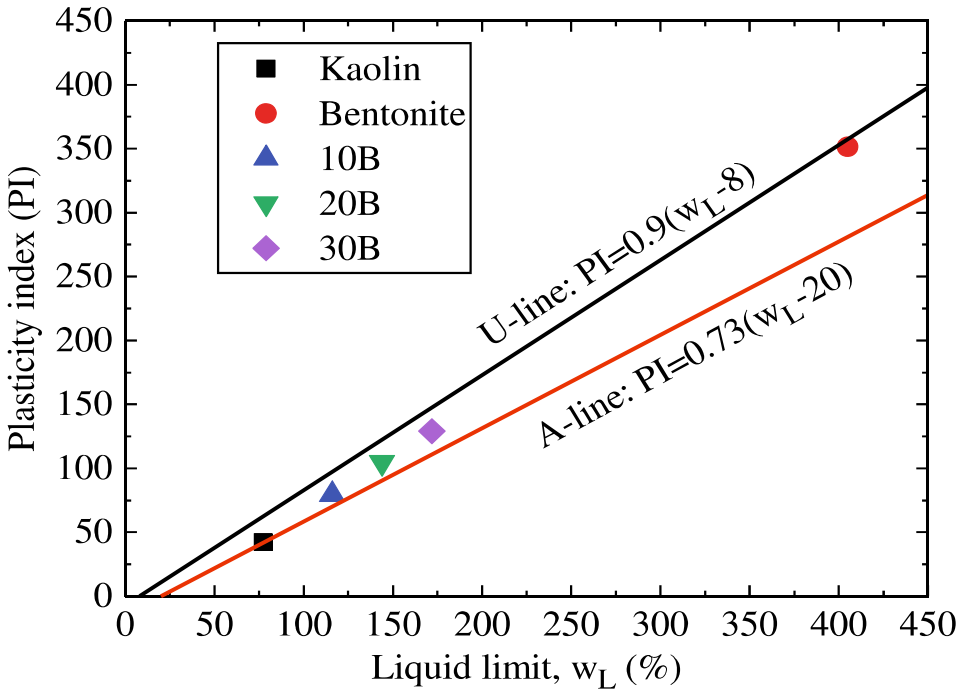

Figure 3.5 Casagrande's plasticity chart

3.4. Sample and specimen preparation

A set of samples containing kaolin and kaolin–bentonite mixtures were prepared for ring shear tests by the pre-consolidation process in a large consolidation tank (Fig. 3.6).

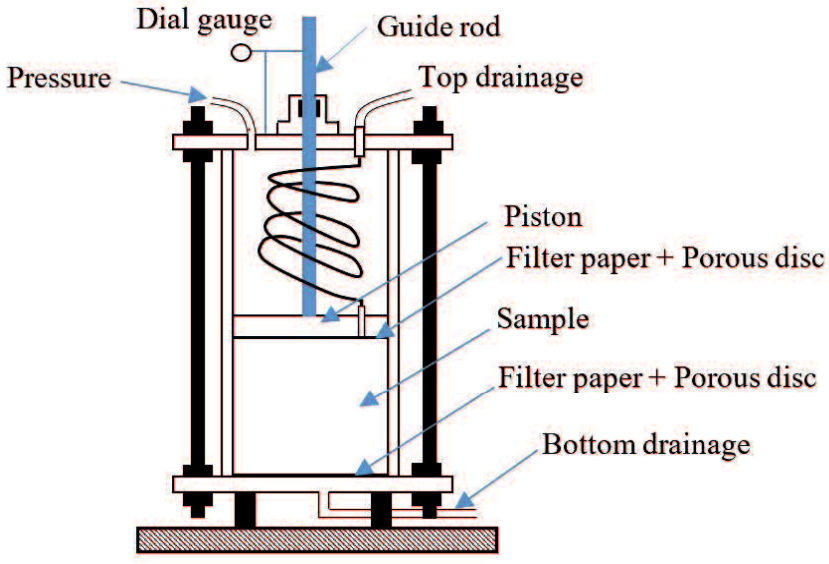

Figure 3.6 Consolidation tank for sample pre-consolidation

The dry powder clays were mixed with distilled water into slurries at about twice their liquid limits and then kept for 24 h to hydrate and reach a homogeneous state. The

slurries were then poured into a large consolidation tank, and a vacuum pressure of 70 kPa was applied for at least 1 h to release air bubbles. The slurry samples were preconsolidated until the primary consolidation was completed. The primary consolidation time was determined based on the 3t method (Japanese Geotechnical Society, JGS 0560–2009).

The specimens used in the ring shear test were cut from the preconsolidated samples to have an outer diameter (D) of 10 cm, an inner diameter (d) of 6 cm(d/D = 0.6), and a height of 2 cm (Fig. 3.7).

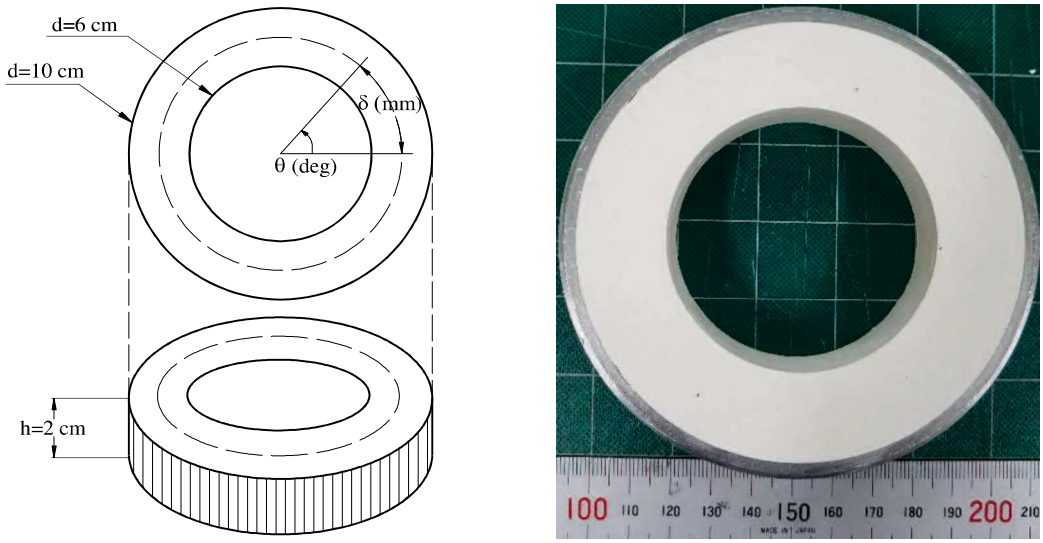

Figure 3.7 Size of annular intact specimen used in ring shear apparatus

Ring-shaped specimens may cause the non-uniformity of strain and shear stress during shearing in the ring shear apparatus, especially specimens with a low ratio of inner diameter to outer diameter. This effect can be reduced by decreasing the outer diameter, but will lead to an increase in wall friction. The increase of this ratio can minimize the non-uniformity. However, when this ratio is increased, it requires a large torque to shear. According to ASTM 6467, the ratio of the inside diameter to the outside diameter of the annular specimen should not be less than 0.6, the inside diameter should not be less than 5 cm, and the height of the specimen before shearing should not be less than 5 mm. The maximum particle size is limited to 10% of the initial specimen height. The feature of ring-shear devices and ring-shaped specimens are presented in Table 3.2. Generally, the size of the specimen will more or less affect the shear strength of the soil. Wu et al. (2008) and Moayed et al. (2017) reported that the peak strength decreased with the increase in the specimen size in the direct shear test. However, the residual strength is almost

independent of the specimen size (Moayed et al., 2017). Therefore, the use of small specimens with an outer diameter of 10 cm, an inner diameter of 6 cm, and a height of 2 cm, has no effect on the residual strength.

Table 3.2 Features of ring-shear devices and ring-shaped specimens

Authors	Type of apparatus	Affiliation	Outer diameter (D) cm	Inner diameter (d) cm	Ratio of d/D	Height of specimen (H) cm
La Gatta (1970)	Harvard Rotation Shear (Bromhead's type)	Harvard Univ	7.11	5.08	0.71	0.1-2.5
Bishop et al. (1971)	Bishop	Imperial College, London	15.24	10.16	0.67	1.91
Bromhead (1979)	Bromhead	Kingston Univ	10	7	0.7	0.5
Hungr and Morgenstern (1984)	Bishop	Alberta Univ	30	22	0.73	2
Gibo et al. (1987)	Bishop	Ryukyus Univ	10	6	0.6	3
Yatabe et al. (1991)	Bishop	Ehime Univ	16	10	0.63	2
Stark et al. (1993)	Bromhead	Illinois Univ	10	7	0.7	0.5
Stark et al. (1996)	Bromhead[a]	Illinois Univ	10	7	0.7	1
Tiwari et al. (2003)	Bishop	Niigata Univ	20	13	0.65	4.5
Sadrekarimi and Olson (2009)	Bromhead[b]	Illinois Univ	26.9	20.3	0.75	2.6
Sassa et al. (From 1984)	Bishop[c]	Kyoto Univ	14-35	10-27	0.71-0.77	5.2-15
Suzuki et al. (From 1997)	Bishop	Yamaguchi Univ	10	6	0.6	2

Note: Bishop's type: the shear surface is located at the mid-height of the specimen

Bromhead's type: the shear surface is located at or near the top of the specimen

[a] Constant volume ring shear apparatus

[b] The shear surface is located at the bottom of the specimen

[c] Specimens can be sheared under drained, undrained, static, or dynamic conditions

3.5. Test procedures

The specimens cut from the pre-consolidated samples were placed in the shear box and then reconsolidated under the desired effective normal stress until the end of the primary consolidation. The double drainage condition during consolidation and shearing in the shear box was allowed through the two porous stones located at the top and bottom of the specimen. The primary consolidation time was calculated based on the 3t method. In the case of over-consolidated conditions, the specimens were firstly consolidated to reach the primary consolidation, and then the normal stress was decreased to obtain the desired over-consolidation ratio (OCR). At the decreased effective normal stress, the specimens also were kept until the end of the dilatancy process before shearing at this stress.

In this study, the normal stress and the shear rate were controlled individually, and the shear stress was measured (strain-controlled). The net normal stress was calculated based on the measured frictional force in order to obtain the correct values for the strength parameters. The gap between the rings was kept closed during consolidation to prevent soil leakage and then left open during shearing to mitigate any influence exerted by the contact friction between the rings. Before shearing, the screw connecting the upper and lower rings was removed, and the suitable gap was set to 0.1 mm to minimize the influence of the soil leakage and the change in shear strength (Suzuki, 2008). The net normal stress was manually modified to be constant when the gap was set before shearing. However, the net normal stress was not always modified during shearing. Hence, the net normal stress fluctuated, but was correctly calculated by the continuous measurement of the frictional force.

The shear displacement, vertical displacement, shear force, and other data were recorded automatically during the shearing. The shear displacement rate was controlled by the shear controller. In the single-stage procedure, the shear displacement angle (the angle of rotation around the loading axis) was set to 450° as the maximal degree. This shear angle is equal to a shear displacement, δ, of about 314 mm. Here, δ is defined as an intermediate circular arc between the inner and outer rings. Skempton (1985) noted that the residual state of clay could be reached after a shear displacement of about 300 mm. Distilled water was poured into the water bath, but the water level was kept lower than the shear surface in order to avoid the penetration of free water from the water bath into the shear surface and to accurately determine the water content in the shear zone. The

shear box was then covered by a wet towel to prevent the sample from drying during testing.

The hyperbolic approximation method was applied to determine the residual shear strength from the test results. In this method, the relationship between $\theta/(\tau/\sigma_N)$ and shear displacement angle θ was plotted ($\theta>\theta_p$ for which θ_p is the shear displacement angle at the peak stress). Hyperbolic approximation parameters *a* and *b* are given by the segment, and the gradient of the straight line is fitted to the measurement of the relationship between $\theta/(\tau/\sigma_N)$ and θ by the least squares method. If the approximated hyperbola is in good agreement with the measurement, $(\tau/\sigma_N)_r$ is given as the inverse of *b*. The validity of the data fitting can be assessed using the correlation coefficient, R^2 (Fig. 3.8) The application of this method was based on the results of tests on kaolin and natural clays under various test conditions (Suzuki et al., 1997).

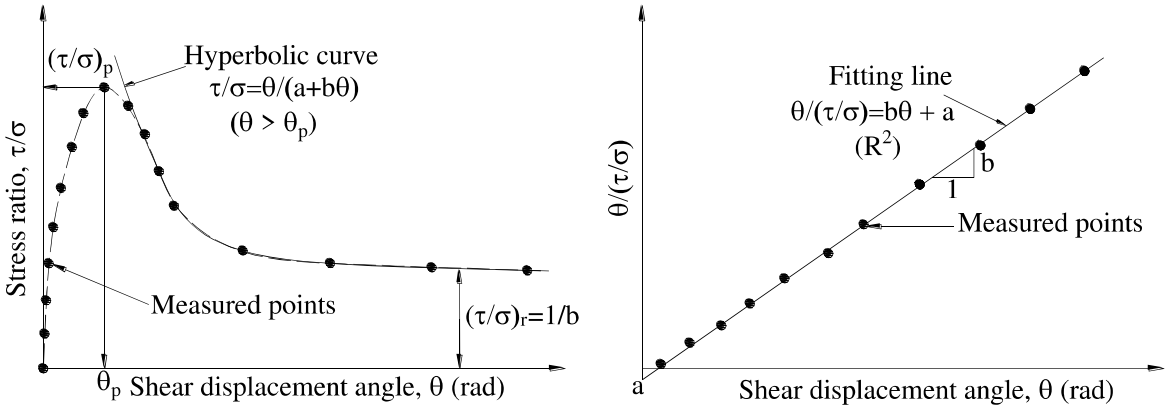

Figure 3.8 Schematic diagram for determining residual strength by hyperbolic curve approximation method (Suzuki et al., 1997)

CHAPTER 4. RATE EFFECT ON RESIDUAL SHEAR STRENGTH OF KAOLIN AND KAOLIN–BENTONITE MIXTURES

4.1. Introduction

The addition of bentonite to kaolin samples can easily change the physical properties of the mixture. Therefore, the use of kaolin–bentonite mixtures is controllable and useful in the investigation of the rate effect on the residual strength in relation to the physical properties. In this study, 10%, 20%, and 30% bentonite (dry weight) were mixed with 90%, 80%, and 70% kaolin, respectively. These samples are referred to herein as 10B, 20B, and 30B, respectively.

A set of kaolin and kaolin–bentonite mixture samples was prepared for ring shear tests by the pre-consolidation process in a large consolidation tank. The slurry and pre-consolidated samples were prepared as described in sub-section 3.4. The slurry samples were pre-consolidated in the consolidation tank under a consolidation pressure of 98 kPa until the primary consolidation was completed. The specimens to be used in the ring shear tests were cut from pre-consolidated samples with an outer diameter of 10 cm, an inner diameter of 6 cm, and a height of 2 cm. The specimens were placed in the shear box and then reconsolidated under a normal stress of 98 kPa (OCR=1).

To evaluate the effect of the shear rate on the residual strength, a single-stage shearing rate procedure was conducted on different specimens at shear rates ranging from 0.02 to 20 mm/min under an effective normal stress of 98 kPa. Suzuki et al. (2003) investigated the residual shear strength of kaolin and bentonite by means of a ring shear device. Their test results indicated that the residual shear strength of both kaolin and bentonite is almost independent of the effective normal stress at or above 98 kPa. Moreover, the rate effect is thought to be more evident at effective normal stress levels below 100 kPa (Stark and Hussain, 2010; Kimura et al., 2013; Gratchev and Sassa, 2015). Therefore, to evaluate the rate effect clearly, an effective normal stress of 98 kPa was applied in this study. The specimens were sheared continuously to the shear displacement of about 314 mm. After each test, the water content of the soil within the shear zone was measured immediately after removing the sheared specimen from the shear box. A thin layer of soil (a band), about 3 mm in thickness, was cut from the middle of the shear zone of the specimen and then divided into three parts to determine the water content. The

average water content was calculated as that of the soil within the shear zone. A summary of the test procedure is presented in Fig. 4.1.

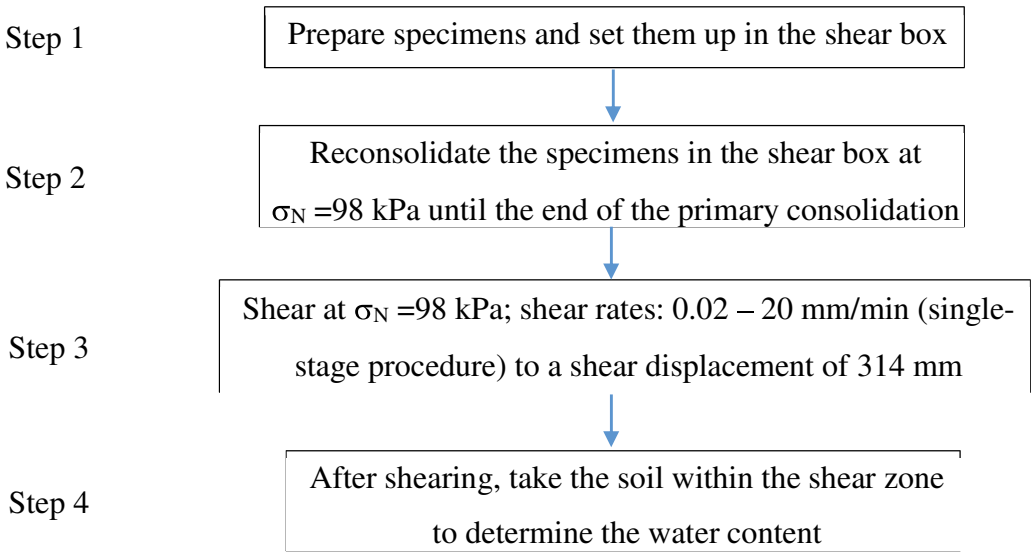

Figure 4.1 Test procedure for kaolin and kaolin-bentonite mixtures

4.2. Ring shear behaviour of kaolin and kaolin–bentonite mixtures

The ring shear test results for thirty-two specimens of kaolin and kaolin–bentonite mixtures are shown in Figs. 4.2(a)–(d) and Table 4.1. Figs. 4.2(a)–(d) show the relationship between shear stress τ and vertical displacement ν with respect to the shear displacement at different shear rates. From these figures, it is clear that the shear stress increases rapidly and reaches the peak when shear displacement δ is around 5–10 mm. The shear stress then decreases with further increases in shear displacement. All the samples reached their residual states after a shear displacement of approximately 300 mm. The vertical displacements of the mixture samples exhibited different types of behaviour from that of the kaolin sample, particularly at fast shear rates. This may lead to a difference in the shear strength behaviour of the kaolin and the mixture samples at fast shear rates.

Table 4.1 summarises the initial conditions of the specimens and the test results for the peak and residual strengths of the kaolin and the mixture samples. The experimental results of Tiwari and Marui (2003) revealed that the residual cohesion of kaolin and kaolin–bentonite mixtures was not equal to zero. However, this value was insignificant. Skempton (1964, 1985) noted that cohesion in the residual state can be very low. In addition, the test results of Di Maio and Fenelli (1994) showed that the residual

cohesion of kaolin and kaolin–bentonite mixtures was approximately zero. Thus, the residual cohesion was assumed to be zero in this study. Residual strength τ_r was then examined in terms of the stress ratio in the residual state, $(\tau/\sigma_N)_r$. The values for $(\tau/\sigma_N)_r$ in Table 4.1 were determined based on the hyperbolic curve approximation method (Suzuki et al., 1997). It should be noted that the stress ratio was calculated based on the total stress (σ_N) because the pore water pressure was not measured in this study. The relationship between the peak stress ratio and that in the residual state, $(\tau/\sigma_N)_r$, is presented in Fig. 4.3, along with the shear displacement rate. In general, the stress ratios for all specimens were found to be dependent on the magnitudes of the shear displacement rates.

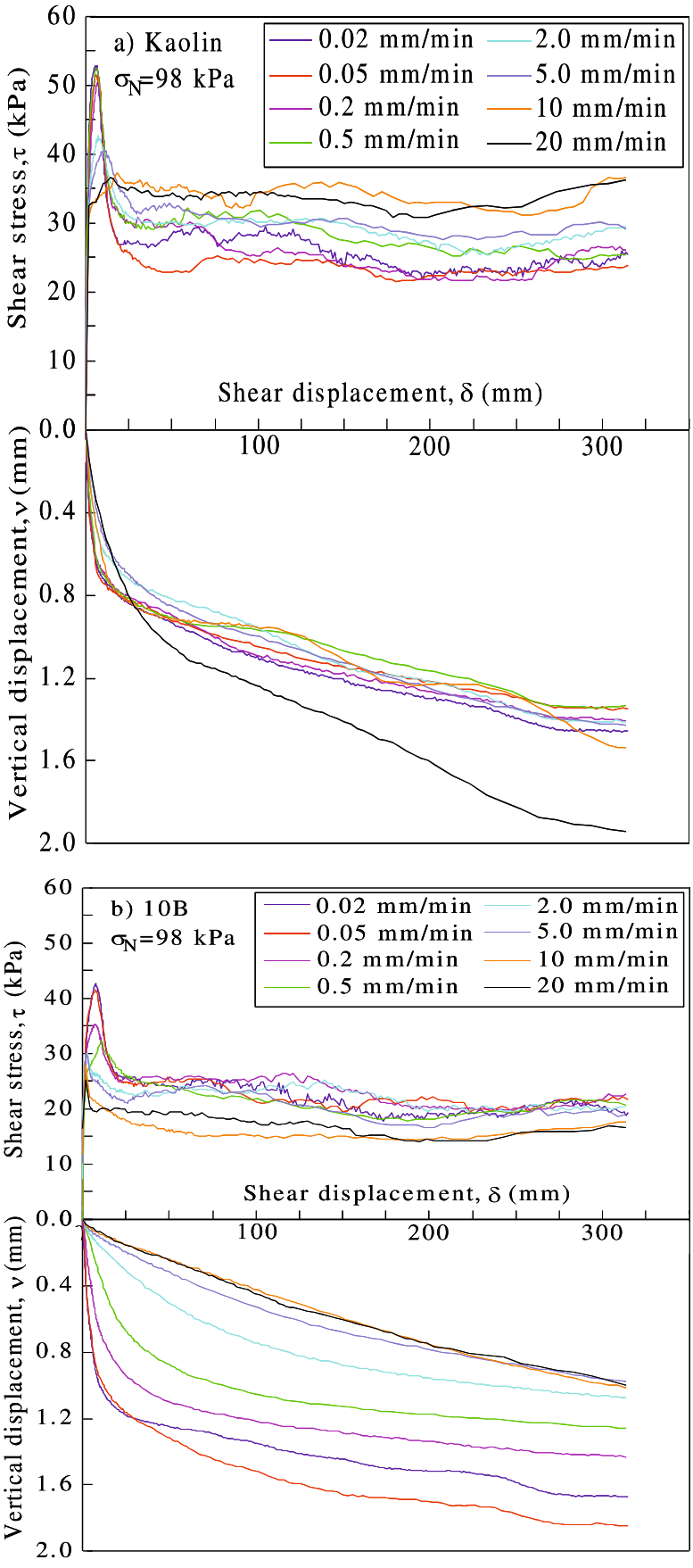
a) Kaolin
σN=98 kPa
0.02 mm/min
0.05 mm/min
0.2 mm/min
0.5 mm/min
2.0 mm/min
5.0 mm/min
10 mm/min
20 mm/min
Shear stress,τ (kPa)
Shear displacement, δ (mm)
Vertical displacement,ν (mm)
b) 10B
σN=98 kPa
0.02 mm/min
0.05 mm/min
0.2 mm/min
0.5 mm/min
2.0 mm/min
5.0 mm/min
10 mm/min
20 mm/min
Shear stress,τ (kPa)
Shear displacement, δ (mm)
Vertical displacement, ν (mm)

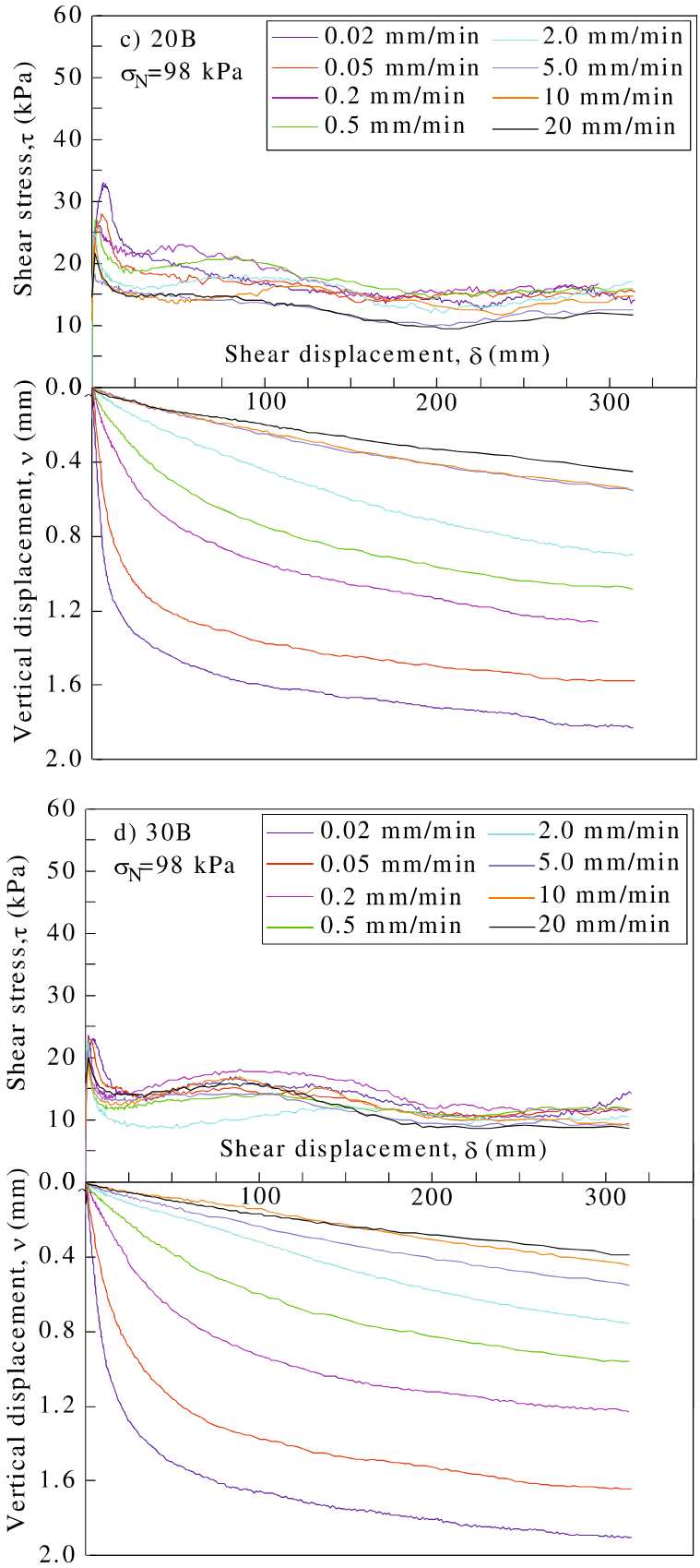

Figure 4.2 Relationship among shear stress, vertical displacement and shear displacement at different shear rates. a) Kaolin, b) 10B sample, c) 20B sample, and d) 30B sample

Table 4.1 Initial conditions of specimens, test cases, and test results

Test group	w_0 (%)	ρ_0 (g/cm^3)	S_{r0} (%)	e_0	σ_C (kPa)	σ_{N0} (kPa)	Shear rate (mm/min)	$(\tau/\sigma_N)_p$	$(\tau/\sigma_N)_r$	τ_p (kPa)	τ_r (kPa)
	66.4	1.547	95.5	1.845	98	98	0.02	0.536	0.235	52.8	23.2
	69.8	1.552	97.5	1.894	98	98	0.05	0.526	0.233	51.5	22.8
	68.8	1.551	96.9	1.879	98	98	0.2	0.512	0.238	50.2	23.4
	66.6	1.554	96.0	1.836	98	98	0.5	0.536	0.260	52.5	25.3
Kaolin	68.3	1.565	97.9	1.844	98	98	2	0.435	0.276	42.6	27.2
	69.5	1.563	98.4	1.868	98	98	5	0.414	0.289	40.5	28.4
	66.6	1.544	95.0	1.860	98	98	10	0.367	0.326	37.2	33.0
	71.7	1.540	97.3	1.949	98	98	20	0.376	0.340	36.7	33.5
	71.4	1.551	98.0	1.934	98	98	0.02	0.435	0.198	42.6	19.3
	73.7	1.556	99.6	1.966	98	98	0.05	0.421	0.207	41.4	20.4
	70.7	1.552	97.7	1.921	98	98	0.2	0.360	0.208	35.2	20.3
	70.7	1.564	98.9	1.899	98	98	0.5	0.326	0.200	32.2	19.6
	71.4	1.556	98.5	1.924	98	98	2	0.307	0.204	30.0	20.0
10B	70.7	1.564	98.9	1.900	98	98	5	0.304	0.188	29.7	18.5
	71.5	1.546	97.6	1.946	98	98	10	0.285	0.160	27.9	15.7
	72.8	1.544	98.0	1.971	98	98	20	0.259	0.153	25.3	15.0
	83.5	1.496	98.0	2.271	98	98	0.02	0.336	0.145	33.1	14.2
	85.2	1.492	98.3	2.311	98	98	0.05	0.285	0.149	27.9	14.6
	80.4	1.517	98.7	2.172	98	98	0.2	0.271	0.157	26.9	15.4
	80.2	1.515	98.5	2.172	98	98	0.5	0.275	0.154	27.1	15.2
20B	86.6	1.484	98.1	2.354	98	98	2	0.256	0.144	24.8	14.1
	82.6	1.497	97.8	2.253	98	98	5	0.246	0.137	23.9	13.6
	80.4	1.513	98.4	2.180	98	98	10	0.225	0.115	21.9	11.3
	80.1	1.509	97.9	2.183	98	98	20	0.223	0.107	21.6	10.4
	97.1	1.434	97.0	2.681	98	98	0.02	0.239	0.113	23.4	11.2
	101.4	1.419	97.0	2.801	98	98	0.05	0.236	0.113	23.1	11.1
	100.5	1.428	97.5	2.759	98	98	0.2	0.237	0.121	23.2	11.9
	105.6	1.417	98.0	2.884	98	98	0.5	0.235	0.117	22.9	11.4
	101.0	1.426	97.5	2.775	98	98	2	0.226	0.105	22.3	10.3
30B	97.4	1.435	97.2	2.684	98	98	5	0.214	0.094	21.0	9.3
	102.1	1.422	97.4	2.805	98	98	10	0.201	0.099	19.5	9.7
	97.9	1.432	97.1	2.724	98	98	20	0.205	0.087	20.0	8.5

w_0: Initial water content

ρ_0: Initial wet density

S_{r0}: Initial degree of saturation

σ_{N0}: Initial normal stress

σ_N: Normal stress

σ_C: Consolidation pressure

$(\tau/\sigma_N)_p$: Stress ratio at peak state; τ_p: Peak strength

$(\tau/\sigma_N)_r$: Stress ratio at residual state determined by hyperbolic curve approximation method

τ_r: Residual strength determined by hyperbolic curve approximation method

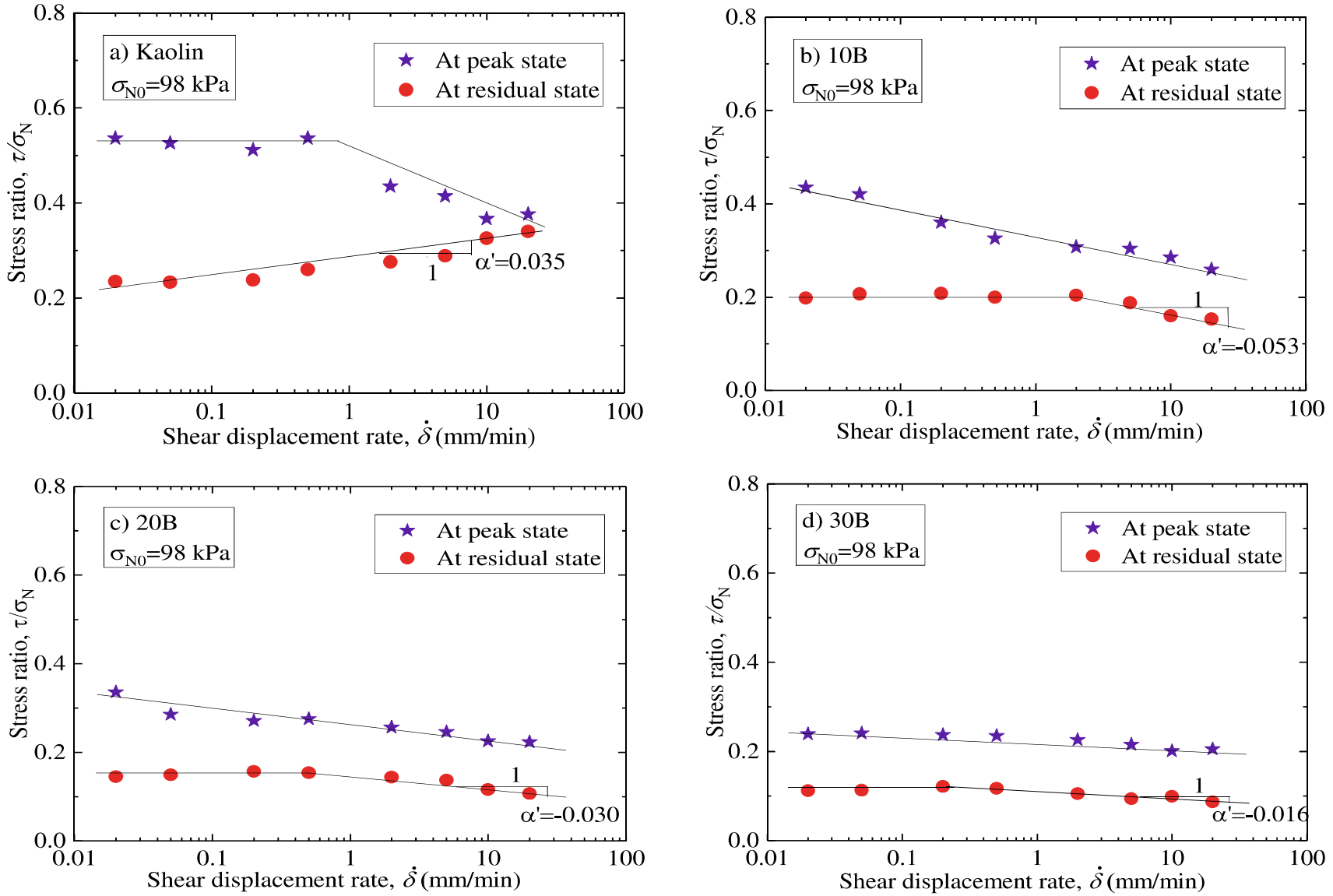

Figure 4.3 Relationship between stress ratio and shear displacement rate: a) Kaolin, b) 10B sample, c) 20B sample, and d) 30B sample.

4.3. Volume change of specimens during ring shearing

As mentioned above, the pore water pressure was not measured in the present study. The vertical displacements can be considered to reflect the characteristics of contraction or expansion of the soil and the structural changes within the shear zone because the specimens were kept almost saturated during testing. When a normally consolidated specimen is sheared, the platy particles of the sample around the shear surface tend to align themselves parallel to the shearing direction. This decreases the void ratio, which results in contractive behaviour (the vertical displacement is higher than zero). The test results show that all of the samples exhibited this contractive behaviour during shearing (Figs. 4.2(a)–(d)). Fig. 4.2(a) reveals that, for all shear rates, the vertical displacement of kaolin decreases significantly in the first 10 to 25 mm of shear displacement. In the drained test, the excess pore pressure was not generated. Thus, the volume of the specimen was changed. The fast reduction in vertical displacement was caused by the fast dissipation of excess pore water inside the kaolin sample. In other words, the volume change due to the dissipation of pore water is almost complete after a small shear displacement. The volume change after the first 10 to 25 mm of shear displacement is mostly due to the loss of soil through the gap. Fig. 4.4 shows the relationship between the final vertical displacement and the shear displacement rates for all of the samples. It can be seen that the final vertical displacement of the kaolin sample tends to increase with the shear displacement rate, especially at fast shear rates. The increase in vertical displacement with the shear displacement rate is mainly attributable to the extrusion of soil through the gap between the two halves of the shear box. Bromhead (2004) stated that more rapid shear rates will result in more extrusion of the soil in both the Bishop-type and the Bromhead-type ring shear devices. In contrast, the final vertical displacement of the mixture samples is small at the fast shear rates and tends to decrease with an increasing shear displacement rate. This indicates that higher shear rates will lead to less contraction in the mixture samples. In addition, Figs. 4.2(b)–(d) show that the relation between the vertical displacement and the shear displacement at low shear rates is apparently different from that at high shear rates (it is almost linear at high shear rates, i.e., >2 mm/min, but curvilinear at slow shear rates). In contrast, for kaolin, the relationship between the vertical displacement and the shear displacement is the same (i.e., curvilinear) for all the shear rates, as shown in Fig. 4.2(a). This is because

of the significant difference in permeability between the kaolin and the mixture samples. For example, for the sample with 10% bentonite, the permeability coefficient was lower than that of the kaolin sample by a factor of about 10 (Table 4.1). As the permeability coefficient of the mixture samples was very low, the consolidation (dissipation of excess pore water) was insignificant during fast shearing. Therefore, the vertical displacement of the mixture samples under fast shear rates was smaller than that under slow shear rates. In this case, the vertical displacement under fast shearing is mainly caused by the loss of soil through the gap. However, a comparison with the vertical displacement of the kaolin sample reveals that under fast shear rates, higher plasticity soil will result in reduced soil extrusion.

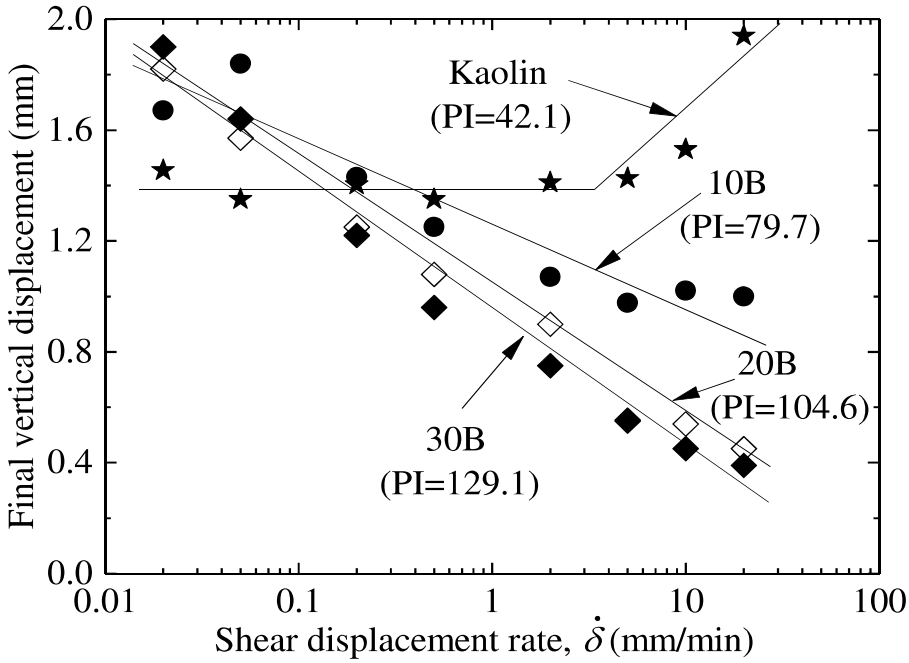

Figure 4.4 Plot of final vertical displacement and shear displacement rates

Since the specimens were kept almost saturated during shearing, the water content of the soil will reflect the void ratio and the density of the sheared specimen. The higher water content reflects a higher void ratio and less contraction of the specimens. Fig. 4.5 illustrates the relationship between the water content of the specimens within the shear surface after the shear test and the shear displacement rate. As seen in this figure, although the water content within the shear zone of the mixture samples tends to increase with an increasing shear displacement rate (especially at fast shear rates), it remains almost constant in the case of kaolin. This is consistent with the behaviour of the vertical displacement shown in Figs. 4.2 and 4.4. Accordingly, changes in the water content

within the shear zone after shearing may reflect changes in the vertical displacement as the shear displacement rates increase. The higher water contents within the shear zone of the mixture samples exhibit lower values of vertical displacements at fast shear rates. In addition, the higher water contents after shearing may lead to lower residual strength (Chowdhury et al., 1977; Lupini et al., 1981; Tiwari and Marui, 2003).

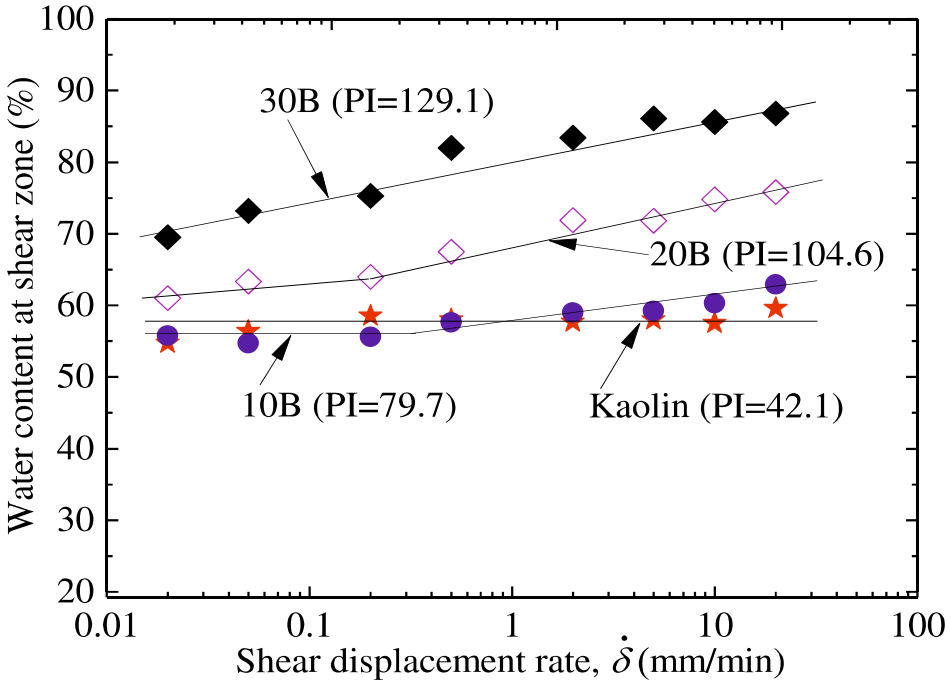

Figure 4.5 Relationship between water content measured at shear zone after shear test and shear displacement rate

4.4. Rate effect on ring shear behaviour

Fig. 4.3(a) shows that, although the peak stress ratio for kaolin is almost constant in the range of 0.02 to 0.5 mm/min and decreases above 0.5 mm/min, the residual stress ratio increases linearly with respect to the logarithm of the shear rate over the range of 0.02 to 20 mm/min. At low shear rates, the drained condition can be achieved even at the peak state, so the change in the peak stress ratio with respect to the shear rate under slow shear rates is insignificant. However, the fully drained condition cannot be obtained at the peak state under fast shear rates. Hence, if the specimens were normally consolidated, its peak stress ratio would decrease with an increasing shear rate because of the delayed dissipation of excess pore water pressure. The peak strength of kaolin at shear rates exceeding 0.5 mm/min could be expressed as partially drained strength. The peak stress

ratio of the kaolin sample is consistent with the results of Suzuki et al. (2001, 2009). The increase in residual strength with respect to the shear rate can be attributed to the change from the sliding mode to turbulent shear mode (structural change) as the shear rate increases (e.g., Skempton, 1985; Tika et al., 1996; Bhat, 2013). In addition, soil extrusion via the clearance between the upper and lower rings may also cause the residual strength to increase. As mentioned above, the loss of soil through this gap tends to increase with the shear rate in the kaolin sample. The greater the amount of soil loss, the more the amount of new soil that enters the shear zone. This phenomenon serves to decrease the degree of orientation among the soil particles inside the shear zone, which results in higher residual strength. The effect of soil extrusion on the "fast" residual strength can be referred to as the mechanical effect. Thus, the gap between the lower and upper parts of the ring shear box should be as small as possible.

In addition to the structural change and soil extrusion, the increase in the fast residual strength of kaolin may also be attributed to the shear viscosity of the soil (Tika et al., 1996; Lemos, 2003; Carrubba and Colonna, 2006). Furthermore, Van Asch et al. (2007), Mahajam and Budhu (2008), and Massey et al. (2013) noted that the shear viscosity should be considered in order to understand the post-failure behaviour. The shear viscosity (viscosity) is the resistance of fluids to flow. In general, it is calculated as the ratio of the shear stress to the shear velocity. The viscosity of soil can have an effect on the shear stress when increasing the shear rates (shear viscosity effect). However, the viscosity of the kaolin sample in this study may be low. Iannicelli and Millman (1966) found that the viscosity of a kaolin–water suspension consisting of 50% solids and a montmorillonite content of less than 5% was very low. Thus, the effect of shear viscosity on the residual strength of kaolin is insignificant. Therefore, the change in the shear mode and the soil extrusion seem to be the primary mechanisms behind the increase in the fast residual strength of kaolin.

Fig. 4.6 shows the relationship between the shear displacement rate and the residual stress ratio of kaolin samples in previous investigations using ring shear tests (Tika et al., 1996; Suzuki et al., 2001, 2007, 2017; Bhat, 2013; Scaringi and Di Maio, 2016). As this figure shows, the positive rate effect on the residual strength of kaolin observed in the present study is in good agreement with the results of previous studies.

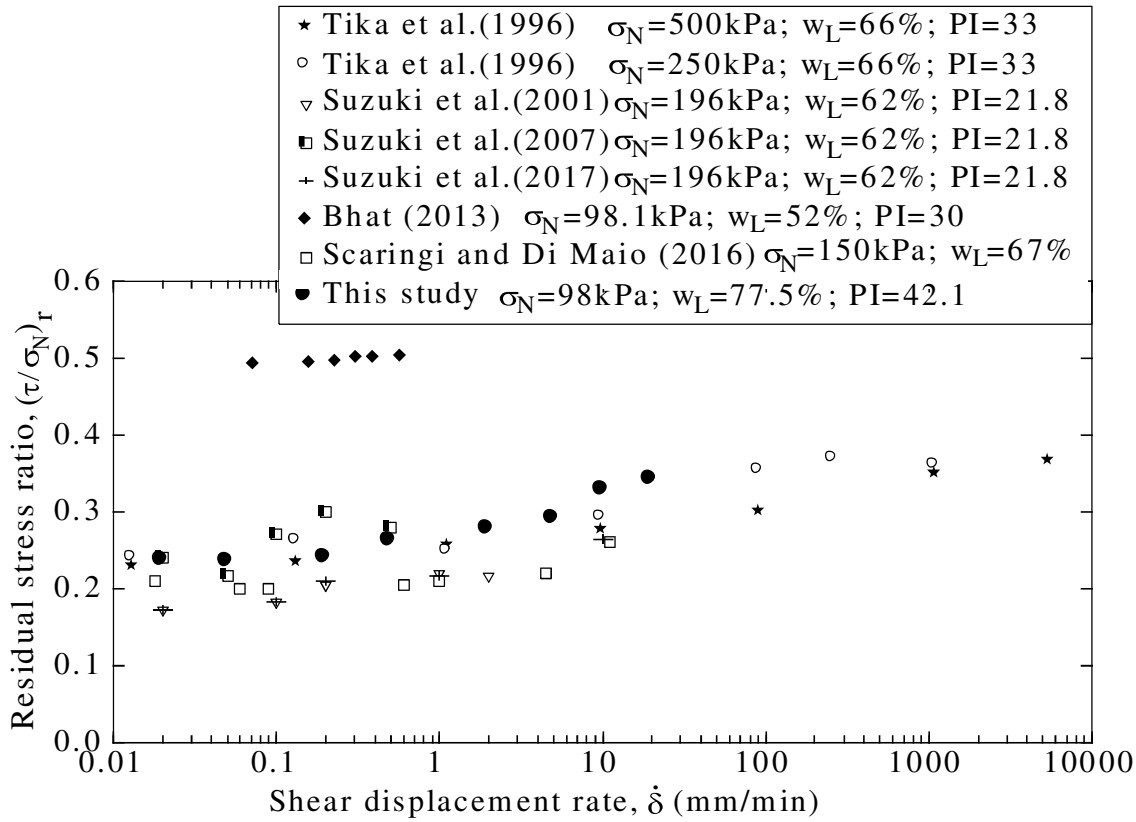

Figure 4.6 Relationship between residual stress ratio and shear rate for kaolin sample

Next, Figs. 4.3(b)–(d) show that the peak stress ratios of the mixture samples decrease linearly as the logarithm of the shear displacement rate increases from 0.02 to 20 mm/min, whereas the residual stress ratios are independent of the slow shear rates before decreasing as the shear rate increases. Unlike kaolin, the permeability of the mixture samples was quite low, so the fully drained condition could not be reached at the peak state, even at low shear rates. This phenomenon led to a decrease in the peak stress ratio as the shear displacement rate increased. In this case, the peak strength of the mixture samples could be considered as partially drained strength. However, different from the peak state, the fully drained condition could be attained at the residual state at low shear rates, meaning that the excess pore water pressure generated inside the specimens did not substantially change the effective normal stress on the shear surface. This leads to the neutral rate effect on the residual strength of the mixture samples in the low range of shear rates. Toyota et al. (2009) also indicated that the residual strength of high plasticity soils was independent of shear rates ranging from 0.0002 to 0.2 mm/min. At fast shear rates, although the presence of bentonite is insignificant in terms of changing the clay fraction, the trend in the rate effect on the residual strength changes from positive to negative (as

shown in Fig. 4.7). In other words, the rate dependency of the residual strength of soil can be changed by the plasticity index and permeability. This indicates that, in addition to the clay content, the presence of smectite minerals may be influential in controlling the rate effect. This phenomenon has also been observed in sand–bentonite mixtures (Saito et al., 2006, 2007). As was mentioned in the Introduction, there are various reasons for the reduction of fast residual strength. However, in this study, the water in the water bath was kept below the shear surface, so that no penetration of free water could cause a negative rate effect. The reduction in fast residual strength may also be caused by an increase in finer particles in the shear zone due to the breakage of angular particles (Fukuoka and Sassa, 1991) or larger particles being moved out of the shear zone (Saito et al., 2007; Li et al., 2017). Nevertheless, as the samples in this study were fine-grained cohesive soils, these explanations are not applicable.

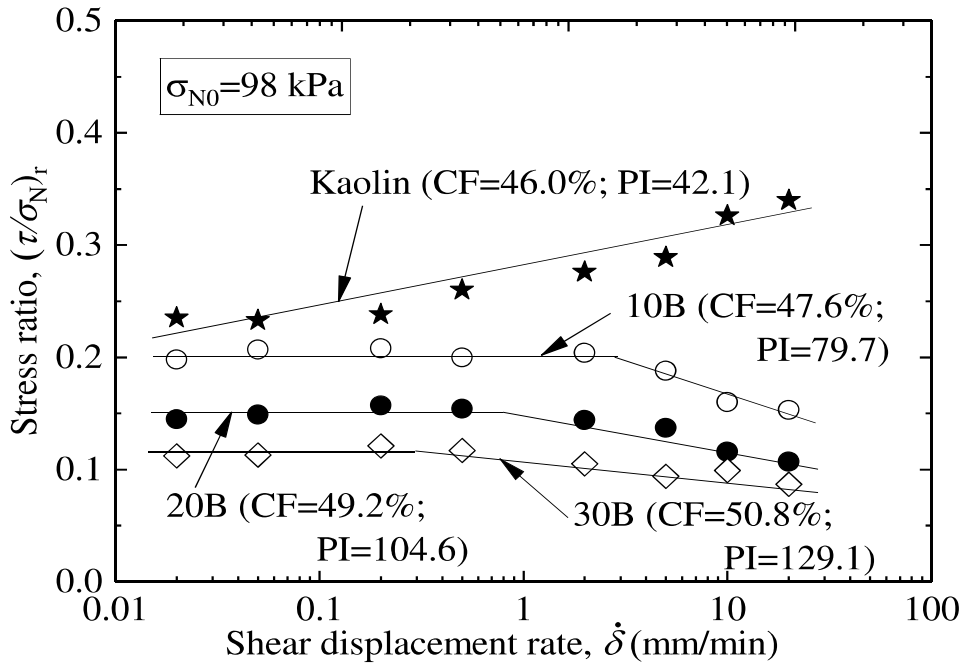

Figure 4.7 Relationship between stress ratio at residual state and shear rates

Gratchev and Sassa (2015) conducted a multi-stage shearing rate procedure on clay and measured the pore water pressure build-up during shearing. The test results showed an increase in residual strength with a decreasing shear displacement rate. They believed that this negative rate effect was related to the rate of broken bond recovery and particle rebound and that the excess pore water pressure did not affect the residual strength. Nevertheless, the shearing time was only 3 minutes, which was not sufficient

for the excess pore water pressure to equalize inside the specimen. Thus, the measured excess pore water pressure might not reflect the actual value. More recently, following experiments using a single-stage procedure, Li et al. (2017) concluded that the excess pore water pressure did not cause a negative rate effect on the residual strength of silty sand. The high permeability of silty sand causes the effect of the excess pore water pressure on the fast residual strength to be insignificant. However, in the present study, the presence of smectite minerals in the kaolin–bentonite mixtures led to a significant decrease in the permeability coefficient (k) and an increase in the plasticity index (PI) (see value in Table 1). In addition, as mentioned above, the behaviour of the vertical displacement of the mixture samples is totally different from that of kaolin, especially at fast shear rates. Thus, the negative rate effect on the residual strength of the mixture samples was probably caused by the development of excess pore water pressure during fast shearing. The delayed dissipation of pore water pressure and the shear viscosity may simultaneously affect the residual strength of soil under fast shear rates. This delayed dissipation will result in a decrease in the fast residual strength, whereas the shear viscosity effect may lead to an increase in the fast residual strength. However, in the single-stage procedure, the effect of pore water pressure on the residual strength of the mixture samples may dominate that of the shear viscosity at fast shear rates. Thus, the residual strength of the mixture samples at fast shear rates could be referred to as partially drained strength.

The effect of the excess pore water pressure generated during fast and slow shearing on the peak and residual strength is depicted in Figs. 4.8(a)–(c). During slow shearing, the excess pore water is generated and instantly dissipated in both the peak and residual states. Hence, the excess pore water pressure does not substantially change the effective normal stress acting on the shear surface. Therefore, the peak and residual stress ratios are almost constant at slow shear rates (points A and B in Fig. 4.8). In contrast, during fast shearing, the excess pore water does not have enough time to dissipate, even in the residual state in the case of the mixture samples. This action decreases the effective normal stress and results in a decrease in the peak and residual strength (points A′ and B′ in Fig. 4.8).

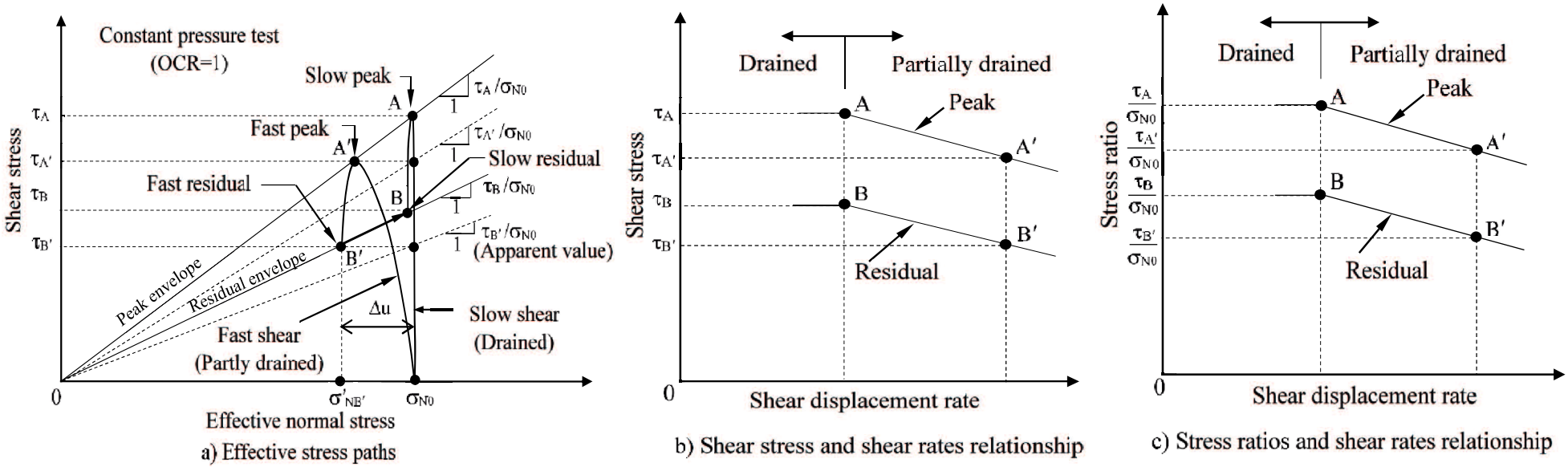

Figure 4.8 Schematic diagram of changes in effective stress paths, shear stress, and stress ratios during slow and fast shearing

The drained shear behaviour and partially drained shear behaviour observed in ring shear tests are consistent with those observed in triaxial tests and direct shear tests. In the triaxial tests, the test results of Asaoka et al. (1994) indicated that, while the undrained strength increased, the partially drained strength decreased as the strain rates increased. Quinn and Brown (2011) investigated the shear strength of kaolin over a wide range of strain rates in the triaxial tests and reported that the shear strength was not dependent on the low strain rates (drained strength); it decreased at intermediate strain rates (partially drained) and increased at fast strain rates (undrained). In the direct shear tests, Thermann et al. (2006) also demonstrated three types of shear strength behaviour with the increasing shear rates. In this study, the drainage conditions inside the specimen may change because of the decrease in permeability. It should be emphasized that the change in the drainage conditions of the specimens has not been discussed in previous studies on the rate effect. The negative rate effect from the delayed dissipation of pore water pressure may be apparent, but it is not a true physical mechanism. In other words, it does not produce any change in the internal friction angle in terms of effective stress.

4.5. Rate effect coefficient

To quantitatively evaluate the rate effect on the residual strength of soil, the rate effect coefficient (α') is proposed:

$$\alpha' = \frac{d\left(\tau/\sigma_N\right)_r}{d(\log\dot{\delta})} \tag{4.1}$$

If $\alpha' < 0$, the rate effect is negative; if $\alpha' > 0$, the rate effect is positive; if $\alpha' = 0$, the residual strength is independent of the shear displacement rate (neutral rate effect). The magnitude of α' reflects the level of rate dependency of the residual strength. The rate effect coefficients of the kaolin and mixture samples in this study are shown in Figs. 4.3(a)–(d). The negative rate effect coefficients are -0.053, -0.030, and -0.016 for the 10B, 20B, and 30B samples, respectively. This shows that the absolute value of the negative rate effect coefficient decreases as the bentonite content increases. In other words, the magnitude of the negative rate effect decreases as the plasticity index increases.

Table 4.2 Previous results showing negative rate effect on residual strength

Type of soil	Liquid limit (%)	Plasticity index	Clay fraction (%)	Normal stress (kPa)	Shear rate (mm/min)	$(\tau/\sigma_N)_r$	α'	Reference
Clayey siltstone	39	17	10	200	10 100 400 830	0.537 0.379 0.152 0.178	-0.232	Tika et al. (1996)
Clayey siltstone	39	18	20	200	10 100 400 700	0.430 0.270 0.160 0.150	-0.159	
Clayey siltstone	44	21	8	200	10 100 460 870 2150 5600	0.396 0.275 0.182 0.137 0.130 0.148	-0.115	
Clayey siltstone	44	24	25	230	11 100 400 2000 5400	0.347 0.254 0.144 0.160 0.150	-0.076	
Clayey siltstone	53	26	37	240	0.0462 1.0689 9.5 95 2600	0.181 0.159 0.146 0.149 0.080	-0.018	
Claystone	55	28	39	200	0.01 10 100	0.181 0.170 0.140	-0.009	
Claystone	62	36	52	210	0.05 0.9237 10 100 400 6000	0.164 0.161 0.140 0.121 0.124 0.082	-0.016	
Mauritius	36	6	11	220	12 360 1000 2000	0.710 0.658 0.319 0.282	-0.191	
Mt Ontake B	63	13	14	250	100 1000 2500 6000	0.603 0.556 0.550 0.450	-0.069	
Fiji B	85	22	55	200	0.015 1100 2400	0.232 0.205 0.153	-0.012	
Lower Cromer till	22	10	14	220	0.0001 0.014 3.6 133	0.600 0.552 0.534 0.354	-0.037	

Type of soil	Liquid limit (%)	Plasticity index	Clay fraction (%)	Normal stress (kPa)	Shear rate (mm/min)	$(\tau/\sigma_N)_r$	α'	Reference
Lower Cromer till	26	14	22	220	0.025 0.133 133 1200	0.564 0.564 0.253 0.338	-0.04	Tika et al. (1996)
Cowden till	35	19	32	200	0.0089 0.01 0.1 1 10 140	0.540 0.520 0.510 0.530 0.600 0.350	-0.05	
Landslide soils	86	21	-	55.9	0.002 0.02 0.2 2	0.370 0.300 0.220 0.200	-0.06	Nakamura and Shimizu (1978)
Sand+10% bentonite	50.8	20.3	20	100	60 600	0.828 0.682	-0.145	Saito et al. (2007)
Sand+20% bentonite	64.3	37.8	28	100	0.6 6 60 600	0.680 0.647 0.230 0.250	-0.225	
Pepper shale	70.5	49	-	100	0.0056 0.056	0.152 0.141	-0.012	La Gatta (1970)
Kaolin	50.3	28.3	100	200	3.6 36 360	0.310 0.250 0.280	-0.016	Li et al. (2013b)
80% kaolin+ 20% beads	43.8	24	80	200	3.6 36 360	0.450 0.430 0.420	-0.016	
60% kaolin+ 40% beads	33.8	17.5	60	200	3.6 36 360	0.480 0.450 0.420	-0.030	
50% kaolin+ 50% beads	27.2	12.3	50	200	3.6 36 360	0.490 0.460 0.380	-0.055	
40% kaolin+ 60% beads	22.8	9.3	40	200	3.6 36 360	0.520 0.460 0.380	-0.07	
Brown clay	88.2	54.5	19	100	12 60 120 180 240 270 300	0.367 0.337 0.316 0.301 0.297 0.292 0.292	-0.055	Gratchev and Sassa (2015)

Table 4.3. Previous results showing positive rate effect on residual strength

Type of soil	Liquid limit (%)	Plasticity index	Clay fraction (%)	Normal stress (kPa)	Shear rate (mm/min)	$(\tau/\sigma_N)_r$	α'	Reference
Kaolin	66	33	74	250	0.0131 0.1328 1.1248 9.9349 90.831 260	0.238 0.260 0.247 0.291 0.352 0.367	0.031	Tika et al. (1996)
Kaolin	62	21.8	35.3	196	-	-	0.030	Suzuki et al. (2001)
Mudstone	63	25.5	24		-	-	0.139	
Kaolin	62	21.8	35.3	196	0.02 0.1 0.2 1 2 10	0.172 0.183 0.205 0.220 0.217 0.264	0.032	Suzuki et al. (2009)
Shimajiri mudstone	91.4	61.4	55.5		0.02 0.05 0.1 0.2	0.140 0.160 0.197 0.205	0.070	
Yuya A	89	53.1	87		0.02 0.1 0.2 0.5 1	0.368 0.368 0.385 0.400 0.415	0.029	
Yuya B	43.3	19.9	32		0.02 0.076 0.1 0.2 0.4	0.483 0.490 0.487 0.509 0.524	0.032	
Yuya C	49	28.6	34.5		0.02 0.05 0.1 0.2 0.5	0.467 0.464 0.475 0.489 0.504	0.029	
Kaolin	52	30	26	98.1	0.073 0.162 0.233 0.313 0.398 0.586	0.491 0.492 0.495 0.499 0.500 0.502	0.013	Bhat (2013)
Kaolin	62	21.8	35.3	196	0.02 0.1 0.2 1 10	0.173 0.183 0.210 0.217 0.264	0.033	Suzuki et al. (2017)
Kaolin	67	-	74	150	0.09 0.6 1 4.5 11.1	0.200 0.205 0.210 0.220 0.060	0.042	Scaringi and Di Maio (2016)
					0.073 0.162	0.457 0.457		

Type of soil	Liquid limit (%)	Plasticity index	Clay fraction (%)	Normal stress (kPa)	Shear rate (mm/min)	$(\tau/\sigma_N)_r$	α'	Reference
Krishnabhir landslide	34.1	13.4	21	98.1	0.233 0.313 0.398 0.586	0.458 0.461 0.465 0.469	0.023	Bhat and Yatabe (2015)
Shikoku landslide	47.5	16.3	20		0.073 0.162 0.233 0.313 0.398 0.586	0.254 0.254 0.255 0.258 0.266 0.275	0.039	
Toyooka-kita landslide	96.5	37.5	24		0.073 0.162 0.233 0.313 0.398 0.586	0.091 0.090 0.095 0.100 0.109 0.121	0.055	
80% beads +20%kaolin	13.4	2.3	20	200	3.6 36 360	0.580 0.610 0.610	0.012	Li et al. (2013b)
Zentoku	39.2	18.7	2.7	98	-	-	0.015	Yatabe et al.(1991)
Sagayama II	42.5	15.7	25	98	-	-	0.028	
Utsugi	26.3	11.6	7.5	98	-	-	0.020	

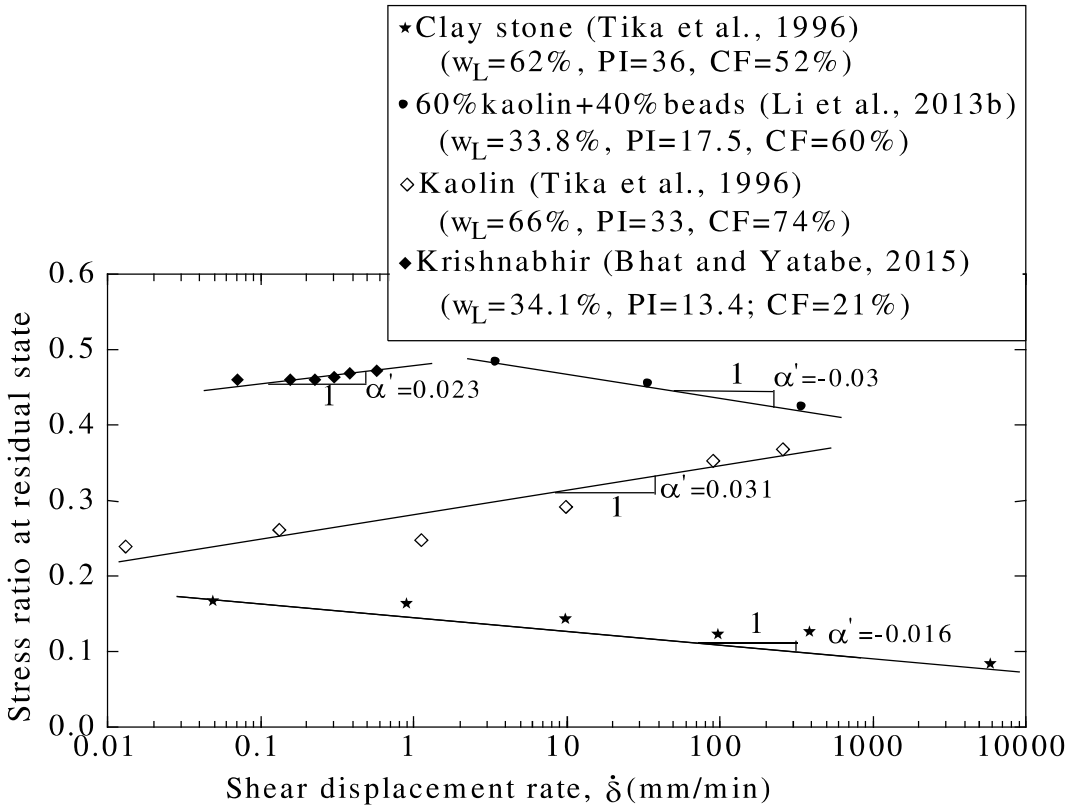

Figure 4.9 Rate effect coefficient in some previous studies

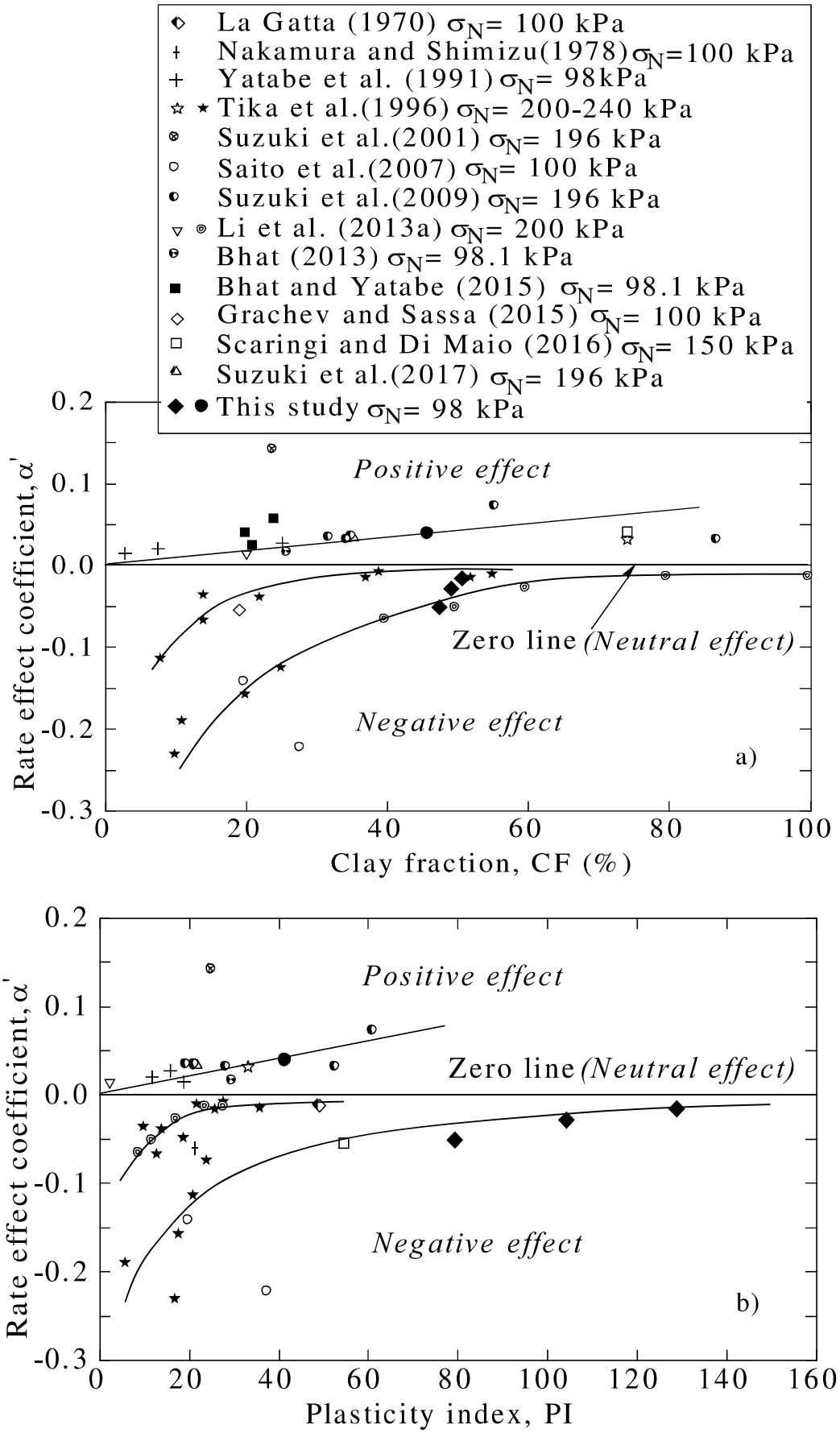

Figure 4.10 Relationships between: a) Rate effect coefficient and clay fraction and (b) Rate effect coefficient and plasticity index

Suzuki et al. (2001, 2009) stated that there was a correlation among the positive rate effect coefficient, the clay fraction, and the plasticity index. However, their data were limited. In this study, data used to establish the relationships among the rate effect coefficient, the clay fraction, and the plasticity index were collected from many previous studies (the details are summarised in Tables 4.2 and 4.3). As the magnitude of the normal stress affected the level of the rate effect (Stark and Hussain, 2010; Kimura et al., 2013; Gratchev and Sassa, 2015), the data in these tables were selected to correspond to effective normal stress levels in the range of 55.9 to 250 kPa. Fig. 4.10 shows some examples of how to determine α' based on the collected data. The relationships between α' and the clay fraction and α' and the plasticity index are plotted in Figs. 4.10(a) and (b), respectively. Although the positive rate effect coefficient seems to increase with the increasing clay fraction and plasticity index, the absolute value of the negative rate effect coefficient decreases with the clay fraction and plasticity index. In other words, the coefficient of the rate effect on the residual strength of soil depends on some physical properties of the soil, such as the clay fraction and plasticity index. In addition, Figs. 4.10(a) and (b) suggest that the positive and negative rate effect coefficients observed in this study are consistent with the results of previous investigations. In particular, Fig. 4.10(b) shows the coefficient of negative rate effect on the residual strength of high-plasticity soil which was not investigated in the literature.

4.6. Summary

In this chapter, ring shear tests were conducted on thirty-two samples of kaolin and kaolin-bentonite mixtures with shear displacement rates ranging from 0.02 mm/min to 20 mm/min under the normal stress of 98 kPa. The test results have been analysed and compared with the previous research results. The results of this chapter can be summarised as follows:

1. The relationship between the vertical displacement and the shear displacement of the kaolin sample is curved at all shear rates in the range from 0.02 to 20 mm/min, whereas it is almost linear in the cases of the kaolin-bentonite mixtures at fast shear rates. This difference may lead to the difference in the shear strength of the kaolin and the kaolin-bentonite mixtures, especially at fast shear rates.

2. The vertical displacement of the kaolin samples tends to increase with the increasing shear rates. This shows that the soil extrusion through the gap between the upper and lower parts may occur significantly at fast shear rates. In contrast, the vertical displacement of the mixture samples decreases as the shear rate increases. The difference in the vertical

displacement between the kaolin and the mixture samples may affect the rate dependency of the residual strength.

3. The water content of the soil within the shear zone of the kaolin sample is independent of the shear rates in the range used. In contrast, the water content of the soil within the shear zone of the kaolin-bentonite mixtures tends to increase as the shear rates increase.

4. The peak strength of the kaolin is independent of the slow shear rates whereas it decreases as the shear rates exceed 0.5 mm/min. In contrast, the peak strength of the mixture samples decreases as the shear rates increase from 0.02 to 20 mm/min.

5. The residual strength of the kaolin sample increases linearly with the logarithm of the shear rates (positive rate effect). However, after adding bentonite to the kaolin sample, the residual strength of the kaolin-bentonite mixtures decreases with the increasing shear rates (negative rate effect). This indicates that the bentonite significantly affects not only the residual strength but also its rate dependency.

6. The negative rate effects on both the peak strength and the residual strength are attributed to the delayed dissipation of the excess pore water pressure. In addition, the negative rate effect on the residual strength of the mixture samples can be related to the increasing water content within the shear zone after shearing with increasing shear rates.

7. The positive rate effect on the residual strength of kaolin clay can be caused by the structural changes and accelerated by the soil extrusion through the gap between the upper and lower parts of the shear box.

8. The relationship between the coefficient of the rate effect on the residual strength (α') and some soil physical properties (clay fraction and plasticity index) was established. The results show that the magnitude of the positive rate effect increases, while the negative rate effect decreases as the clay fraction and the plasticity index increase.

CHAPTER 5. RATE EFFECT ON RESIDUAL INTERFACE STRENGTH BETWEEN KAOLIN AND KAOLIN-BENTONITE MIXTURES

5.1. Introduction

In landslides, a shear zone often develops along the bedding plane, discontinuous plane or the interface between two soil layers. Tiwari et al. (2005) and Tiwari (2007) showed that the shearing surface of all landslides in Niigata Prefecture is located at the contact between highly weathered and less weathered Tertiary mudstones. The main clay minerals in the Tertiary mudstone are smectite and kaolinite. Many landslides and slope failures often occur in the Tertiary mudstone area due to the presence of expansive minerals. Tiwari et al. (2005) and Tiwari (2007) showed that smectite minerals (expansive) play an important role in triggering landslides along the bedding planes in this area.

Recently, the residual interface strength at the contacts between clay/cemented clay (Suzuki et al., 2017), soil/soil, soil/rock, and rock/rock (Scaringi et al., 2018) has been investigated. To examine the rate dependency of the residual interface strength between two different soil layers, the sample assembly of kaolin and kaolin-bentonite mixtures will be used in this chapter. The second aim of this investigation is to clarify the effect of smectite minerals in the contact surface on the rate dependency of the residual interface strength. A series of combined specimens, comprising one kaolin (K) layer and one kaolin-bentonite mixture layer, was sheared at different shear rates in ring shearing. The kaolin-bentonite mixture layers were denoted as 10B, 20B, and 30B. These notations were defined in Chapter 4. Effective normal stress levels from 98 kPa to 294 kPa and shear rates from 0.02 mm/min to 20 mm/min were applied.

The combined specimens consisted of two halves, each with a height of 1 cm (Fig. 5.1). To ensure that the shear surface would lie between the two halves of the shear box after reconsolidation in the shear box, the pre-consolidated samples were consolidated in the consolidation tank at a normal stress 1.5 times higher than the shear normal stress (equal to OCR=1.5). The combined specimens are denoted as K-10B, K-20B, and K-30B. The former letter in each notation represents the upper layer and the latter one represents the lower layer. The combined specimen with two halves of the kaolin layer (K-K) was also investigated.

The multi-stage procedure for increasing the shear rate from 0.02 mm/min to 20 mm/min was applied to investigate the rate dependency of the residual interface strength. The test results of Suzuki et al. (2017) showed that the residual strength of the combined specimens was reached after a shear displacement of about 60 mm. In addition, Anderson and Hammoud (1988) indicated that in the multi-stage procedure for doubling the normal stress, shear

displacement of about 30 mm was sufficient to obtain the residual strength of kaolin clay. Stark and Eid (1993) also noted that pre-cut specimens required about 15 mm of shear displacement to obtain the residual strength of claystone in the Bromhead-type ring shear device. Therefore, the combined specimens were sheared to a shear displacement of about 60 mm at the first stage (at a shear rate of 0.02 mm/min) to reach the residual state. Then, in the multi-stage procedure, a shear displacement of about 40 mm was set at each shear rate level.

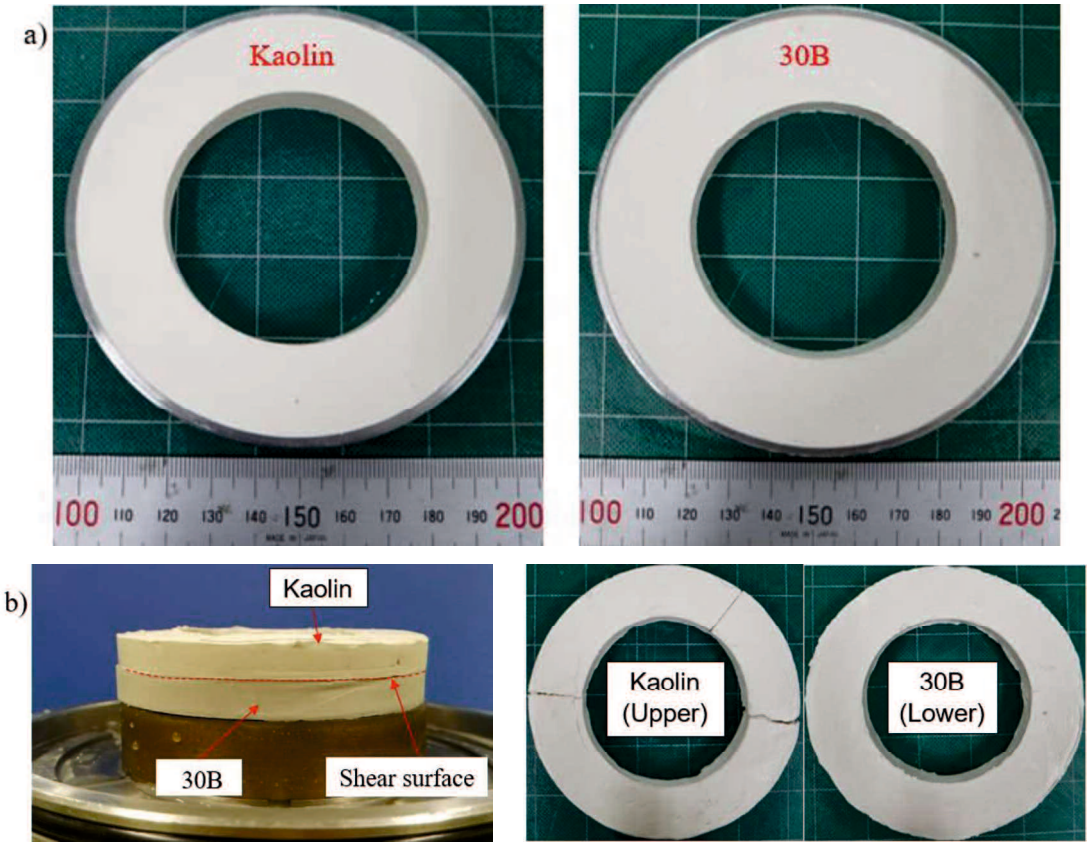

Figure 5.1 Two halves of combined specimen: (a) Before shearing and (b) After shearing

5.2. Shear behavior of combined specimens

The shear stress-shear displacement relationships of the combined specimens (K-K, K-10B, K-20B, and K-30B) at different normal stress levels and shear rates are shown in Figs. 5.2(a)–(d). As shown in these figures, the shear stress increases sharply to reach the peak after a very small shear displacement and then it drops to the residual value. This indicates that the peak strength should not be used in stability analyses of slopes that contain a discontinuous plane. This suggestion is similar to the use of shear strength recovery at the residual state in slope stability. At the residual state, the shear strength may increase after some point in time due to reconsolidation and ageing or healing processes, but it sharply decreases to the residual value after a small shear displacement (e.g., Stark et al., 2005; Stark and Hussain, 2010; Bhat et al., 2013).

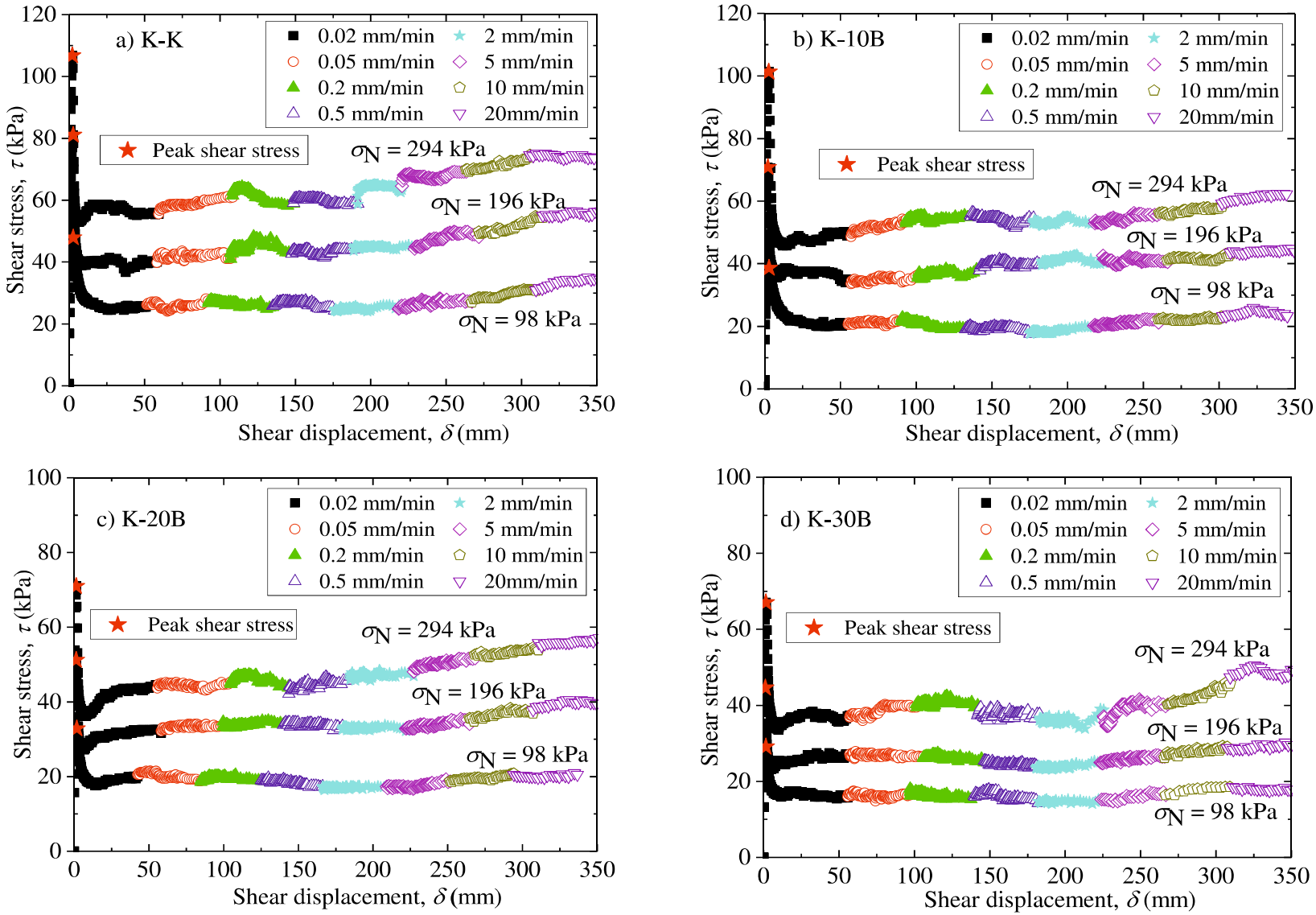

Figure 5.2 Shear stress-shear displacement relationship of combined specimens

5.3. Residual interface strength between two different soil layers

The residual stress ratios of the combined specimens at 98 kPa obtained from the multi-stage procedure for increasing the shear rates are represented in Figs. 5.3 (a)–(d). In these figures, the test results for the combined specimens are also plotted together with those for the intact specimens (obtained from the single-stage procedure, Chapter 4). Fig. 5.3(a) shows that the rate dependency of the residual strength of the K–K specimen is positive and consistent with that of the intact specimens. This confirms that combined specimens or pre-cut specimens can be used to determine the residual strength and to evaluate its rate dependency as well. In other words, the multi-stage procedure for increasing the shear rate is useful for evaluating the rate dependency of the residual strength in order to reduce the testing duration.

Figs. 5.3(b)–(d) show that the rate effect on the residual strength of the combined specimens of the kaolin and kaolin-bentonite mixture samples is insignificant at shear rates lower than 2 mm/min. However, the residual interface strength increases with the shear displacement rates higher than 2 mm/min. The increase in residual interface strength may be caused by the change in shear mode from sliding to turbulent in the kaolin layer and by the viscosity effect in the kaolin-bentonite mixture layer. At a shear rate above 2 mm/min, the rate dependency of the residual strength of the combined specimens and the intact specimens is opposite. It shows a positive rate effect for the combined specimens, while it shows a negative tendency for the intact specimens. The positive rate effect behaviour of the combined specimens is similar to the results of the clay-cemented clay specimens (Suzuki et al., 2017) and of the soil-soil, soil-rock, and rock-rock specimens (Scaringi et al., 2018). These figures also indicate that the residual strength of kaolin clay decreases significantly when the lower half is mixture samples. In particular, the residual strength of the K-10B specimen significantly decreases (about 20%) compared to the residual strength of the K-K specimen and is almost similar to that of the intact 10B specimen at shear rates lower than 2 mm/min (Fig. 5.3(b)). When the lower half is the 20B or 30B specimen, the residual strength at the interface continues to decrease but insignificantly (Fig. 5.4). The higher bentonite content will lead to the lower residual interface strength. This shows that the smectite minerals at the contact surface significantly affect the residual interface strength.

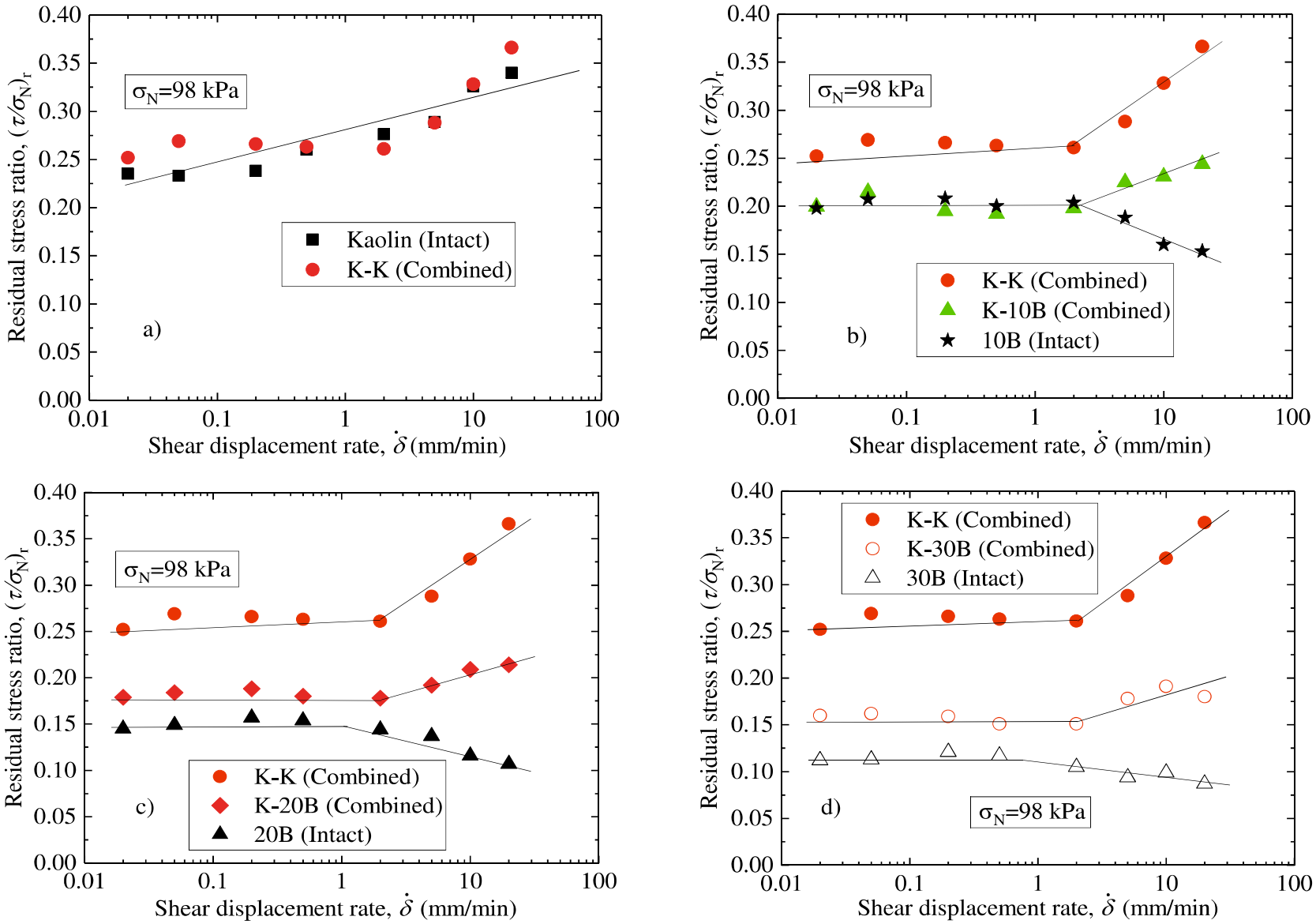

Figure 5.3 Residual stress ratios of combined and intact specimens at different shear rates

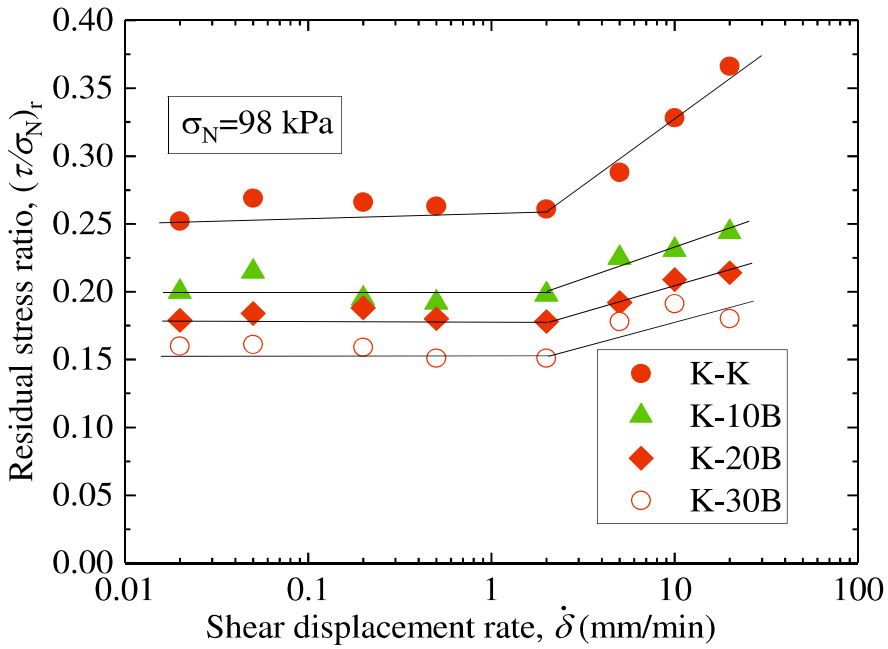

Figure 5.4. Residual stress ratios of combined specimens

The rate dependency of the residual interface strength was also investigated at effective normal stress levels of 196 kPa and 294 kPa. The test results at different effective normal stress levels are presented in Fig 5.5. This figure shows that the residual interface strength seems to decrease as the normal stress increases at all shear displacement rates in the range. This trend is consistent with the previous results for the residual strength of intact samples (Bishop et al., 1971; Townsend and Gibert, 1976; Anayi et al., 1988; Stark and Eid, 1994; Li et al., 2013b, Xu et al., 2018). It can be seen that the residual interface strength of the K-K combined sample is more dependent on the normal stress than that of the K-10B, K-20B, and K-30B samples. The residual interface strength of the K-K sample significantly decreases as the normal stress increases from 98 kPa to 196 kPa. When the normal stress increases from 196 kPa to 294 kPa, the residual interface strength is less dependent on the normal stress (Fig. 5.5(a)). Unlike the K-K sample, the residual interface strength of the K-10B, K-20B, and K-30B combined samples slightly decreases as the normal stress increases from 98 kPa to 294 kPa. This shows that the characteristics of the contact material affect the normal stress dependency of the residual interface strength. In other words, the presence of smectite minerals in the contact surface significantly affects the residual interface strength-stress dependency.

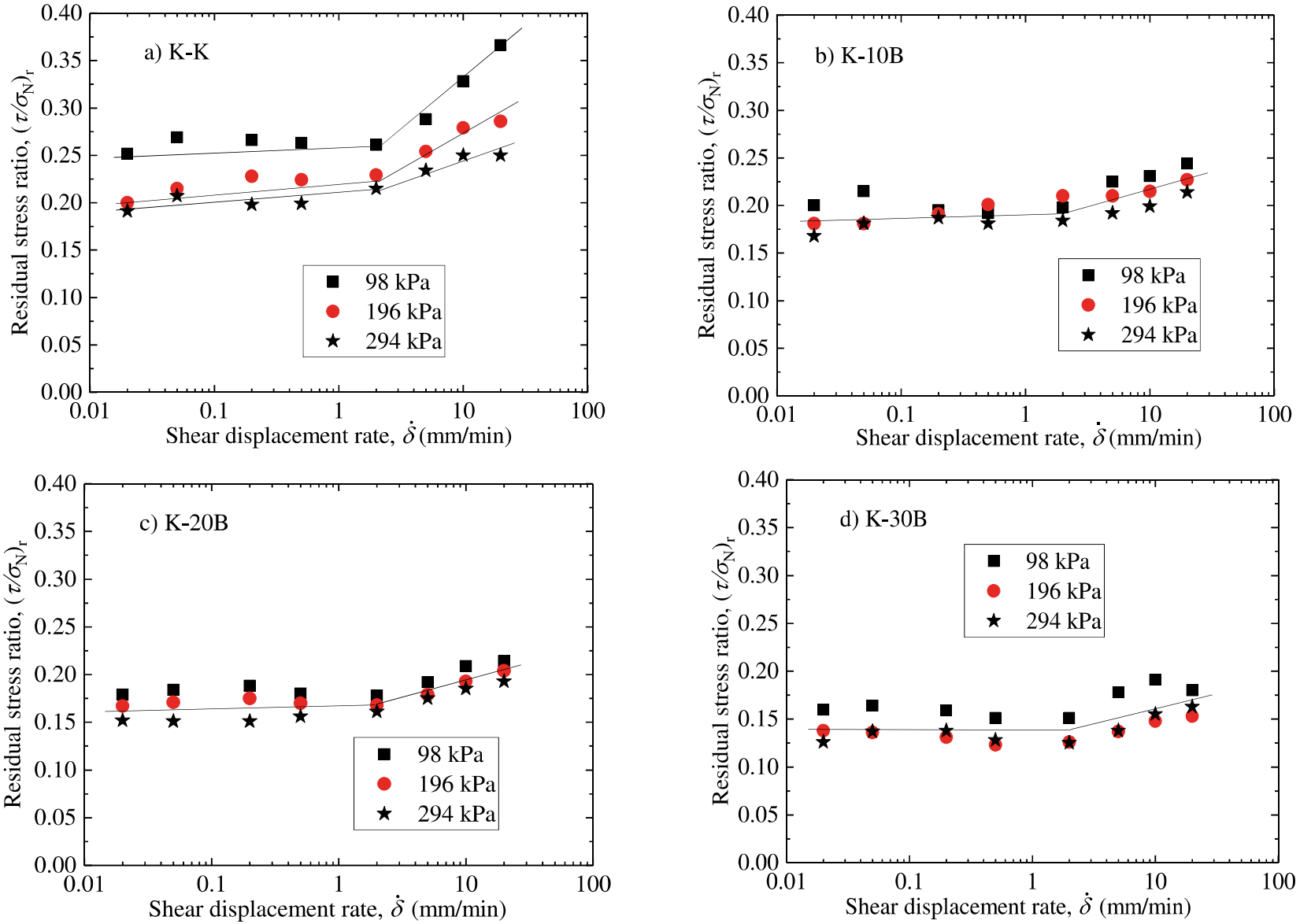

Figure 5.5 Residual stress ratios of combined specimens at different shear rates and different normal stress levels

Regarding the magnitude of the rate dependency of the residual interface strength at different normal stress levels, Fig 5.5(a) shows that the magnitude of the positive rate effect on the residual strength of the K-K sample decreases as the normal stress increases. This behaviour is similar to that shown in previous research results obtained for intact samples (Carrubba and Colonna, 2006; Stark and Hussain, 2010; Kimura et al., 2013; Gratchev and Sassa, 2015). However, for the K-10B, K-20B, and K-30B samples, the effect of the effective normal stress on the magnitude of the positive rate effect is not clear. This indicates that the effect of the effective normal stress on the rate dependency of the residual interface strength also depends on the characteristics of the contact material.

5.4. Summary

This chapter has presented the rate dependency of the residual interface strength between kaolin and kaolin-bentonite mixtures based on the results of ring shear tests conducted on combined specimens (K-K, K-10B, K-20B, and K-30B). The multi-stage procedure was used to increase the shear rates from 0.02 mm/min to 20 mm/min procedure, and effective normal stress levels of 98 kPa, 196 kPa, and 294 kPa were applied. The main research results of this chapter can be summarised as follows:

1. The interface shear strength increases sharply to reach the peak value after a small shear displacement and then drops to the residual value. This shows that the peak interface strength should not be used for the stability of slopes having discontinuous planes or interfaces between two soil layers.

2. The residual strength of combined specimen K-K is almost similar to that of the intact specimen of kaolin clay at all shear rates in the range. This indicates that pre-cut specimens can be used to determine the residual shear strength and to evaluate its rate dependency as well.

3. The residual interface strength decreases significantly with the presence of 10% bentonite in the lower layer. When the bentonite content in the lower layer is increased, the residual interface strength continues to decrease, but this decrease is insignificant.

4. The effect of normal stress on the magnitude of the rate dependency of the residual strength is also exhibited in the residual interface strength. However, this behaviour seems to depend on the characteristics of the contact material. A decrease in the magnitude of the positive rate effect on the residual interface strength with an increasing normal stress is exhibited considerably in the K-K specimen, whereas it is insignificant in the cases of the K-10B, K-20B, and K-30B specimens.

CHAPTER 6. RATE EFFECT ON SHEAR STRENGTH OF OVER-CONSOLIDATED KAOLIN CLAY

6.1. Introduction

A series of ring shear tests (Bishop's type) (Bishop et al., 1971) was conducted on remoulded kaolin clay with different overconsolidation ratios (OCRs) under different shear displacement rates. The main objective was to examine the rate dependency of both peak and residual strengths of OC clay and their relationship to the OCRs in ring shearing. The variations in cohesion and friction angles at both peak and residual states of the OC clay at different shear rates were also clarified. In addition, the multi-stage procedure for decreasing the normal stress was also applied to determine the residual strength parameters of the OC clay. The strength parameters from this procedure were compared with those obtained from the single-stage procedure which was conducted on individual OC samples.

A commercial kaolin clay in the form of powder was used; its physical properties were shown in Chapter 3. The pre-consolidated samples were prepared according to the procedure presented in Chapter 3. A series of ring shear tests was carried out on reconstituted kaolin clay at different OCRs. The OCR is theoretically defined as the ratio of the maximum pre-consolidation pressure recorded in the stress history of a soil mass to the current pressure. In order to create an artificial OCR, the specimens were firstly consolidated at a given consolidation pressure (σ_c) to reach the primary consolidation. The primary consolidation time was calculated based on the 3t method. Subsequently, the load was decreased to the required vertical pressure. The specimens were kept under this normal stress until the end of the dilation process and later sheared at this stress. The duration for completing the dilation was also confirmed based on the 3t method.

To investigate the rate effect on the shear strength of the OC clay, specimens with artificial OCRs of 1, 4, and 6 were used. These OCRs of 1, 4, and 6 consist of stress combinations of 98/98 kPa, 392/98 kPa, and 588/98 kPa, respectively, in which the former value of each combination represents the consolidation pressure and the latter represents the normal stress at shear. The specimens were sheared at shear displacement rates, $\dot{\delta}$, in the range of 0.02 mm/min to 20 mm/min to a shear displacement of about 314 mm under an effective normal stress of 98 kPa.

To investigate the variations in cohesion and friction angles of OC clays at different shear rates, the specimens were firstly consolidated at 588 kPa and then sheared at effective normal stress levels of 588, 392, and 98 kPa, which correspond to OCRs of 1, 1.5, and 6,

respectively. The single-stage procedure was conducted on individual OC specimens with shear displacement rates from 0.02 to 2 mm/min. The multi-stage procedure for decreasing the normal stress was also applied in order to make a comparison with the results of tests conducted with the single-stage procedure. In the multi-stage procedure, the specimens were firstly consolidated at 588 kPa and then sheared at this stress to the shear displacement of about 314 mm to reach the residual state. Next, the normal stress was decreased to 392 kPa (equal to an OCR of 1.5) and kept at this stress until the end of the dilation process. At this normal stress, the specimens were sheared again to obtain the residual strength. Anderson and Hammoud (1988) showed that in the multi-stage procedure for doubling the normal stress, the shear displacement of about 30 mm was sufficient to obtain the residual strength of kaolin clay. Stark and Eid (1993) also noted that the pre-cut specimens required about 15 mm of shear displacement to obtain the residual strength in the Bromhead-type ring shear apparatus. Therefore, in this study, the shear displacement in the multi-stage procedure was set at about 40 mm to attain the residual strength. Finally, the normal stress was reduced to 98 kPa (equal to an OCR of 6). The process was repeated for the OCR of 1.5. The test procedure for the OC kaolin clay is shown in Fig. 6.1.

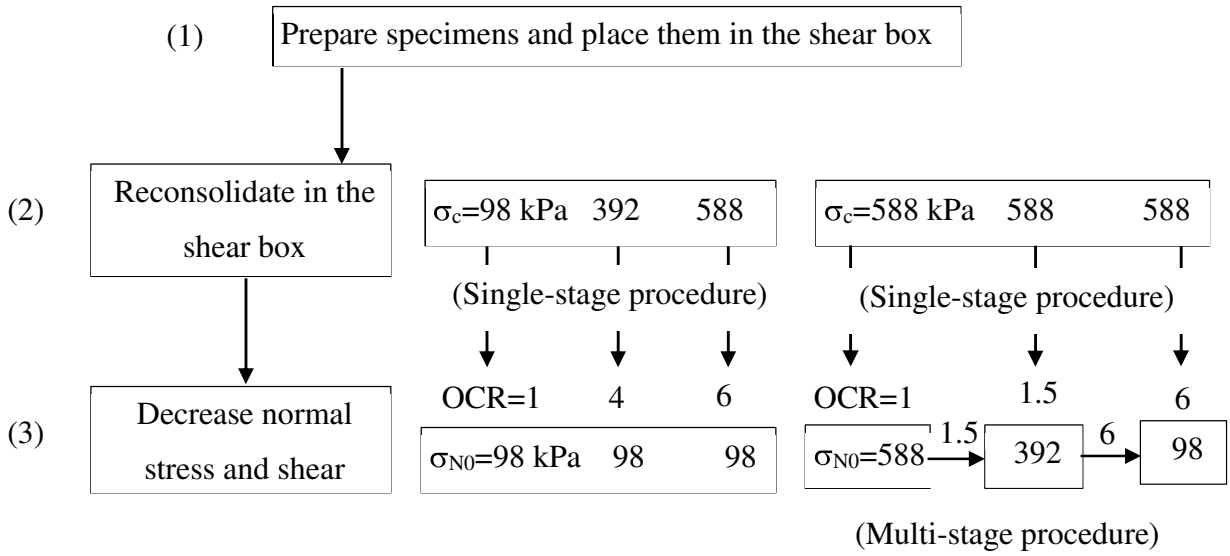

Figure 6.1 Test procedure for OC kaolin clay

6.2. Ring shear behaviour of OC clay under different shear rates

The initial conditions and the test results of kaolin samples at different OCRs under different shear displacement rates are shown in Table 6.1. The residual strength, τ_r, and the residual stress ratio, $(\tau/\sigma_N)_r$, were determined based on the hyperbolic curve approximation

method (Suzuki et al., 1997). The relationships of the shear stress (τ), vertical displacement (v), and normalized normal stress (σ_N/σ_{N0}) to the shear displacement (δ) at different OCRs are presented in Figs. 6.2(a)–(c). As shown in Fig. 6.2(a), the shear stress increases rapidly to reach the peak strength at a small shear displacement and then begins to decline, accompanied by an increase in shear displacement.

Fig. 6.2(b) shows the behaviour of the vertical displacement of the samples at different OCRs during shearing at different shear rates. For the NC sample (OCR of 1), contraction is seen during shearing at all shear rates from 0.02 to 20 mm/min ($v>0$). In contrast for the OCRs of 4 and 6, the samples show expansion at the initial stage of shearing ($v<0$) and contraction at the residual state ($v>0$).

Fig. 6.2(c) presents the fluctuation in normal stress during shearing at different shear rates and different OCRs. The fluctuation in normal stress is expressed through the normalised ratio of σ_N/σ_{N0}, in which σ_{N0} is the initial normal stress and σ_N is the normal stress during shearing. It can be seen that the normal stress during the shearing of the NC samples fluctuates less than that during the shearing of the OC samples. The high fluctuation of the normal stress during the shearing of the OC samples may be caused by the dilation behaviour.

The relationship between the shear displacement at the peak state (δ') and the different OCRs under shear displacement rates from 0.02 mm/min to 20 mm/min is shown in Fig. 6.3. This figure shows that the shear displacement required to reach the peak state decreases with the increasing OCRs for all shear displacement rates in the range. This confirms that an increase in the OCR leads to more brittle failure in the shear behaviour. However, the required shear displacement becomes mostly constant at OCRs of 4 and 6. This result is in good agreement with the results of Vithana et al. (2012).

Table 6.1 Initial conditions, test cases, and test results of kaolin samples at different OCRs

No	Shear rate (mm/min)	p_c (kPa)	w_0 (%)	ρ_0 (g/cm^3)	e_0	S_{r0} (%)	σ_c (kPa)	e_1	σ_{N0} (kPa)	OCR ($=\sigma_c/\sigma_{N0}$)	τ_p (kPa)	$(\tau/\sigma_N)_p$	$(\tau/\sigma_N)_r$	τ_r (kPa)	e_2	δ' (mm)
1-1a	0.02	98	66.4	1.547	1.845	95.2	98	1.587	98	1	52.8	0.536	0.235	23.2	1.380	5.5
1-1b	0.02	196	60.7	1.580	1.691	95.0	196	1.505	196	1	83.6	0.428	0.185	36.2	1.288	3.9
1-1c	0.02	392	54.6	1.629	1.511	95.6	392	1.320	392	1	157.6	0.403	0.177	69.1	1.120	5.0
1-2	0.05	98	69.8	1.552	1.894	97.5	98	1.575	98	1	51.5	0.526	0.233	22.8	1.379	6.1
1-3	0.2	98	68.8	1.550	1.879	96.9	98	1.597	98	1	50.2	0.512	0.238	23.4	1.395	6.5
1-4	0.5	98	66.6	1.551	1.836	96.0	98	1.611	98	1	52.5	0.536	0.260	25.3	1.420	6.1
1-5	2	98	68.3	1.565	1.844	97.9	98	1.604	98	1	42.6	0.435	0.276	27.2	1.403	7.3
1-6	5	98	69.5	1.563	1.868	98.4	98	1.600	98	1	40.5	0.414	0.289	28.4	1.396	10.6
1-7	10	98	66.6	1.544	1.854	95.0	98	1.602	98	1	37.2	0.367	0.326	33.0	1.384	18.2
1-8	20	98	71.7	1.540	1.949	97.3	98	1.617	98	1	36.7	0.376	0.340	33.5	1.331	14.2
2-1	0.02	392	55.6	1.630	1.525	96.5	392	1.280	98	4	61.2	0.624	0.283	27.3	1.248	4.1
2-2	0.05	392	56.5	1.610	1.571	95.1	392	1.253	98	4	65.0	0.657	0.291	28.3	1.204	3.6
2-3	0.2	392	55.2	1.620	1.534	95.2	392	1.261	98	4	61.4	0.637	0.306	30.0	1.222	2.4
2-4	0.5	392	53.8	1.640	1.480	96.1	392	1.204	98	4	62.7	0.640	0.292	28.0	1.160	2.5
2-5	2	392	54.9	1.640	1.489	96.9	392	1.190	98	4	67.2	0.672	0.321	30.9	1.170	2.4
2-6	5	392	54.6	1.640	1.493	96.7	392	1.219	98	4	75.9	0.684	0.333	32.7	1.178	2.5
2-7	10	392	54.4	1.637	1.495	96.3	392	1.166	98	4	70.3	0.706	0.337	33.0	1.150	4.1
2-8	20	392	53.8	1.650	1.465	97.1	392	1.147	98	4	73.8	0.725	0.356	34.9	1.123	6.1
3-1	0.02	392	53.1	1.667	1.429	98.3	588	1.110	98	6	56.9	0.581	0.214	20.7	1.086	2.4
3-2	0.05	392	52.7	1.650	1.448	96.3	588	1.210	98	6	59.8	0.602	0.228	22.0	1.166	2.5
3-3	0.2	392	55.4	1.614	1.547	94.7	588	1.246	98	6	59.3	0.604	0.236	23.0	1.225	3.2
3-4	0.5	392	58.5	1.621	1.586	97.5	588	1.139	98	6	65.7	0.650	0.211	20.8	1.129	1.5
3-5	2	392	57.9	1.613	1.589	96.4	588	1.214	98	6	69.3	0.660	0.227	22.7	1.169	3.0
3-6	5	392	56.8	1.590	1.608	93.4	588	1.189	98	6	65.2	0.651	0.259	25.3	1.178	1.5
3-7	10	392	56.2	1.640	1.519	97.8	588	1.104	98	6	66.0	0.673	0.272	27.1	1.095	3.0
3-8	20	392	55.7	1.631	1.525	96.6	588	1.194	98	6	68.3	0.696	0.277	26.8	1.179	4.1

4-1	0.02	392	55.0	1.638	1.503	96.8	588	1.131	392	1.5	161.8	0.414	0.165	65.9	0.978	4.1
4-2	0.05	392	54.0	1.622	1.511	94.5	588	1.128	392	1.5	151.1	0.384	0.186	73.3	0.948	3.6
4-3	0.2	392	55.4	1.631	1.520	96.4	588	1.119	392	1.5	165.4	0.426	0.192	75.4	0.939	5.1
4-4	0.5	392	58.0	1.626	1.570	97.7	588	1.145	392	1.5	165.6	0.422	0.213	83.8	0.981	5.6
4-5	2	392	55.3	1.636	1.511	96.8	588	1.129	392	1.5	151.6	0.385	0.236	92.9	0.981	7.3
5-1	0.02	392	57.1	1.616	1.571	96.1	588	1.120	588	1	224.5	0.380	0.155	91.1	0.905	4.9
5-2	0.05	392	59.3	1.601	1.632	96.1	588	1.149	588	1	229.7	0.393	0.169	101.5	0.777	4.1
5-3	0.2	392	55.2	1.628	1.522	96.0	588	1.087	588	1	232.3	0.395	0.191	112.5	0.898	6.5
							→392	0.904	392	1.5	–	–	0.197	77.5	0.908	–
							→98	0.969	98	6	–	–	0.224	22.9	0.970	–
5-4	0.5	392	56.8	1.626	1.551	96.9	588	1.079	588	1	238.7	0.406	0.206	121.5	0.742	5.1
							→392	0.750	392	1.5	–	–	0.212	83.4	0.731	–
							→98	0.804	98	6	–	–	0.230	23.0	0.797	–
5-5	2	392	58.0	1.613	1.591	96.4	588	1.133	588	1	222.7	0.378	0.231	136.1	0.806	6.3
							→392	0.815	392	1.5	–	–	0.253	98.8	0.807	–
							→98	0.858	98	6	–	–	0.347	34.3	0.872	–

p_c: Consolidation pressure in consolidation tank (preparing sample)

w_0: Initial water content; e_0: Initial void ratio

ρ_0: Initial wet density

S_{r0}: Initial degree of saturation

σ_c: Consolidation pressure in shear box

σ_{N0}: Initial normal stress

$(\tau/\sigma_N)_r$: Residual stress ratio determined by hyperbolic curve approximation method

$(\tau/\sigma_N)_p$: Stress ratio at peak state; τ_p: Peak strength

τ_r: Residual strength determined by hyperbolic curve approximation method

e_1: Void ratio before shearing; e_2: Void ratio after shearing

OCR: Overconsolidation ratio

δ': Required shear displacement to reach peak strength

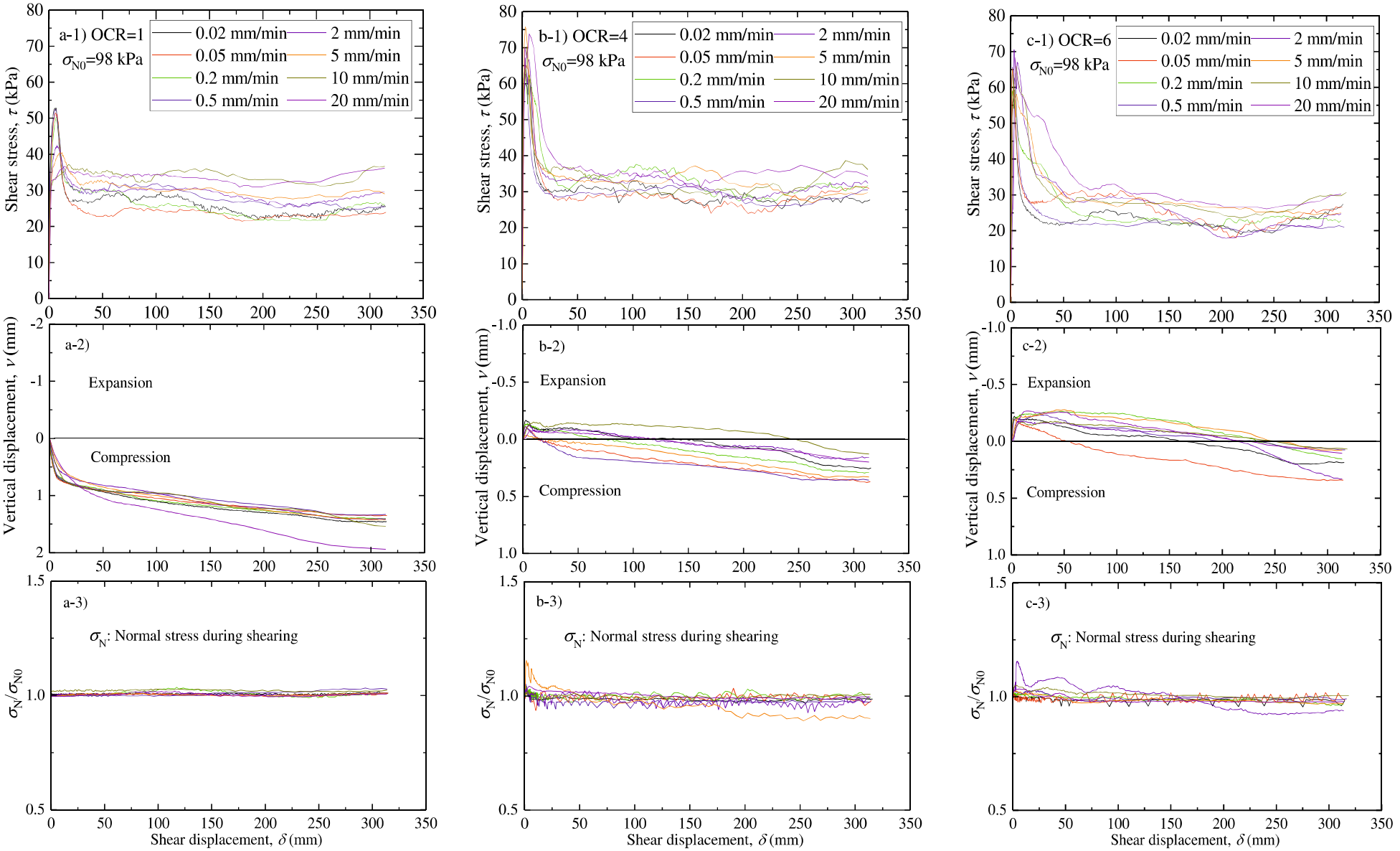

Figure 6.2 Relationships of shear stress (τ), vertical displacement (ν), and normalized normal stress (σ_N/σ_{N0}) to shear displacement (δ) at different OCRs

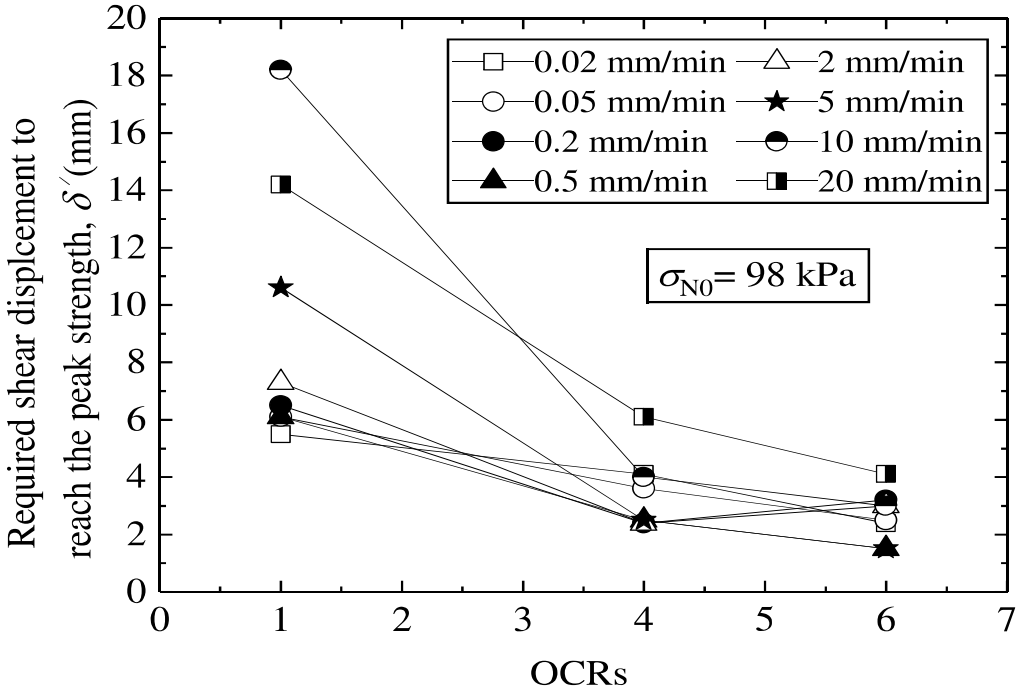

Figure 6.3 Required shear displacement to reach peak strength at different OCRs

6.3. Rate effect on peak strength of OC clay

Fig. 6.4 presents the relationship between the peak stress ratio, $(\tau/\sigma_N)_p$, and the shear displacement rates of kaolin samples at different OCRs. It can be seen from this figure that in the case of the OCR of 1, $(\tau/\sigma_N)_p$ is almost constant at slow shear rates (less than or equal to 0.5 mm/min) and decreases with an increase in the shear rates above 0.5 mm/min. These trends may be caused by the lack of any effect of the excess pore water pressure at slow shear rates and the delayed dissipation of the excess pore water pressure during fast shearing at the peak state. The peak strengths of the NC samples at shear rates below and above 0.5 mm/min can be referred to as the drained and partially drained/undrained shear strengths, respectively. Like the NC specimens, the ratios of the peak strength, $(\tau/\sigma_N)_p$ of the specimens at the OCRs of 4 and 6 are also irrespective of the slow shear rates (less than or equal to 0.2 mm/min) (drained shear strength behaviour). Unlike the NC specimens, however, the peak strength ratios of the OC specimens tend to increase at shear displacement rates equal to or higher than 0.5 mm/min. The test results show that the peak strengths of the OC specimens are higher than those of the NC specimens. Nevertheless, the difference in the peak strengths of the kaolin clay at the OCRs of 4 and 6 is insignificant. This is consistent with the test results of Vithana et al. (2012). Although Vithana et al. (2012) noted that the peak friction coefficient of Kamenose soil at the OCR of 4 was equal to that at the OCR of 6, it did not reflect the effect of the shear displacement rates on the peak strength at the OCRs of 4 and 6. In the present study, the peak strength of kaolin clay at different OCRs

was determined at different shear displacement rates from 0.02 mm/min to 20 mm/min. The test results show that the peak strength of kaolin at the OCR of 4 is almost similar to that at the OCR of 6, regardless of the shear displacement rates (Fig. 6.4).

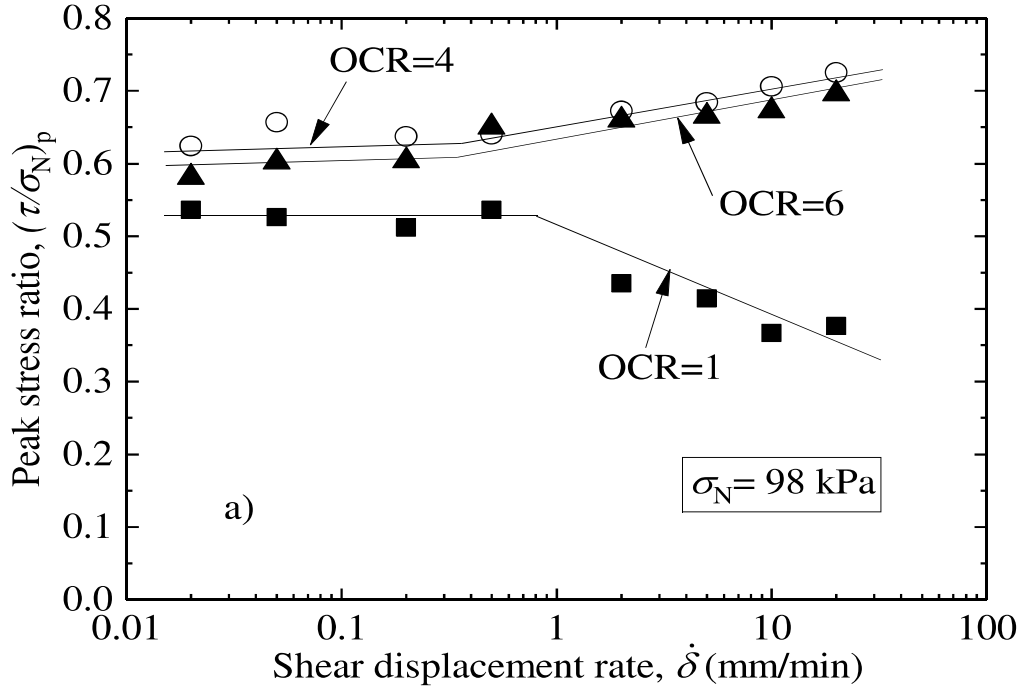

Figure 6.4 Relationship between peak stress ratio and shear displacement rate at different OCRs

In this study, when over-consolidated (OC) specimens are subjected to shear in ring shearing, the specimens show dilation behaviour at the initial stage of shearing. This process leads to an increase in the void ratio and a decrease in the shear-induced pore water pressure. The pore water pressure may decrease to a negative value. At slow shear rates, there is sufficient time for the dissipation of pore water pressure until failure occurs. Thus, the peak shear strengths at these shear rates are drained strengths. At shear rates above 0.5 mm/min, there is a tendency for the changes in peak strength to increase as the shear rates increase. This may be attributed to the delayed dissipation of negative pore water pressure. The test results showed that the peak strength of the OC specimens was reached after a very small shear displacement (Fig. 6.3). In other words, at shear rates above 0.5 mm/min, the required time to reach the peak strength is short and may be insufficient for the dissipation of negative pore water pressure if failure occurs. Hence, in this case, the peak strength can be considered as partially drained or undrained behaviour. However, the shear-induced pore water pressure was not measured in the ring shear tests. Therefore, it is difficult to distinguish between the partially drained behaviour and the undrained shear behaviour in this case. The shear behaviour may be moderately changed from drained to undrained through partially drained conditions as the shear rates increase.

The behaviours of the peak shear strengths of the NC and OC samples with increasing shear rates in the ring shear tests are presented in Fig. 6.5. These behaviours are consistent with those in triaxial tests (Richardson and Whitman, 1963; Lefebvre and Lebouef, 1987; Asaoka et al., 1994, 1998; Sheahan et al., 1996; Quinn and Brown, 2011; Mun et al., 2016) and direct shear tests (Thermann et al., 2016), in which, the drained shear strength is independent of the slow shear rates due to lack of any effect of the excess pore water pressure. The behaviours of the partially drained and undrained shear strengths with increasing shear rates are attributed to the delayed dissipation of the shear-induced pore water pressure.

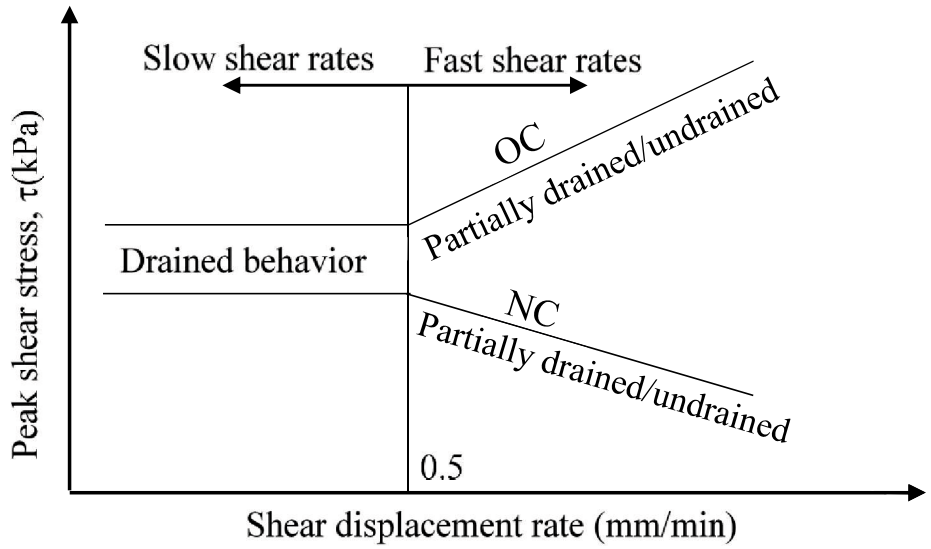

Figure 6.5 Variations in peak strength of NC and OC samples at different shear rates

6.4. Rate effect on residual strength of OC clay

Fig. 6.6 presents the relationship between the residual stress ratio, $(\tau/\sigma_N)_r$ and the shear displacement rates. For all the cases of OCRs, namely, 1, 4, and 6, the residual stress ratios show an increasing trend with the logarithm of shear displacement rates from 0.02 mm/min to 20 mm/min. The increase in the residual strength of the kaolin clay with increasing shear displacement rates could be induced by the change in shear mode from sliding to turbulent (e.g., Skempton, 1985; Tika et al., 1996; Lemos, 2003; Carrubba and Colonna, 2006; Bhat, 2013). In addition, the increase in the residual strength of the NC clay can also be related to the soil extrusion through the gap between upper and lower rings of the shear box (Duong et al., 2018). The soil extrusion will lead to an increase in the final vertical displacement. Fig. 6.7 shows the relationship between the final vertical displacement, v, and the shear displacement rates for both NC and OC specimens. It can be seen from this figure that the final vertical displacements of the OC specimens are almost similar, but much lower than those of the NC specimens, so that the positive rate effect on the residual strength of the OC clay may not be related to the soil extrusion. This reveals that OC

samples should be used to determine the residual strength of soil using the Bishop-type ring shear device in order to reduce the soil leakage through the gap. This suggestion is similar to that of Stark and Eid (1993) and Stark (1995) who used OC samples to determine the residual strength in the Bromhead-type ring shear device.

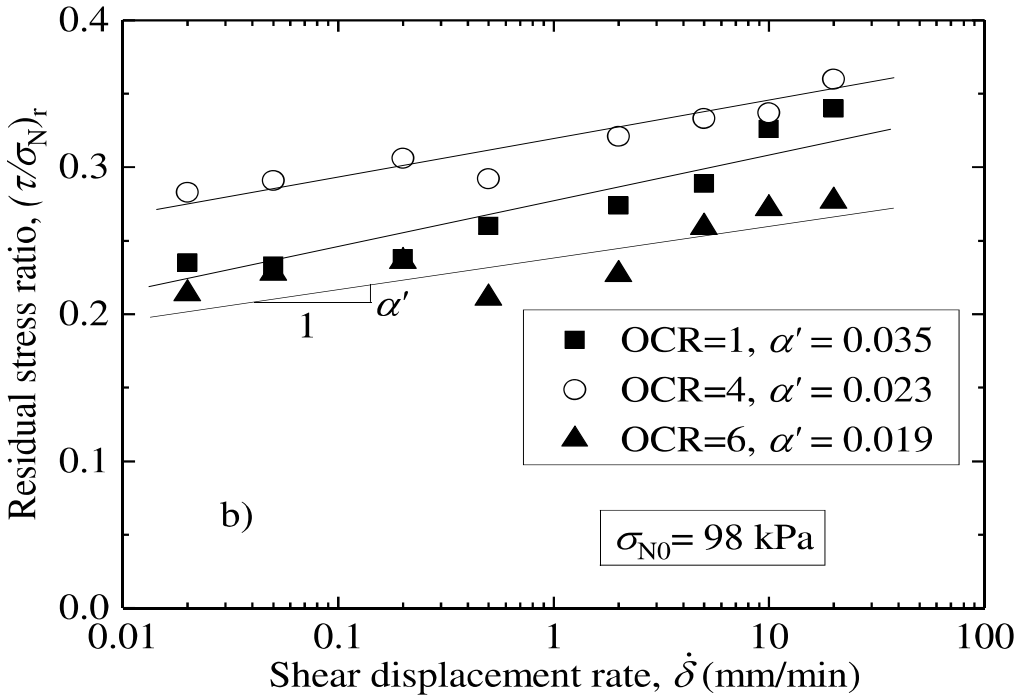

Figure 6.6 Relationship between residual stress ratio and shear rate at different OCRs

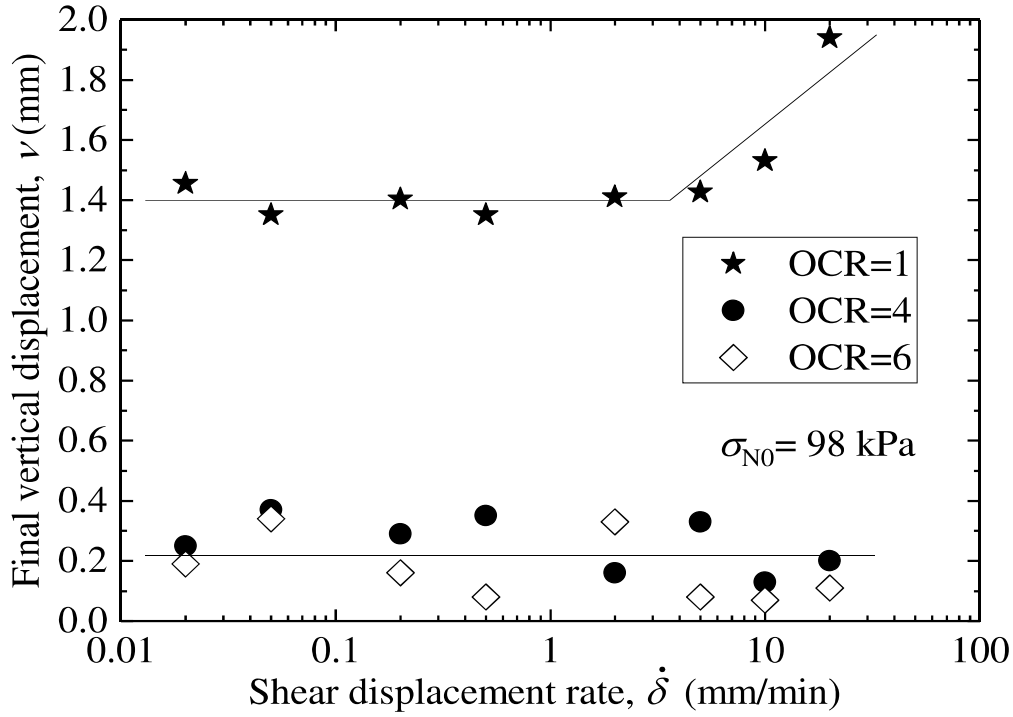

Figure 6.7 Relationship between final vertical displacement and shear rates at different OCRs

For the OC samples, in addition to the structural change, the increase in residual strength at fast shear rates may be attributed to the existence of negative pore water pressure caused by dilation. However, the data in Figs. 6.2 and 6.7 show contractive behaviour for all samples at the residual state, including the OC specimens. Hence, the effect of the negative pore water pressure on the residual strength of the OC clay can be excluded.

Li et al. (2017) and Xu et al. (2018) also investigated the rate dependency of the residual strength of OC clay. Nevertheless, the test results were still limited, so no quantitative relationship between the OCRs and the magnitude of the rate effect could be drawn. In this chapter, the rate effect coefficient (α'), as shown in section 4.5, will be used to quantitatively evaluate the effect of the OCR on the rate dependency of the residual strength.

$$\alpha' = \frac{d\left(\tau/\sigma_N\right)_r}{d(\log\dot{\delta})}$$

The coefficient of the rate effect on the residual strength of kaolin at different OCRs is shown in Figs. 6.6 and 6.8, in which coefficient α' in Fig. 6.6 is calculated based on the samples pre-consolidated at different stress levels (σ_c=588, 392, and 98 kPa), but sheared at the same effective normal stress (σ_{N0}=98 kPa). In contrast, the α' in Fig. 6.8 is based on the samples pre-consolidated at the same stress level (σ_c=588 kPa), but sheared at different normal stress levels (σ_{N0}=588, 392, and 98 kPa). The values for α' are summarized in Table 6.2. The relationship between the rate effect coefficient (α') and the OCRs is shown in Fig. 6.9.

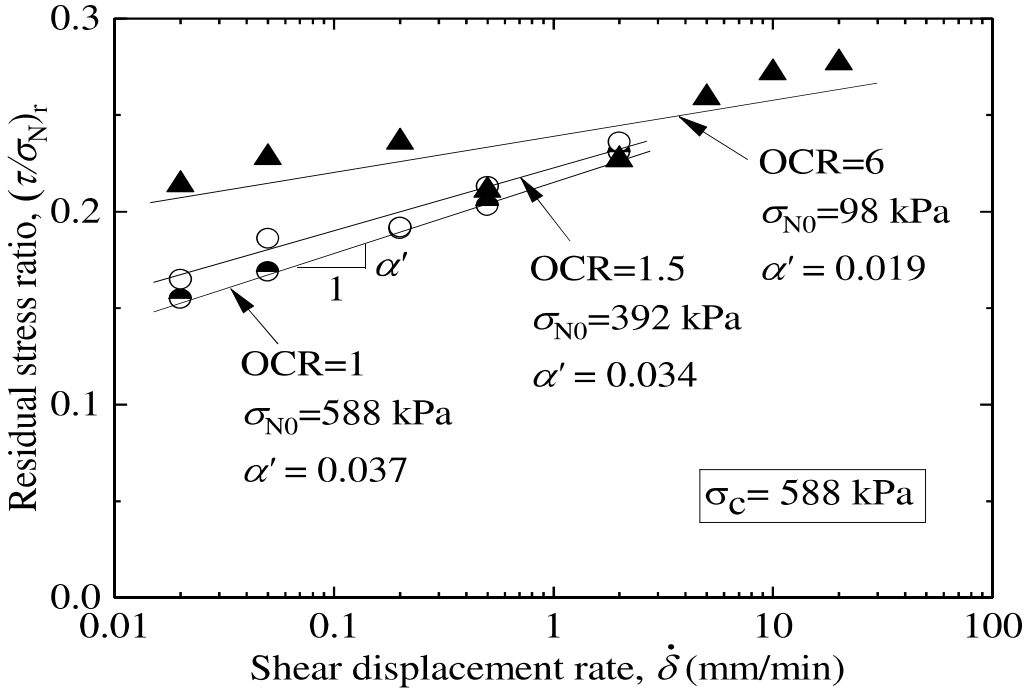

Figure 6.8 Coefficient (α') of kaolin samples sheared at different normal stress levels

Table 6.2 Rate effect coefficient (α')

σ_c (kPa)	σ_{N0} (kPa)	OCR ($=\sigma_c/\sigma_{N0}$)	Shear rates (mm/min)	α'
98	98	1	0.02 – 20	0.035
392	98	4	0.02 – 20	0.023
588	98	6	0.02 – 20	0.019
588	392	1.5	0.02 – 2.0	0.034
588	588	1	0.02 – 2.0	0.037

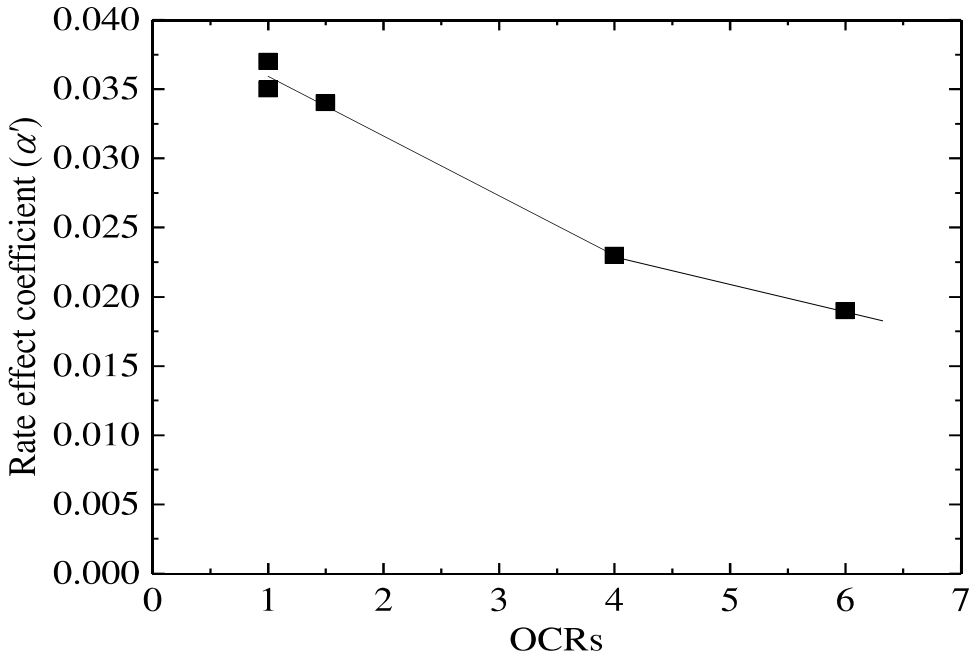

Figure 6.9 Relationship between α′ and OCRs

Fig. 6.9 shows that the positive rate effect coefficient decreases as the OCRs increase, regardless of the shearing effective normal stress (σ_N). In other words, the magnitude of the positive rate effect on the residual strength tends to decrease with the increasing OCRs. As mentioned before, the main reason for the positive rate effect is relevant to the change in shear mode from sliding to turbulent. Vithana et al. (2012) stated that the shear surface structure of OC soil may be disturbed by the dilation process. This leads to a difficulty in reversing the face-face particle orientation (sliding) to turbulent shear behaviour. This phenomenon may result in a lowering of the magnitude of the positive rate effect. In addition, the increase in soil extrusion of the NC specimens through the gap at fast shear rates, as mentioned above, may lead to an increase in the positive rate effect on the residual strength of the NC clay.

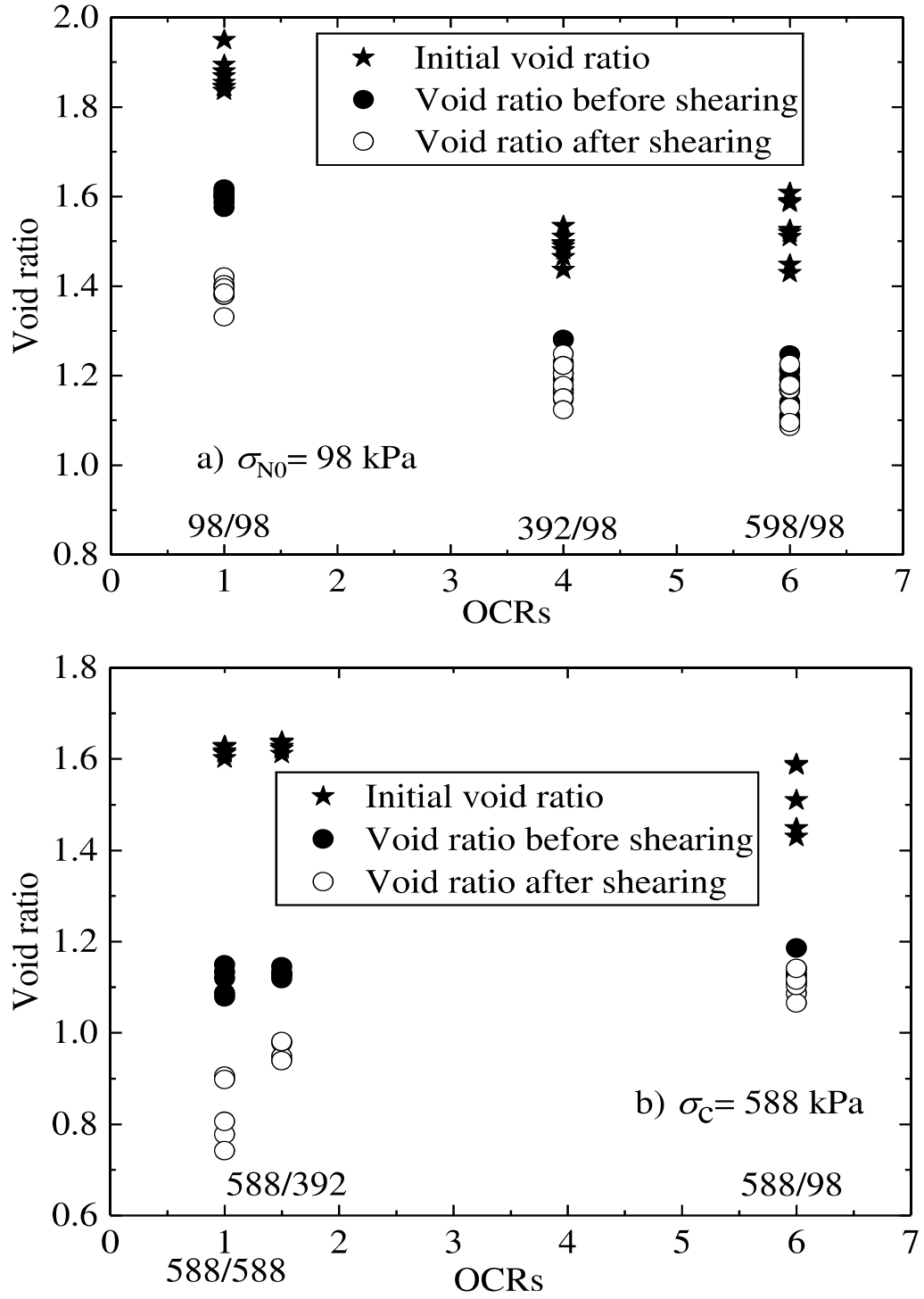

Figure 6.10 Variation in void ratio of samples at different OCRs: a) Pre-consolidated at different pressures and sheared at same effective normal stress and b) Pre-consolidated at same pressure and sheared at different effective normal stress levels

In addition, the magnitude of the rate dependency of the residual strength may be related to the void ratio of the samples. Li and Aydin (2013) indicated that the level of positive rate effect may be decreased by the increase in soil density (decrease in void ratio). Figs. 6.10(a) and (b) show the variation in the void ratio of the samples at different OCRs in the case of shearing at the same

effective normal stress and at different effective normal stress levels, respectively. The void ratios before and after shearing were calculated based on the changes in the vertical displacement of the specimens. It should be noted that the void ratio after shearing may not totally reflect the real values because of the soil leakage through the gap between the upper and lower parts of the shear box, especially at the OCR of 1. However, it may more or less reflect the relationship between the soil density and the rate dependency of the residual strength. As shown in Fig. 6.10(a), the void ratios before and after shearing decrease with the increasing OCRs. Hence, the findings of Li and Aydin (2013) seem to be consistent with the change in the positive rate effect coefficient when shearing at the same effective normal stress. However, Fig. 6.9(b) indicates that the void ratios before and after shearing tend to increase with the OCRs due to the dilation behaviour during the unloading process. This reveals that the magnitude of the positive rate effect on the residual strength of OC samples may not totally relate to the change in the void ratio (soil density). Therefore, the disturbance of the shear surface structure of OC samples due to the dilatancy when the sample is subjected to shear, especially at fast shear rates and the soil extrusion of the NC samples, may be the major causes of the decrease in the magnitude of the positive rate effect with increasing OCRs.

6.5. Variations in cohesion and friction angles of OC clay under different shear displacement rates

The variations in the cohesion and friction angles of the OC samples were investigated under shear displacement rates of 0.02 to 2 mm/min. The single-stage procedure was conducted on individual specimens under different effective normal stress levels equal to different OCRs. Accordingly, at each shear rate, three specimens were firstly consolidated under the effective normal stress of 588 kPa; then they were sheared at effective normal stress levels of 588, 392, and 98 kPa, respectively (Table 6.1).

The relationships between the effective normal stress and the shear stress at the peak and residual states is shown in Fig. 6.11. It can be seen that all the linear regressions are almost parallel at the peak state (Fig. 6.11(a)) whereas at the residual state, the slope of linear regression increases with increasing shear displacement rates (Fig. 6.11(b)). This may reflect the difference in the variations in cohesion and friction angles at the peak and residual states of the OC samples.

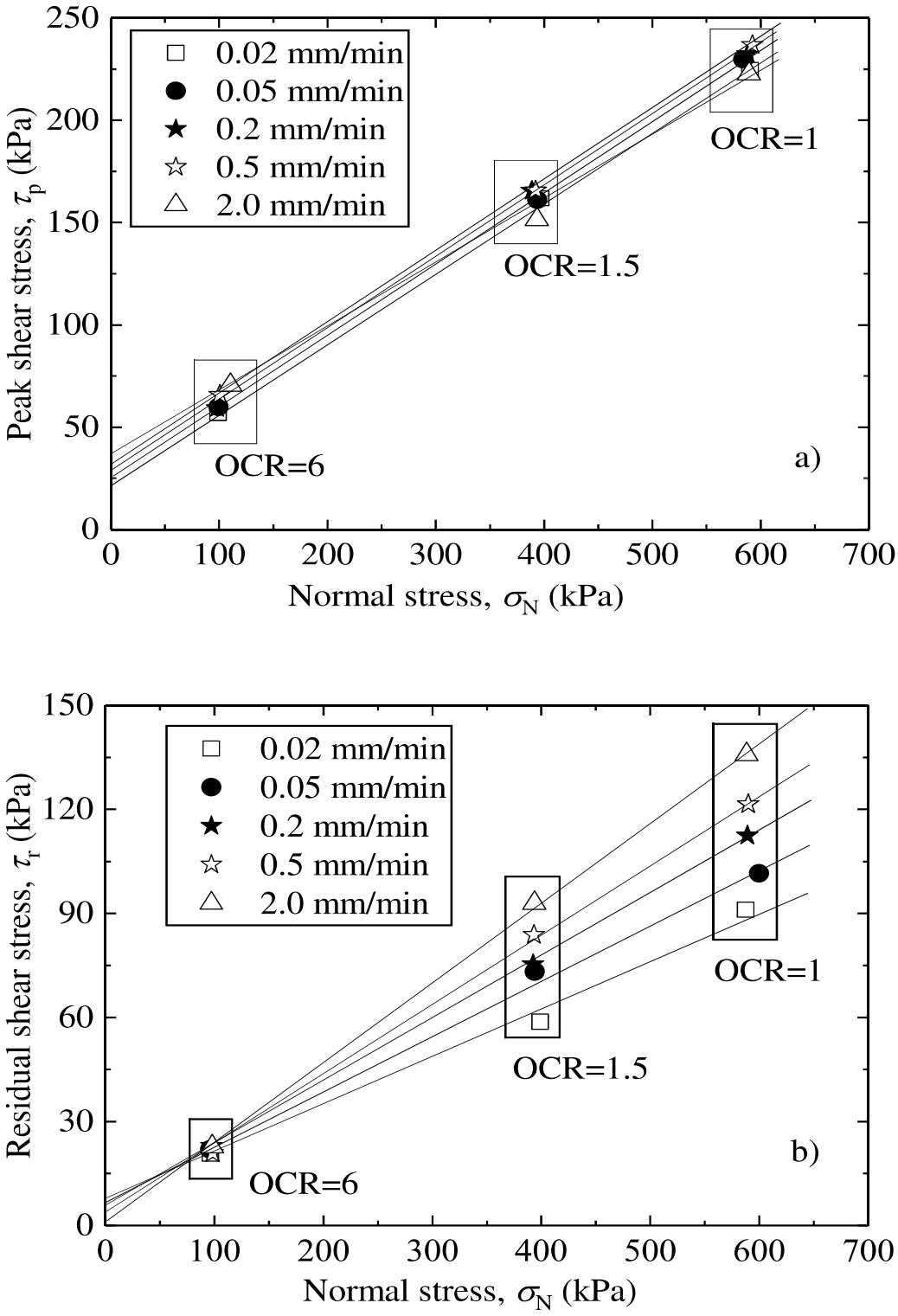

Figure 6.11 Relationships of (a) Shear stress at peak state and (b) Shear stress at residual state to effective normal stress

The calculated results for cohesion and friction angles at both the peak and the residual states of the OC specimens are summarized in Table 6.3. The residual strength parameters of the NC kaolin sample at a slow shear rate of 0.02 mm/min were also determined. The results confirm that the stress history (OCR) has almost no effect on the residual strength.

Table 6.3 Results of cohesion intercept and friction angle of OC clay

No	Shear rate (mm/min)	Specimen types	Test procedure	Peak strength		Residual strength	
				Cohesion intercept c_p (kPa)	Internal friction angle, ϕ_p (deg)	Cohesion intercept c_r (kPa)	Internal friction angle, ϕ_r (deg)
1a	0.02	OC	Single-stage	24.3	18.8	7.3	8.1
1b	0.02	NC	Single-stage	15.8	19.8	6.8	9.0
2	0.05	OC	Single-stage	24.5	19.3	7.8	9.0
3	0.2	OC	Single-stage	25.5	19.5	4.9	10.3
4	0.5	OC	Single-stage	30.3	19.1	1.2	11.6
5	2.0	OC	Single-stage	34.0	17.5	0.5	13.0

The variations in cohesion and friction angles at the peak and residual states under different shear displacement rates are presented in Figs. 6.12 and 6.13. As shown in Fig. 6.12, the peak cohesion intercept tends to increase as the shear rates increase, especially above 0.2 mm/min while the peak friction angle is almost independent of the shear rates in the range of 0.02 to 2 mm/min. The increase in peak cohesion, especially above 0.2 mm/min, can be attributed to the delayed dissipation of the negative pore water pressure. With the existence of negative pore water pressure, the total peak cohesion can be composed of the effective cohesion and the apparent cohesion; this is caused by the negative pore water pressure (Fredlund et al., 1995). This indicates that the negative pore water pressure will lead to an increase in the total peak cohesion of the OC samples with increasing shear rates. In contrast, the negative pore water pressure may have no effect on the peak friction angle (Peterson, 1990; Nishimura and Fredlund, 2000). This results in the independence of the friction angle with increasing shear rates. The research results of Han et al. (2014) also indicated that the apparent peak friction angle of highly over-consolidated clay (OCRs from 7 to 56) in the triaxial tests appeared to be independent of the strain rates.

Unlike at the peak state, at the residual state, the friction angle increases, whereas the cohesion tends to decrease as the shear displacement rates increase (Fig. 6.13). Although the residual cohesion decreases with shear displacement rates, it has no effect on the overall tendency of the residual stress ratio, as mentioned above, because the residual cohesion is insignificant.

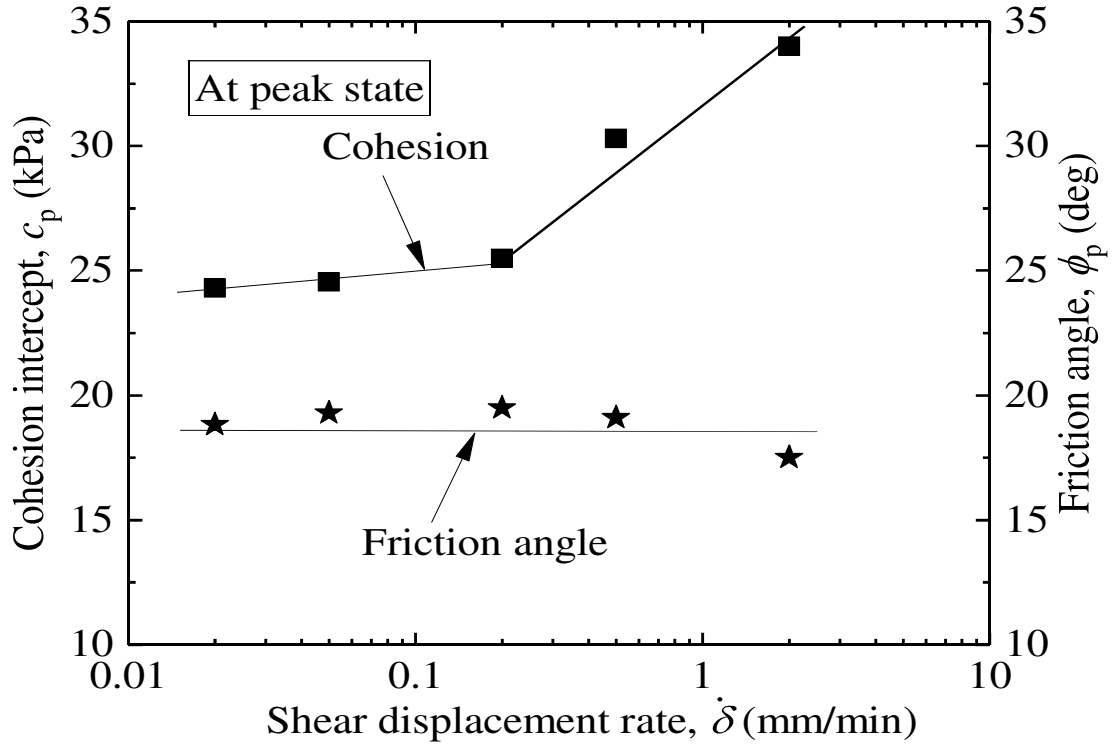

Figure 6.12 Variations in peak cohesion and friction angles of OC clay at different shear rates

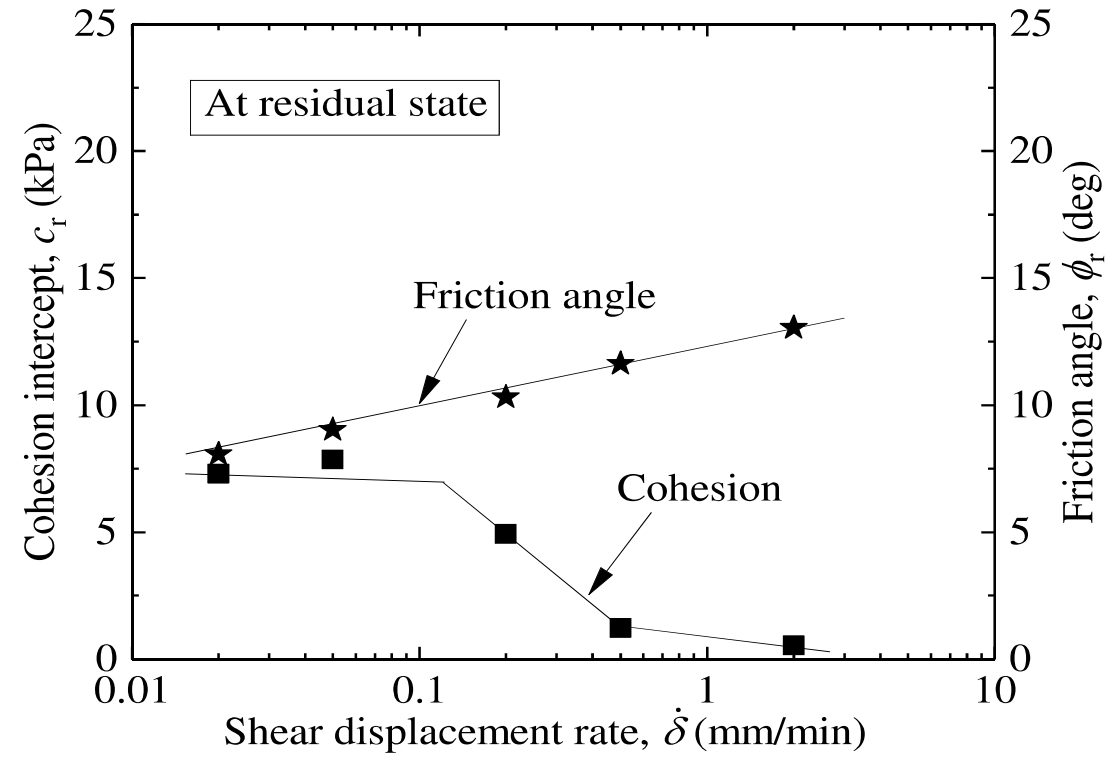

Figure 6.13 Variations in residual cohesion and friction angles of OC clay at different shear rates

6.6. Multi-stage procedure for determining residual strength of OC clay

The multi-stage test procedure has been investigated and applied for many years to determine the residual strength (e.g., Anderson and Hammoud, 1988; Stark and Vettel, 1992; Stark, 1995; Tiwari and Marui, 2004; Xu et al., 2018). Recently, Xu et al. (2018) concluded that the residual strength obtained from the multi-stage procedure was almost similar to that obtained from the single stage procedure. However, these investigations did not reflect the effect of the shear displacement rate on the test results obtained from the multi-stage test procedure. In addition, most of these investigations used the multi-stage procedure for increasingthe normal stress. In the present study, the multi-stage procedure for decreasing the normal stress was applied to determine the residual strength of OC specimens at shear displacement rates of 0.2, 0.5, and 2.0 mm/min. In this procedure, at each shear rate, one specimen was sheared under different effective normal stress levels equal to different OCRs (OCRs of 1, 1.5, and 6). The test results of the single- and multi-stage procedures are summarised in Table 6.4.

Table 6.4 Test results of single- and multi-stage procedures for OC kaolin clay

No	Shear rate (mm/min)	Specimen types	Test procedure	Peak strength		Residual strength	
				Cohesion intercept c_p (kPa)	Internal friction angle, ϕ_p (deg)	Cohesion intercept c_r (kPa)	Internal friction angle, ϕ_r (deg)
1	0.2	OC	Single stage	25.5	19.5	4.9	10.3
			Multi-stage	–	–	4.3	10.4
2	0.5	OC	Single stage	30.3	19.1	1.2	11.6
			Multi-stage	–	–	3.4	11.3
3	2.0	OC	Single stage	34.0	17.5	0.5	13.0
			Multi-stage	–	–	14.7	11.8

The results of the residual cohesion intercept and the residual friction angle of the single- and multi-stage procedures at different shear rates are presented in Fig. 6.14. Fig. 6.14(a) shows that the residual friction angle obtained from the single-stage procedure is consistent with that obtained from the multi-stage procedure, regardless of the shear displacement rates. However, there is a difference in the residual cohesion intercept obtained by the two procedures. While the residual cohesion of the two procedures is almost similar at the shear rates of 0.2 and 0.5 mm/min, the residual cohesion of the multi-stage procedure is much higher than that of the single-stage

procedure at the fast shear rate (2 mm/min) (Fig. 6.14(b)). Therefore, the multi-stage procedure for decreasing the normal stress should be applied to determine the residual strength of OC kaolin clay at shear displacement rates less than or equal to 0.5 mm/min.

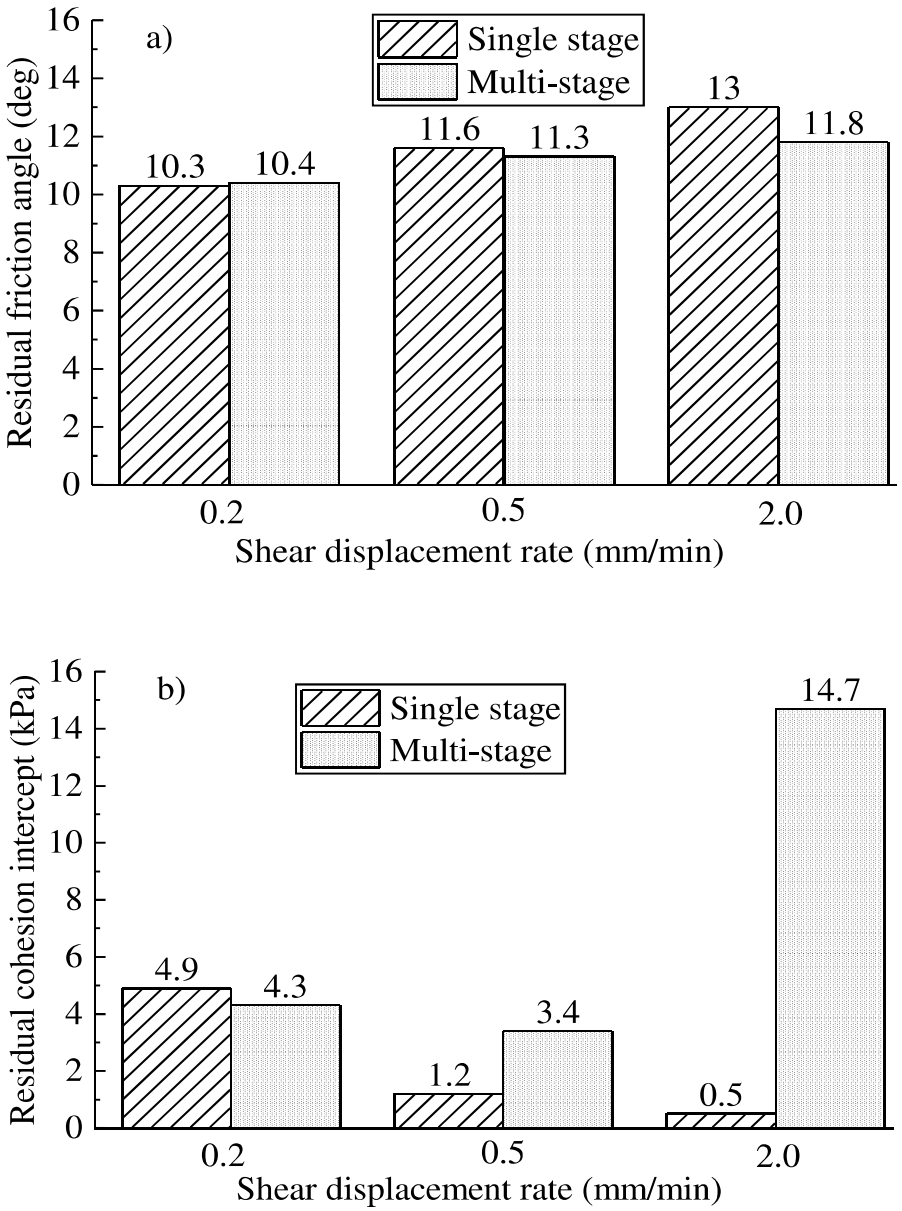

Figure 6.14 Test results of single- and multi-stage procedures for OC kaolin clay at residual state.

6.7. Summary

This chapter has presented an experimental investigation of ring shear tests conducted on kaolin clay at OCRs ranging from 1 to 6. The tests were conducted at shear rates from 0.02 mm/min to 20 mm/min and normal stress levels of 98 kPa, 392 kPa, and 588 kPa. Both single- and multi-stage procedures were employed in this chapter. The main research results of this chapter can be summarised as follows:

1. The peak strengths of NC and OC kaolin clays are independent of shear rates less than 0.5 mm/min. However, at fast shear rates, the rate effect on the peak strengths of NC and OC clays is opposite. It shows a downward trend for NC clay, whereas it shows an upward one for OC clay. The difference in the peak strengths of kaolin clay at OCRs of 4 and 6 is insignificant under all the shear displacement rates in the range of 0.02 mm/min to 20 mm/min.

2. At shear rates above 0.5 mm/min, the peak shear strength can be considered as showing partially drained or undrained shear behaviour. These behaviour is closely related to the delayed dissipation of shear-induced pore water pressure.

3. The positive rate effect on the residual strength is exhibited in both NC and OC kaolin clays. However, the magnitude of the positive rate effect on the residual strength decreases as the OCRs increase. The disturbance of the shear surface structure of the OC samples and the soil leakage of the NC samples during shearing seem to be the major causes of the decrease in the magnitude of the rate dependency of the residual strength.

4. The variations in cohesion and internal friction angles of OC kaolin clay at peak and residual states under different shear displacement rates are different. At the peak state, the cohesion is almost constant at slow shear rates (less than or equal to 0.2 mm/min), but it tends to increase as the shear rates increase above 0.2 mm/min. However, the peak friction angle is almost independent of the shear rates. Unlike the peak state, at the residual state, the friction angle increases whereas the cohesion tends to decrease with an increase in the shear displacement rates.

5. The multi-stage procedure for decreasing the normal stress can be used instead of the single-stage procedure to determine the residual strength of OC kaolin clay in order to reduce the test duration. However, this multi-stage procedure should not be used to determine the residual strength of OC clay at shear rates above 0.5 mm/min.

CHAPTER 7. ACCELERATION EFFECT ON RESIDUAL STRENGTH

7.1. Introduction

In a pre-existing slide, the velocity or shear displacement rate of a landslide block is not always constant. As shown in Fig. 1.1(b), the initial shear displacement rates of a reactivated landslide block can be very slow. However, they can increase gradually at certain times after the initial slope failure under a constant effective normal stress. This movement is known as residual-state creep (post-peak creep) (Bhat et al., 2011, 2013). The creep behaviour of soil can manifest under undrained or drained shear conditions. For undrained creep, the creep rupture is caused by the migration of pore water (Walker et al., 1969; Asaoka et al., 1998). Although drained creep (real creep) has not been clarified, it is thought to be controlled by the viscous property of soils (Mitchell and Soga, 2005). At a slow residual state, the creep behaviour is regarded as a type of drained creep. In large-scale landslides, the creep behaviour is mostly exhibited in soils containing clay minerals, such as bentonite, chlorite, illite, and mica (Bhat et al., 2011). The shear displacement rate (creep rate) varies according to the creep stage: decreasing in the primary creep stage, remaining constant in the secondary creep stage, and increasing dramatically during the tertiary creep stage (Fig. 7.1). The rapid increase in velocity in the tertiary stage may lead to creep rupture or failure. However, changes in velocity in the tertiary creep stage may occur over different durations. The rate of change in velocity over time is defined as acceleration. Therefore, changes in velocity at different times lead to changes in acceleration, which may affect the shear strength in the residual state (this is known as an acceleration effect). Acceleration has been used to forecast the time failure of creep landslides. Xu et al. (2011) considered the displacement–time curve and the acceleration threshold in establishing pre-warning criteria for creep slope failure. However, reliable information on how the acceleration effect influences the residual strength is not yet available.

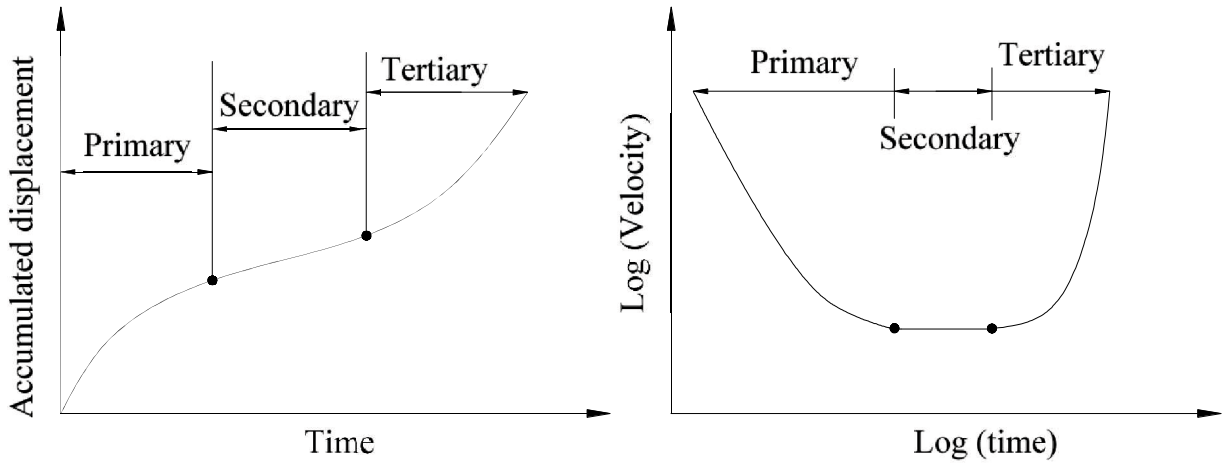

Figure 7.1 Three typical stages of shear creep process (after Augustesen et al., 2004)

To investigate the acceleration effect, a multi-stage shearing rate procedure with different acceleration values was applied to a kaolin sample and a mixture of 10% bentonite and 90% kaolin (10B). This procedure consisted of two main steps. First, a ring shear test was conducted at a slow shear rate to obtain the residual state in the fully drained condition. A shear rate of 0.02 mm/min was applied in this step. Second, the multi-stage procedure for increasing shear rates was employed. Once the residual state was reached, the shear rate was increased from very slow (0.002 mm/min) to fast (20 mm/min). Two average accelerations of 0.028 mm/min^2 (100.8 mm/h^2) and 0.014 mm/min^2 (50.4 mm/h^2) were employed in this procedure. The acceleration was calculated as the ratio of the change in velocity (shear rate) to the total time needed for the change. In the case of the acceleration of 0.028 mm/min^2, the shearing time was maintained at each shear rate level for 60 min. In the case of the acceleration of 0.014 mm/min^2, the shearing time was maintained at each shear rate level for 120 min (Fig. 7.2). Mazzanti et al. (2015) made a continuous observation of ten small slides using terrestrial SAR interferometry (TInSAR), and their results indicate that the acceleration of landslides varies from a few mm/h^2 to more than 80 mm/h^2. In addition, in an analysis of the database of rock slope failures at several coal mines, Carlà et al. (2017) showed that the acceleration before failure could reach 120 mm/h^2, although in most cases the average acceleration was less than 40–50 mm/h^2. This indicates that the acceleration before slope failure can reach hundreds of mm/h^2. Therefore, to evaluate the acceleration effect, the accelerations of 100.8 mm/h^2 and 50.4 mm/h^2 applied in this study were appropriate. The effective normal stress applied during this procedure was 98 kPa.

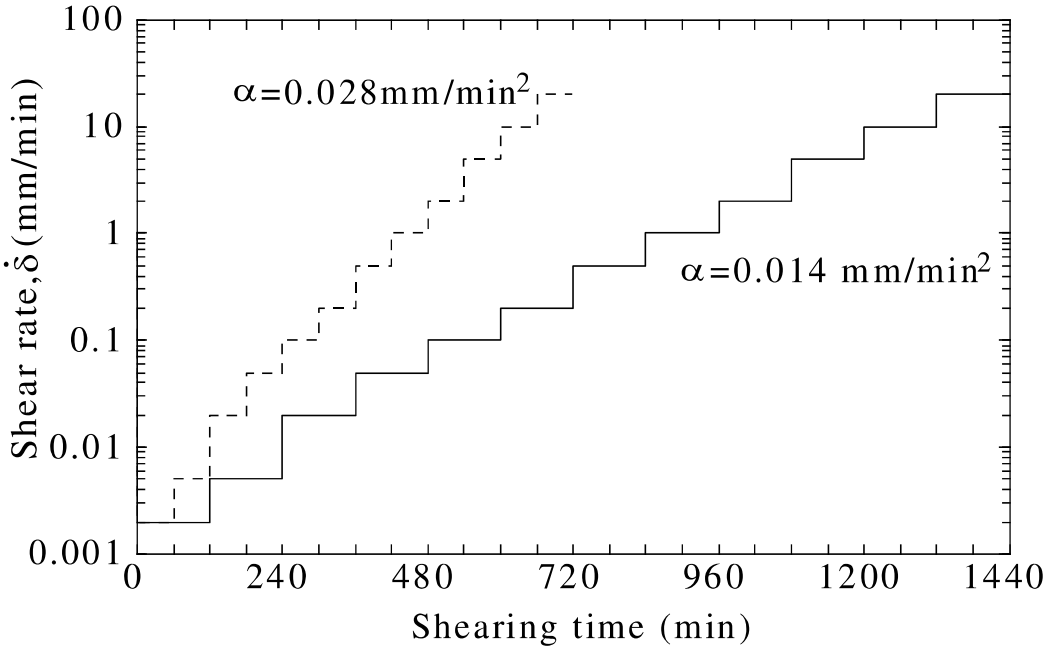

Figure 7.2 Test procedure to investigate acceleration effect on residual strength

7.2. Test results and discussions on acceleration effect

The test results of ring shearing on the kaolin and 10B samples at different acceleration rates are shown in Figs. 7.3 and 7.4.

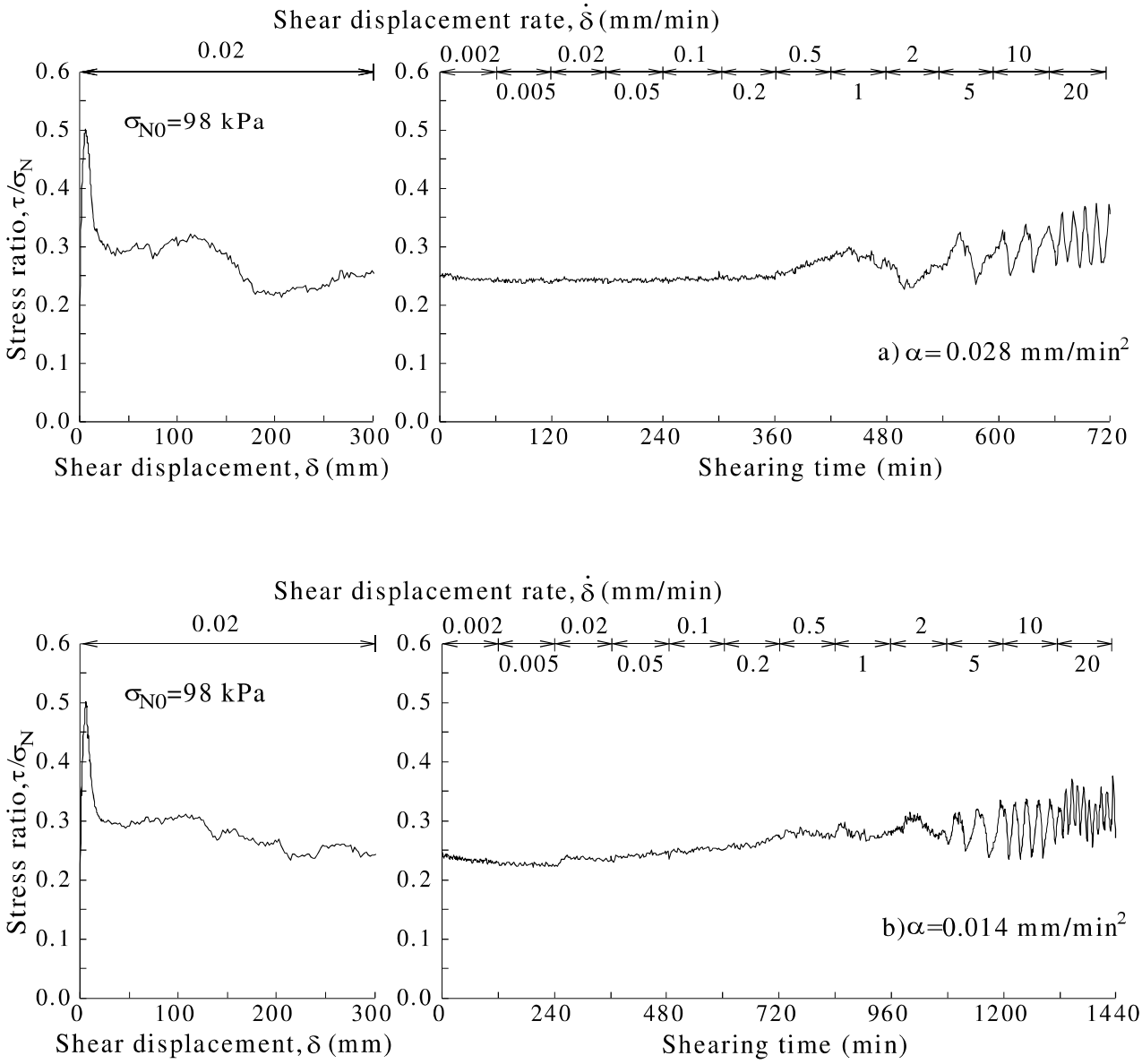

Figure 7.3. Results of multistage test for kaolin sample

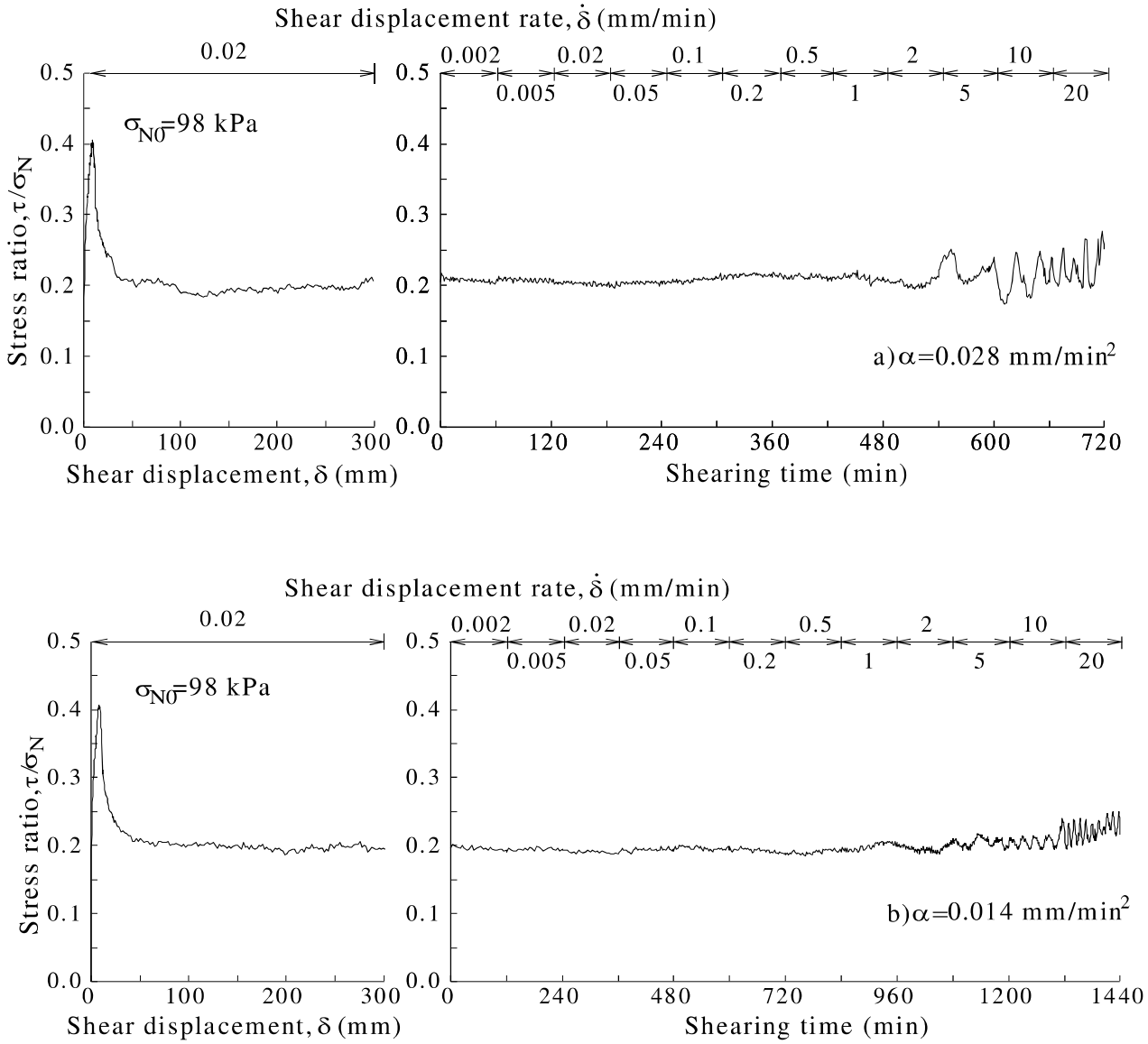

Figure 7.4 Results of multistage test for 10B sample

Figs. 7.3 and 7.4 show the fluctuations in the residual strength under fast shear rates. Accordingly, the fast residual strength sometimes decreased to less than the drained residual strength and sometimes increased to exceed the drained residual strength. A higher acceleration will lead to a higher cyclic increase or decrease in the measured shear strength. The cyclic increase or decrease in the measured shear resistance can be attributed to the cycles of extrusion and replacement of the clay particles by the undisturbed particles along the shearing zone. In addition, the load re-distribution between the two rings and the centre axle (machine effect) may cause fluctuations in the measured residual strength (Meehan et al., 2008).

The residual strength values at different shearing rates and shearing times are shown in Table 7.1.

Table 7.1 Test results at different shearing times and shear displacement rates

α=0.028 mm/min^2					α=0.014 mm/min^2				
Shear-ring time, t (min)	Shear displace-ment rate (mm/min)	Shear displa-cement (mm)	$(\tau/\sigma_N)_r$		Shear-ring time, t (min)	Shear displace-ment rate (mm/min)	Shear displa-cement (mm)	$(\tau/\sigma_N)_r$	
			Kaolin	10B				Kaolin	10B
0	0	0	0.234	0.197	0	0	0	0.245	0.193
60	0.002	0.12	0.243	0.204	120	0.002	0.24	0.230	0.193
120	0.005	0.3	0.242	0.207	240	0.005	0.6	0.225	0.194
180	0.02	1.2	0.244	0.201	360	0.02	2.4	0.234	0.193
240	0.05	3	0.244	0.204	480	0.05	6	0.241	0.194
300	0.1	6	0.246	0.210	600	0.1	12	0.249	0.193
360	0.2	12	0.248	0.215	720	0.2	30	0.263	0.193
420	0.5	30	0.284	0.212	840	0.5	60	0.269	0.193
480	1	60	0.271	0.207	960	1	120	0.271	0.200
540	2	120	0.267	0.209	1080	2	240	0.274	0.201
600	5	300	0.281	0.214	1200	5	600	0.284	0.204
660	10	600	0.315	0.221	1320	10	1200	0.296	0.218
720	20	1200	0.317	0.243	1440	20	2400	0.308	0.226

The relationships of the shear displacement and stress ratio in the residual state with respect to the shearing time for both samples are presented in Figs. 7.5(a)–(c). As shown in the figures, a higher acceleration is associated with higher residual strength. This is because of the positive rate dependency of the residual strength. In addition, Figs. 7.3, 7.4, and 7.5(b) and (c) indicate that the residual strength fluctuates more at higher acceleration rates than at lower acceleration rates. This suggests that higher acceleration may lead to more disordering of the particles within the shear surface.

The stress ratio $(\tau/\sigma_N)_r$ at different accelerations is presented in Table 7.2, and their relationship is shown in Fig. 7.6. The stress ratio was also determined based on the hyperbolic curve approximation method (Suzuki et al., 1997), and the coefficient of determination (R^2) was found to be above 0.98. The residual strength when the acceleration is zero (that is, the shear rate is constant) is calculated as the residual strength obtained from the full drainage shear stage (step 1).

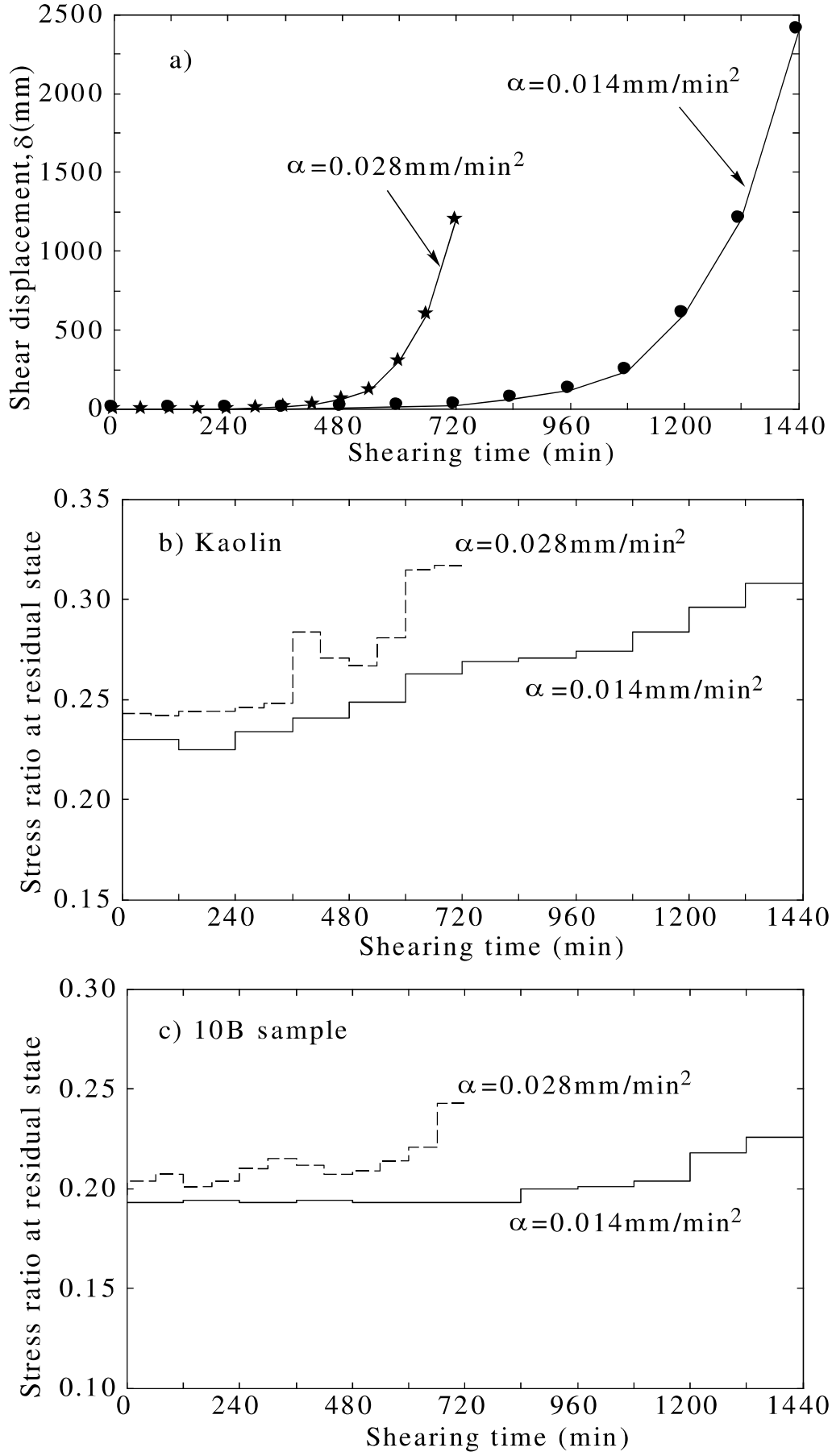

Figure 7.5 a) Shear displacement–time relationship, (b) Stress ratio at residual state–time relationship (Kaolin), and (c) Stress ratio at residual state–time relationship (10B sample)

Table 7.2 Test results at different accelerations

Sample	w_0 (%)	ρ_0 (g/cm^3)	S_{r0} (%)	α (mm/min^2)	σ_{Nr} (kPa)	$(\tau/\sigma_N)_r$	τ_r (kPa)	R^2
Kaolin	66.5	1.572	97.7	0.028	97.6	0.310	30.3	0.986
	68.5	1.568	98.3	0.014	97.4	0.308	30.0	0.986
10B	71.5	1.550	97.9	0.028	98.2	0.223	21.9	0.986
	70.2	1.558	98.1	0.014	97.7	0.223	21.8	0.994

σ_{Nr} : Average effective normal stress at residual state.

R: Coefficient of correlation.

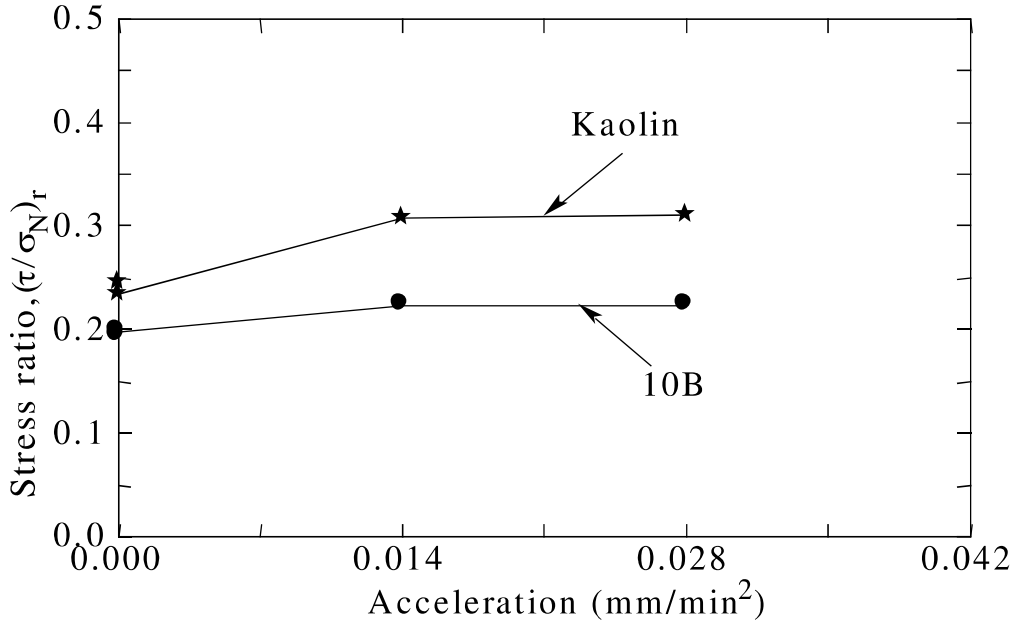

Figure 7.6 Acceleration and stress ratio at residual state

As presented in Fig. 7.6, the residual strength increases slightly as the acceleration changes from 0 to 0.014 mm/min^2 and from 0 to 0.028 mm/min^2. This increase was actually caused by the change in the shear displacement rate. However, when shearing at the same rate occurred for different lengths of time, the residual strength was almost identical at both acceleration rates. This indicates that, although higher acceleration may lead to greater fluctuations in residual strength, the effect of the acceleration on the overall residual strength is negligible. This means that the residual strength is not dependent on the acceleration of the landslide. In reality, many fast landslides are induced by earthquakes. The Newmark method (Newmark, 1965) has been widely used to evaluate the residual displacement of a rigid body after a slope fails due to an earthquake. Additionally, the residual strength is known to be dependent on the rate of movement, especially fast rates. Therefore, when evaluating the sliding displacement of slopes containing a pre-existing shear surface, using the Newmark method, the rate dependency of the residual strength should be considered.

7.3. Effect of test procedure on rate dependency of residual strength

The test results from the single- and multi-stage procedures are shown in Fig. 7.7. For kaolin, the residual strength obtained from the multi-stage procedure increases with an increase in the shear displacement rate, in agreement with the results from single-state shearing. This suggests that the multi-stage procedure with shearing times of 60 min and 120 min for each shear rate level can be used to evaluate the rate effect on the residual strength of kaolin, thus reducing the duration of testing. As kaolin has a relatively high permeability, the excess pore water pressure will be low in the residual state, even in faster single-stage testing.

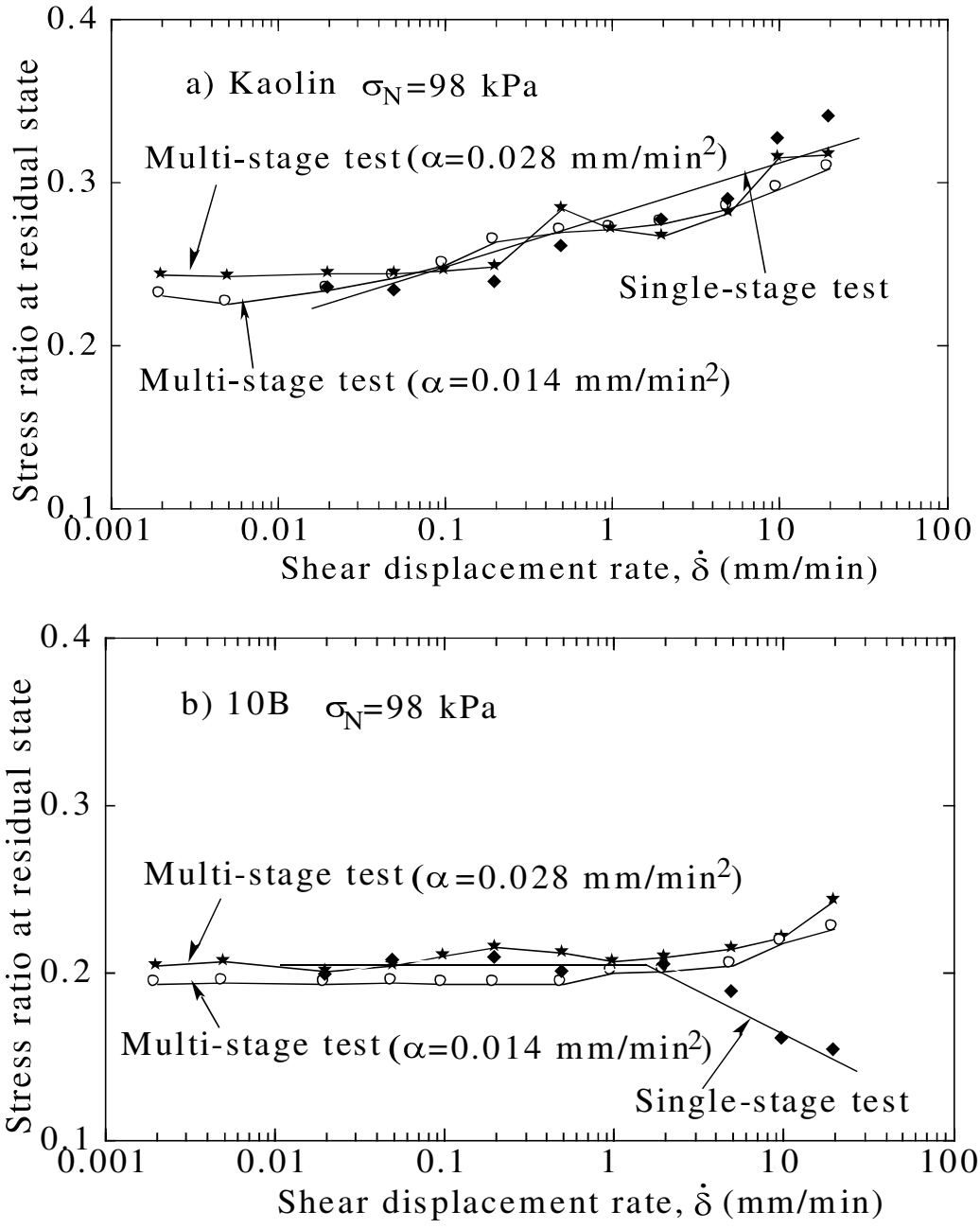

Figure 7.7 Test results for single-stage and multi-stage shear rate procedure

Unlike kaolin, the change in the residual strength of the 10B sample in both the single- and multi-stage shear rate procedures became inverted at shear rates above 2 mm/min. In the single-stage procedure, the fast residual strength exhibited a decreasing trend with increasing shear rates. In contrast, 10B exhibited an increasing trend (positive rate effect) in the multi-stage procedure. The positive rate effect was also observed in sand mixtures with more than 50% bentonite or kaolin in the multi-stage shear rate procedure (Scaringi and Di Maio, 2016). The difference in the rate effect between single- and multi-stage procedures can be attributed to the magnitude of the excess pore water pressure generated during shearing. In the multi-stage procedure, the sample was first sheared in the fully drained condition. Even under the fast shear rate, the specimen reached the residual state; and thus, the excess pore water pressure may be lower and have less of an effect on the fast residual strength. As with kaolin, the increase in residual strength in the multi-stage procedure was caused by the change in the shear mode and the extrusion of soil through the gap between the upper and lower rings. Moreover, as mentioned above, the increase in the fast residual strength might be related to the shear viscosity effect. The viscosity of the 10B sample was much higher than that of kaolin (Iannicelli and Millman, 1966). In the multi-stage procedure, the generation of excess pore water pressure was negligible, so the effect of shear viscosity was dominant. Therefore, unlike the kaolin sample, the shear viscosity effect may lead to an increase in the residual strength of the mixture samples with an increasing shear displacement rate in the multi-stage procedure. Additionally, the change in the rate effect on the residual strength of the 10B sample, from negative to positive when changing the test procedure from single-stage to multi-stage, indicates that the tendency of the rate effect coefficient with respect to certain soil properties may not be generalized. The test results from the multi-stage procedure accurately reflect the rate dependency of residual strength of the 10B sample. Therefore, the multi-stage test procedure should be considered when evaluating the rate dependency of residual strength for low-permeability, high-plasticity soil.

7.4. Summary

Chapter 7 presented the results of ring shear tests on two samples (kaolin and 10B) at different acceleration rates. At each acceleration level, the multi-stage procedure in which the shear displacement rate is increased continuously from 0.002 mm/min to 20 mm/min, was employed. The test results clarified the effect of acceleration on the behaviour of shear strength at the residual state. In addition, the effect of the test procedure on the rate dependency of the residual strength was also investigated based on the results of single- and multi-stage procedures for increasing the shear rates. The main results of this chapter can be summarised as follows:

1. At fast shear rates, the residual strength sometimes decreases to less than the drained residual strength and sometimes increases to exceed the drained residual strength. A higher acceleration may lead to a higher cyclic increase or decrease in the measured residual shear strength. This phenomenon can be attributed to the machine effect and the cycles of soil extrusion and replacement by undisturbed particles along the shearing surface.

2. Higher acceleration might lead to greater fluctuations in the residual strength. However, it does not seem to have an effect on the overall residual strength. Therefore, the acceleration effect can be ignored in the determination of residual strength and in slope stability analyses.

3. The test procedure may affect the type of rate effect on the residual strength of some soils. For kaolin clay, the positive rate effect on the residual strength persists, irrespective of the test procedure. However, for the 10% bentonite–90% kaolin mixture sample (10B), having a very low permeability coefficient, the rate effect on the residual strength changed from a negative rate effect in the single-stage procedure to a positive one in the multi-stage procedure. In the multi-stage procedure, the positive rate effect may be caused by structural changes, soil extrusion through the gap, and/or the shear viscosity effect.

CHAPTER 8. APPLICABILITY OF RESEARCH RESULTS

8.1. Introduction

As described in the above chapters, the shear strength of clay may increase or decrease as the shear displacement rates increase. Thus, the shear displacement rate-dependent increase/decrease in the residual strength will affect the displacement and stability of slopes. If the rate effect on the residual strength is positive, the increase in the shear displacement rate-induced additional strength will resist the sliding. The velocity will decelerate and the slide will come to a rest. In this case, the instability of the slope is restrained. In contrast, if the rate effect is negative, the residual strength will decrease to below the slow residual value. The velocity and displacement will accelerate to potentially catastrophic slides. The rate dependency of the residual strength was used to establish a soil model linking the shear strength on the pre-existing shear surface with the displacement and displacement rates (Skempton et al., 1989; Lemos and Coelho, 1991).

Skempton et al. (1989) analysed the displacement and stability of slopes containing shear zones in the Mam Tor landslide with regard to the positive shear rate effect and the increase in pore water pressure due to rainstorms under static conditions. While an increase in pore water pressure in the shear zone will lead to a decrease in the shear strength, the positive rate effect will result in an increase in the shear strength in the shear zone. Thus, the displacement can be limited to a finite amount. The research results indicated that the rate of movement slowly decreases over the long term and the landslide comes to a rest condition in which the equilibrium can be maintained even under the heaviest rainfall.

Lemos and Coelho (1991) established the constitutive soil model, based on the Newmark method (Newmark, 1965), to predict the displacement and rate of the shear displacement of first-time landslides under the dynamic (earthquake) condition. The research results showed that the reduction in shear strength with the model, giving consideration to the rate effect, was slower than that observed in the laboratory tests. The disturbance of the clay particles in the shear zone at fast shearing affected the rate of reduction in shear strength in the model. Based on the earthquake-induced displacement, these authors showed that the final displacement without the rate effect consideration was about 5-10 times higher than that with the rate effect consideration, for values of a_c/PGA less than 0.5 (a_c-critical acceleration and PGA-peak ground acceleration). However, in this soil model, the critical acceleration remained unchanged during sliding.

In fact, the critical acceleration can change during sliding due to the rate effect on the shear strength. In this chapter, an estimation procedure for the earthquake-induced velocity and displacement of a sliding block at the residual state with the rate dependency of the residual strength, will be presented.

8.2. Earthquake-induced displacement of sliding block

8.2.1. The Newmark method

The Newmark method was proposed by Newmark (1965) and has been widely used to calculate the earthquake-induced displacements of blocks sliding on a plane, dam, embankments, and natural slopes. For slopes, this method models a landslide mass as a single rigid-plastic block with a resistance mobilized along the sliding surface and having a known yield acceleration of (a_c=$K_y g$) (with K_y is the yield seismic coefficient and g is the gravity acceleration) (Fig. 8.1). The yield acceleration is the minimum ground acceleration required to overcome the resistance and cause the failure of a slope or foundation. For a dynamic analysis, the lowest safety factor may not be the most critical one. The most important parameter for seismic analysis is the relationship between the critical acceleration (a_c) and the ground acceleration (a_g). If the earthquake-induced ground acceleration exceeds the yield or critical acceleration, then sliding will occur. Hence, with an earthquake-strong motion record, the parts of the motion record that lie above the critical acceleration will be integrated to derive the velocity-time profile; the velocity-time profile is then integrated to obtain the cumulative displacement of the landslide block.

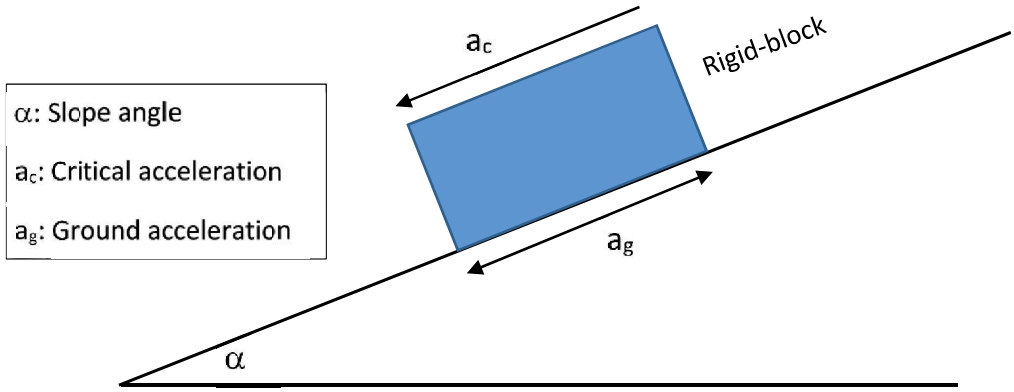

Figure 8.1 Model of rigid-block sliding analysis

Besides the rigid-plastic body assumptions, the Newmark method has some other assumptions for simplicity:

-The shearing resistance of soil is the same under static and dynamic conditions;

-The critical acceleration (or the critical seismic coefficient, *Ky*) is constant during sliding;

-The effect of the dynamic pore water pressure is neglected.

8.2.2. Estimation of block sliding displacement considering the rate effect

In fact, the critical acceleration (a_c) is a function of the geometry and shear strength of the sliding mass corresponding to a safety factor of one. Therefore, changes in geometry, the

deformation within the sliding mass, changes in the shear strength on the shear slip, and changes in the pore water pressure during sliding should be taken into account.

As described above, the residual strength is significantly affected by the increase in shear displacement rates. Thus, a change in the residual strength along the sliding surface will lead to a change in the critical seismic coefficient (*Ky*). In this study, changes in the residual strength during sliding will be considered when evaluating the critical acceleration.

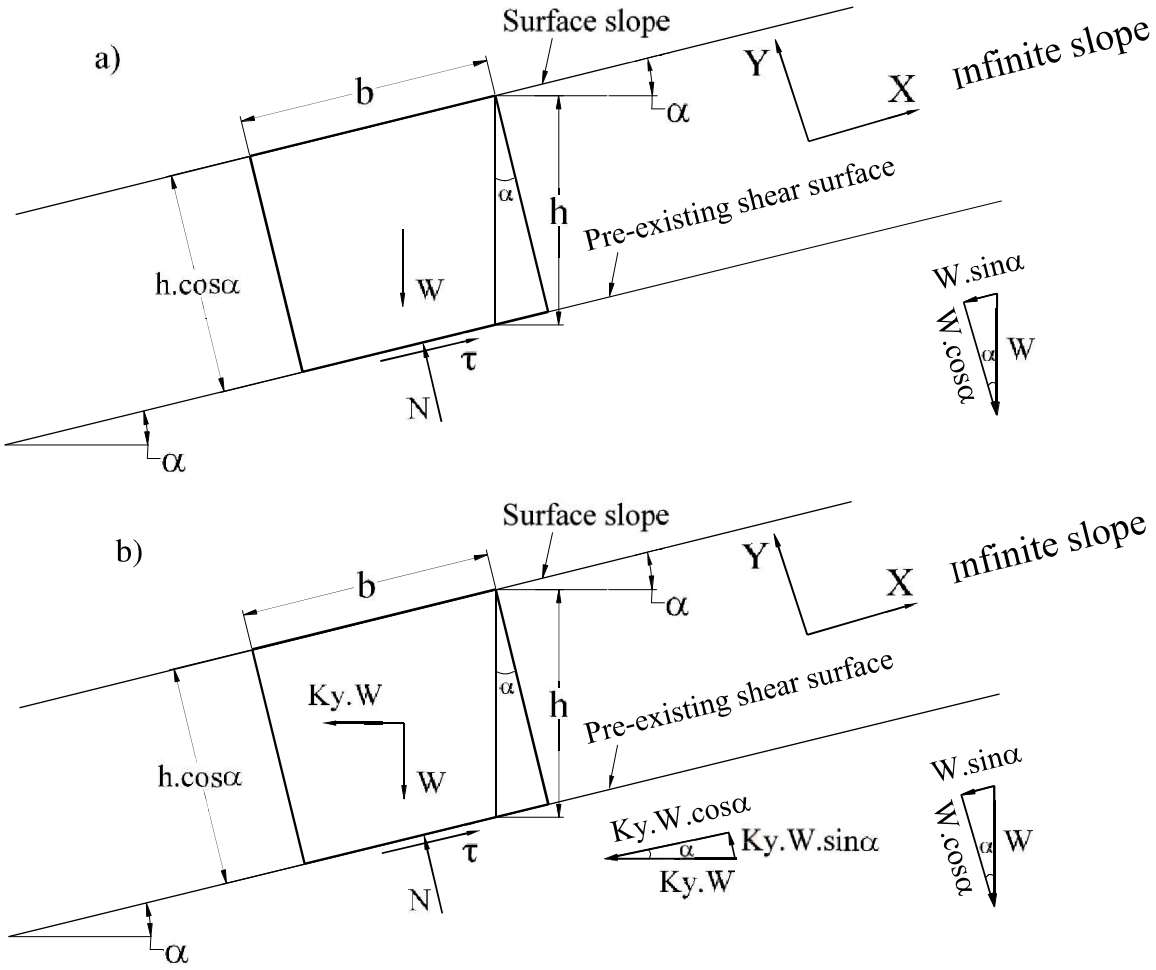

Figure 8.2 Forces acting on single soil block of infinite slope: a) Static and b) Dynamic

The Newmark method will be employed to estimate the displacement of a block sliding at the residual state based on the shear rate dependency of the residual strength. The single soil block on the infinite slope with a pre-existing shear surface (Fig. 8.2) will be used to analyze and estimate the earthquake-induced displacement. The infinite slope is assumed to be at the residual state with a pre-existing shear zone; thus, the effect of the pore water pressure can be disregarded.

The forces acting on the soil block in the static condition are as shown in Fig. 8.2(a). The shear stress and effective normal stress acting on the single block are calculated as follows:

Shear stress: $\tau = \frac{W.\sin\alpha}{b} = \frac{\gamma.b.h.\cos\alpha.\sin\alpha}{b} = \gamma.h.\cos\alpha.\sin\alpha$

Effective normal stress: $\sigma' = \frac{N}{b} = \frac{W.\cos\alpha}{b} = \frac{\gamma.b.h.\cos^2\alpha}{b} = \gamma.h.\cos^2\alpha$

The shear strength mobilizes along the shear surface as follows:

$S = c_r + \sigma' tan\phi_r = \gamma.h.cos^2\alpha.tan\phi_r$

where:

α: Slope angle.

γ: Wet density of soil (kN/m^2)

c_r: Residual cohesion force. At the residual state, c_r is taken as being equal to zero.

ϕ_r: Residual friction angle (deg)

The static global safety factor (*FSt*) is defined as follows:

$$FSt = \frac{ShearStrength}{ShearStress} = \frac{S}{\tau} = \frac{\gamma.h.\cos^2\alpha.\tan\phi_r}{\gamma.h.\cos\alpha.\sin\alpha} = \frac{\tan\phi_r}{\tan\alpha}$$

The critical seismic coefficient (*Ky*) for an infinite slope is calculated as follows:

$$K_y = (FSt - 1).sin\alpha \qquad (8.1)$$ (Newmark, 1965)

The forces acting on the soil block in the dynamic (earthquake) conditions are as shown in Fig. 8.2(b). The shear stress and effective normal stress acting on the shear surface can be expressed as follows:

Shear stress: $\tau = \frac{W(\sin\alpha + K_y.\cos\alpha)}{b}$

$$N = W.cos\alpha - W.K_y.sin\alpha$$

The effective normal stress acts on the shear surface: $\sigma' = \frac{N}{b} = \frac{W(\cos\alpha - K_y.\sin\alpha)}{b}$

The shear strength mobilizes on the shear zone:

$$S = \sigma'.tan\phi_r \quad (c_r=0)$$

$$S = \frac{W.(cos\alpha - Ky.sin\alpha).tan\phi_r}{b}$$

The dynamic safety factor (*FSd*) is defined as follows:

$$FSd = \frac{S}{\tau} = \frac{(cos\alpha - Ky.sin\alpha).tan\phi_r}{(sin\alpha + Ky.cos\alpha)}$$

At a critical condition, *FSd* = 1 or $FSd = \frac{(\cos\alpha - K_y.\sin\alpha).\tan\phi_r}{(\sin\alpha + K_y.\cos\alpha)} = 1$

$$K_y = \frac{\cos\alpha.\tan\phi_r - \sin\alpha}{\cos\alpha + \sin\alpha.\tan\phi_r} = \frac{\tan\phi_r - \tan\alpha}{1 + \tan\phi_r.\tan\alpha} = \tan(\phi_r - \alpha) \qquad (8.2)$$

The above formula (8.2) shows that critical seismic coefficient K_y is a function of ϕ_r (slope angle α is constant during sliding). Therefore, K_y will change as residual strength ϕ_r changes. In other words, K_y is the shear rate-dependent (velocity-dependent) behaviour.

Fig. 8.3 shows the typical earthquake acceleration-time history. The earthquake-induced velocity and displacement of the sliding block can be estimated based on the single and double integration of the acceleration-time record, respectively (Berg and Housner, 1961).

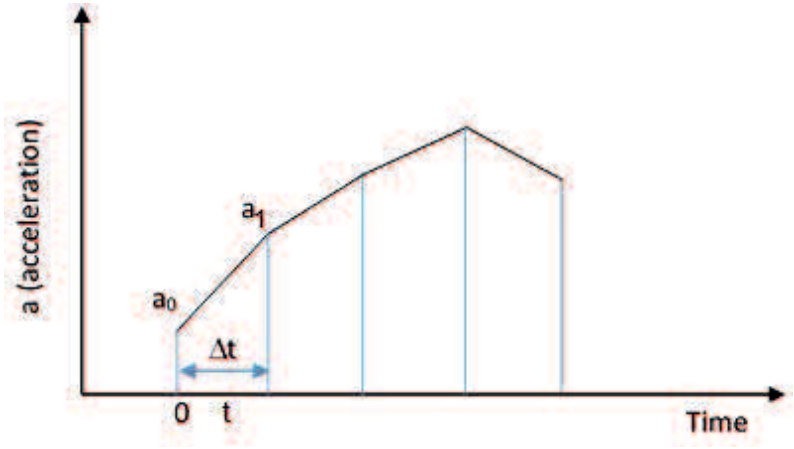

Figure 8.3 Typical earthquake-induced acceleration-time record

$$\Delta a = \frac{1}{\Delta t}(a_1 - a_0)$$

$$a(t) = a_0 + t\Delta a$$

The accumulated velocity is: $v(t) = v_0 + \int_0^t a(t)dt = v_0 + \int_0^t (a_0 + t\Delta a)dt$

$$v(t) = v_0 + a_0 t + \frac{t^2}{2}\Delta a \text{ or } v(t) = v_0 + a_0 t + \frac{t^2}{2}.\frac{1}{\Delta t}(a_1 - a_0)$$

At t=Δt, the accumulated velocity is:

$$v_1 = v_0 + \frac{\Delta t}{2}(a_0 + a_1) \qquad (8.3)$$

The displacement is: $d(t) = d_0 + \int_0^t (v_0 + a_0 t + \frac{t^2}{2}\Delta a)dt$

$= d_0 + v_0 t + \frac{t^2}{2}a_0 + \frac{t^3}{6}\Delta a = d_0 + v_0 t + \frac{t^2}{2}a_0 + \frac{t^3}{6}.\frac{1}{\Delta t}(a_1 - a_0)$

At t=Δt, the displacement will be:

$$d_1 = d_0 + v_0\Delta t + \frac{\Delta t^2}{6}(2a_0 + a_1) \qquad (8.4)$$

In the conventional Newmark method, the critical acceleration is assumed to remain constant during sliding. The block will start moving if the ground acceleration is higher than the critical acceleration (a_c).

In fact, the shear strength during sliding will change as the shear rate changes. Consequently, the critical acceleration that is a function of the safety factor (shear strength) will

change. When considering the rate effect, the critical acceleration (a'_c) will be calculated based on the velocity which is integrated from the acceleration-time record. The velocity and displacement will then be estimated based on the relationship between a'_c and the ground acceleration. The procedure for this calculation is presented in the following flowchart (Fig. 8.4). Steps from 1 to 4 will be conducted until finally $a_g \leq a'_c$.

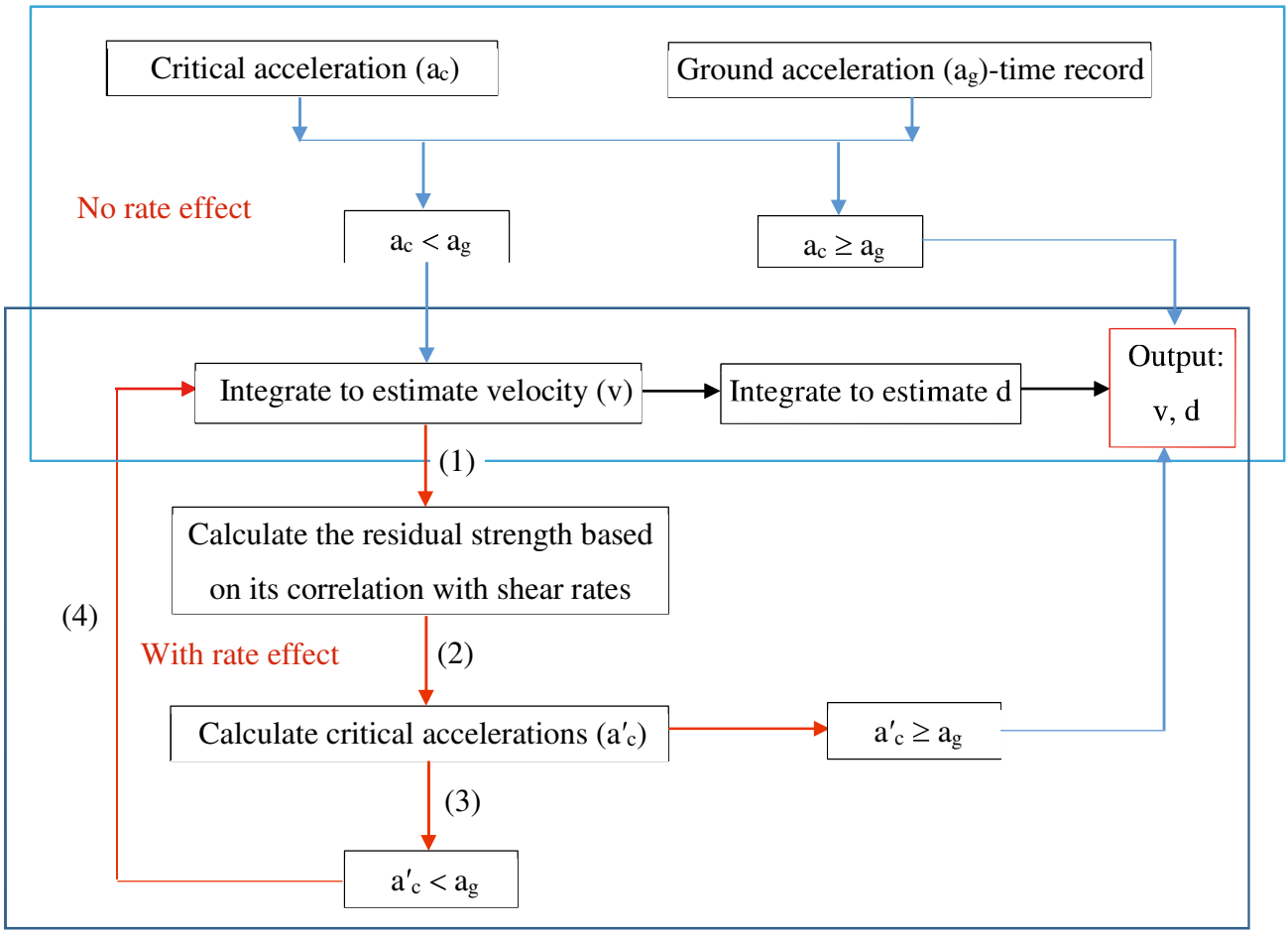

Figure 8.4 Estimation of earthquake-induced velocity and displacement

8.3. An example

Let us take the rate effect on the residual strength of the kaolin sample in this research as an example. The residual strength of kaolin increases linearly with the logarithm of the shear displacement rate (Fig. 4.2(a)). In other words, the residual strength is a function of the shear displacement rate. Based on the test results, the relationship between the residual strength of kaolin and the shear rates is shown in Fig. 8.5 and can be expressed by the following formula:

$$\tan\phi_r = (\tau/\sigma_N)_r = 0.0154\ln v + 0.2775 \quad (R^2 = 0.884) \qquad (8.5)$$

where: v is the shear displacement rate (mm/min) and ϕ_r is the residual strength.

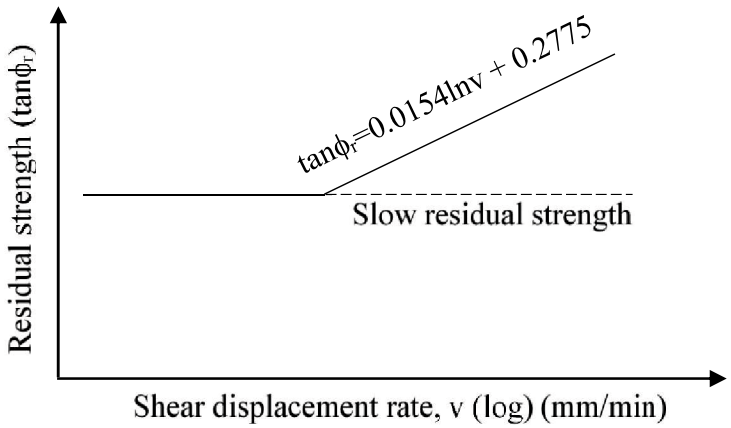

Figure 8.5 Relationship between residual strength of kaolin and shear rates

The infinite slope comprised of kaolin clay (residual strength of kaolin, $\tan\phi_r = 0.22$) has a slope angle (α) of 10^0. This angle is thought to remain constant during sliding. Based on the residual strength value of kaolin, the critical acceleration of this slope (a_c) is 0.04 g.

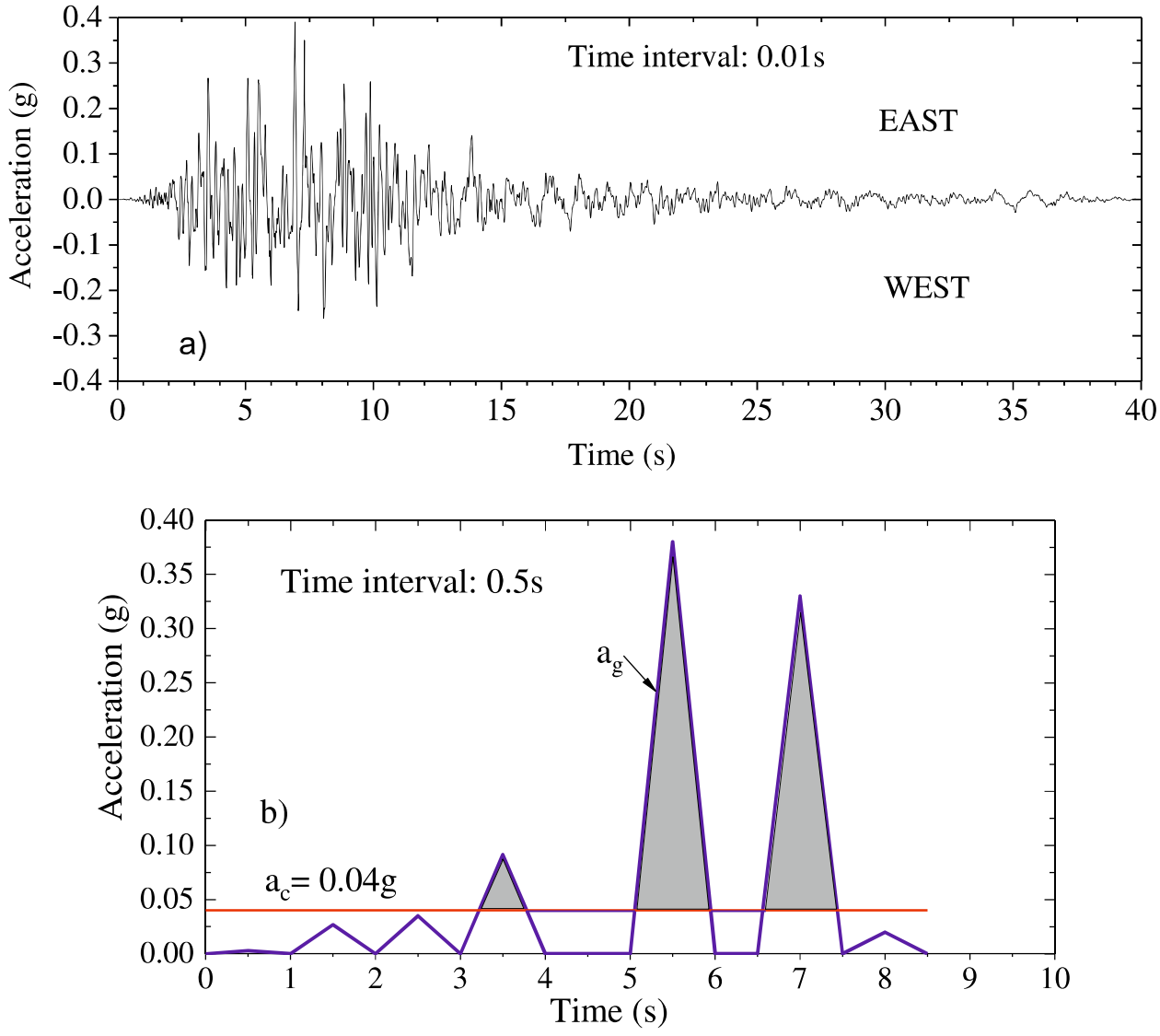

Figure 8.6 a) Earthquake-induced ground acceleration and b) Simplified ground acceleration

An earthquake-induced acceleration-time record will be used to estimate the velocity and displacement of the kaolin clay infinite slope with a pre-existing shear surface (Fig. 8.6(a)). In fact, the earthquake-induced acceleration is very complicated and causes movement, namely, deformation of the landslide block in multi-directions. However, in this study, to shorten the acceleration time and disregard the upslope displacement, the simplified acceleration-time record is used. It is presented in Fig. 8.6(b).

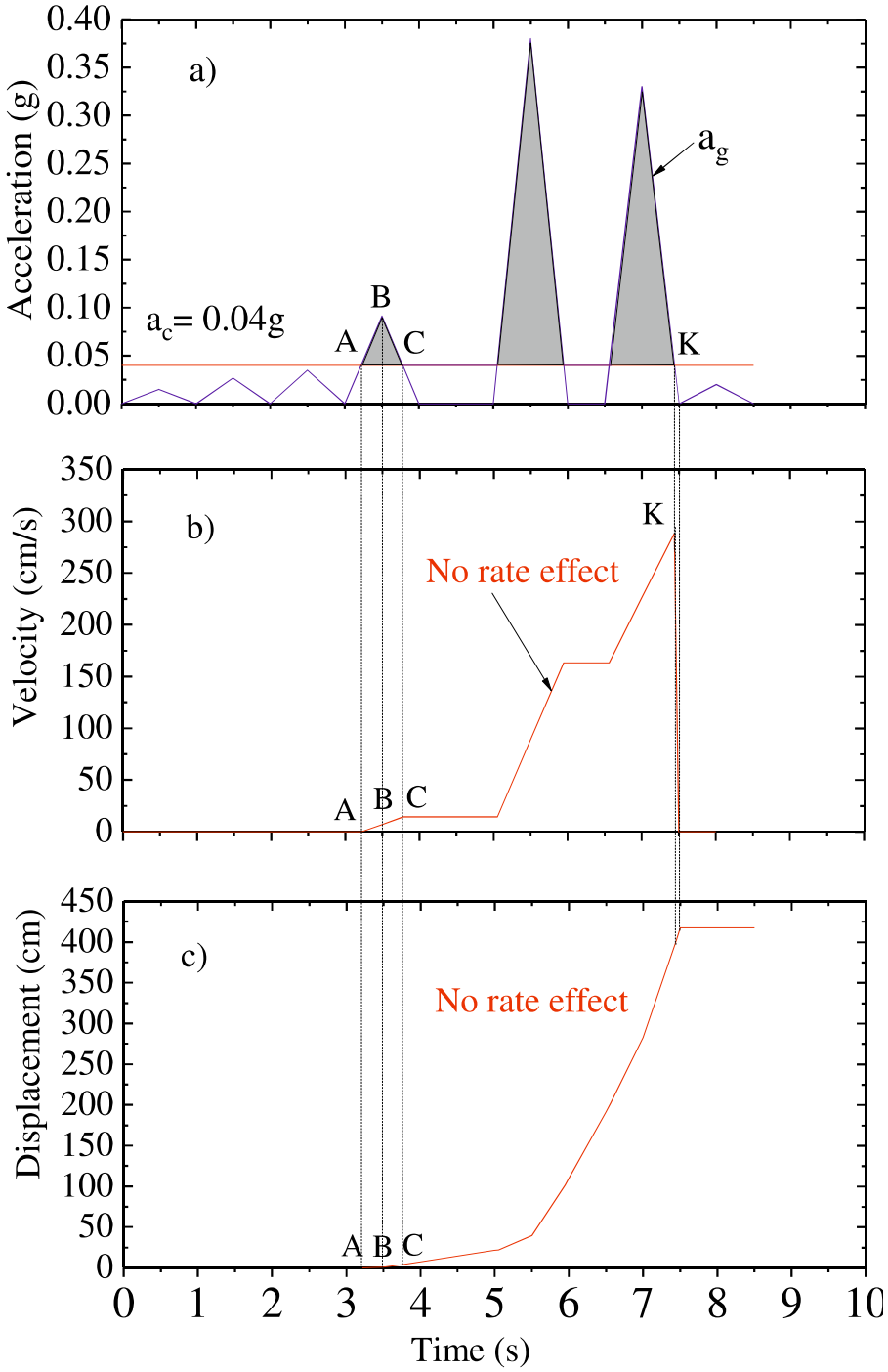

Figure 8.7 Strong ground motion-induced velocity and displacement with constant critical acceleration

Fig. 8.7(a) presents a simplified strong-motion record with constant critical acceleration a_c. To the left of point A, the ground acceleration is less than a_c; the velocity is then zero and no displacement occurs. To the right of point A, those parts of the ground acceleration lying above a_c are integrated over time to obtain the velocity and displacement profiles. In this research, the block is assumed to move only toward the downslope; and thus, the upslope displacement is ignored. Thus, to the right of point A (after starting to move), if the ground acceleration is less than or equal to a_c, the acceleration of the movement will be assumed to equal zero (velocity is constant). To the right of point K, if the ground acceleration is less than a_c, the velocity is zero and no displacement occurs. The estimated velocity and displacement with a constant critical acceleration are presented in Figs. 8.7(b) and (c). The estimated velocity is the area of the triangular pulse.

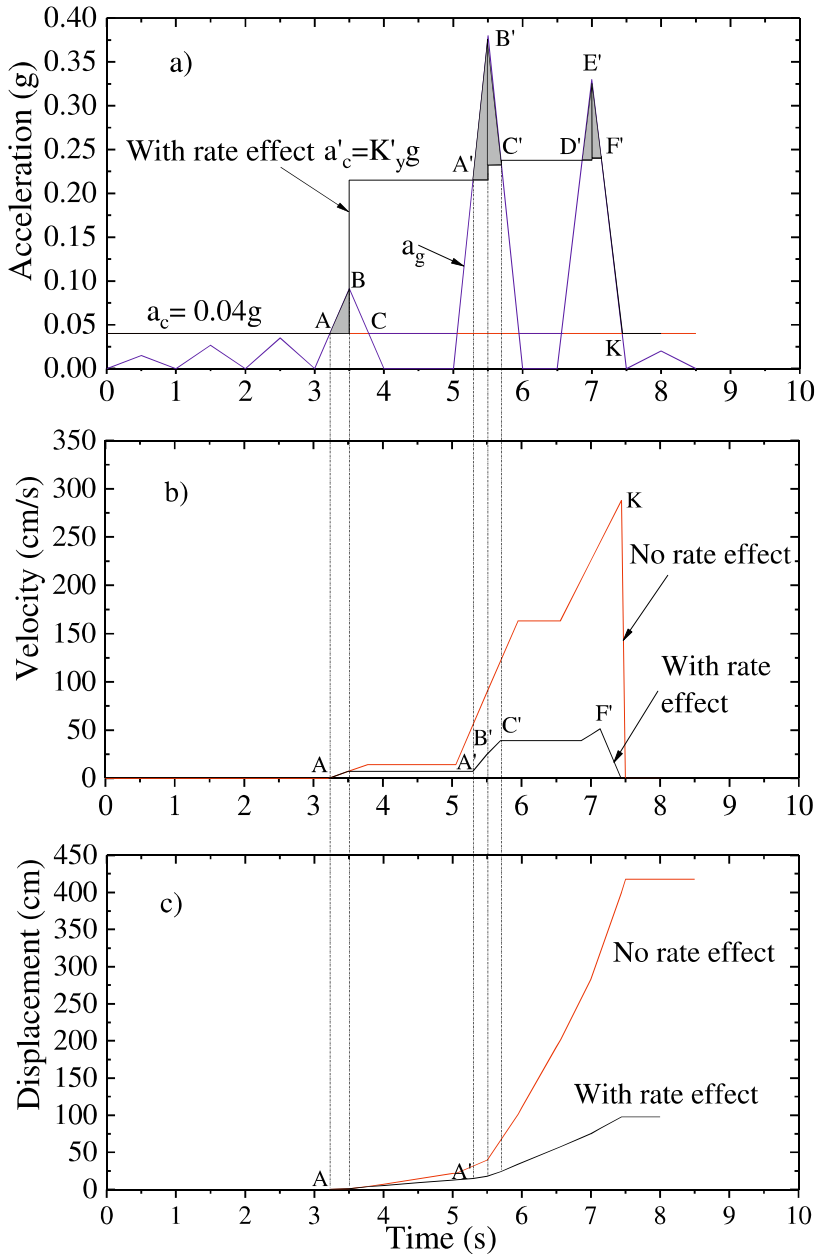

Figure 8.8 Strong ground motion-induced velocity and displacement with changes in critical acceleration

With regard to the rate effect, the residual strength during sliding is estimated based on the above formula (8.5) which is in correlation with the velocity. The residual strength is then used to calculate the critical acceleration. This critical acceleration will include the rate effect on the residual strength. The critical acceleration with the rate effect (a'_c) during sliding is shown in Fig. 8.8(a) with the assumption that a'_c is constant during time step Δt at which time a change in velocity take places. Based on the relationship between a'_c and the ground acceleration, the procedure for estimating the velocity (v) and displacement (d) is similar to that of the cases with no rate effect. The estimated velocity and displacement with the rate effect are shown in Figs. 8.8(b) and (c). A comparison of the estimations with and without the rate effect is shown in Table 8.1.

Table 8.1 Comparison of results with and without rate effect on residual strength

	Without rate effect	With rate effect
Maximum velocity (cm/s)	288.2	51.1
Maximum displacement (cm)	417.5	97.6

It can be seen that when the rate effect is considered, the estimated velocity and displacement of the block sliding at the residual state decreases significantly compared with the case when the rate effect is not considered.

8.4. Summary

In this chapter, the rate effect on the residual strength has been applied to estimate the earthquake-induced velocity and displacement of a block sliding at the residual state based on the Newmark method. The estimated velocity and displacement of the infinite slope of kaolin clay with a pre-existing shear surface and an inclination of 10^0 were investigated. The main results of this chapter can be summarized as follows:

1. The critical seismic coefficient is a function of the residual strength or the shear rate dependent behaviour. An estimation procedure for the earthquake-induced velocity and displacement with regard to the rate effect has been proposed.

2. The rate dependency of the residual strength substantially affects the estimation results of the earthquake-induced velocity and displacement of a block sliding at the residual state. The maximum velocity and displacement of the block sliding with the positive rate effect consideration are significantly smaller than those in the case of no rate effect consideration.

CHAPTER 9. CONCLUSIONS AND RECOMMENDATIONS

9.1. Conclusions

This research was a laboratory-based experimental study of the rate and acceleration effects on the shear strength of various clays in ring shearing. A number of kaolin and kaolin-bentonite mixture samples were used to investigate the rate effect on the residual strength of high-plasticity, low-permeability clay in the range of shear rates from 0.02 to 20 mm/min. In addition, a number of specimen assemblies, comprised of one kaolin layer and one kaolin-bentonite mixture layer were used to investigate the rate dependency of the residual interface strength. Ring shear tests with different shear rates were also conducted on kaolin clay with different overconsolidation ratios (OCRs) ranging from 1 to 6. The acceleration effect on the residual strength was investigated on kaolin and 90% kaolin-10% bentonite samples with acceleration rates of 50.4 mm/h^2 and 100.8 mm/h^2. All the experiments in this research were conducted with a conventional Bishop-type ring shear apparatus. The single- and multi-stage procedures with increasing shear rates and decreasing normal stress levels were applied in ring shear tests. Finally, the rate dependency of the residual strength of kaolin clay was applied to estimate the earthquake-induced velocity and displacement of a block sliding on an infinite slope using the Newmark method. The conclusions from the analysis of the research results can be summarised as follows:

1. The bentonite content significantly affects not only the residual strength, but also its rate dependency. Although the addition of bentonite to kaolin samples leads to insignificant changes in the clay content, it also leads to a significant decrease in the permeability coefficient and affects the rate dependency of the shear strength, especially the residual strength.

2. The rate dependency of the residual strength is related to certain soil properties (clay fraction and plasticity index). This indicates that the rate effect on the residual strength can be affected and changed by the physical properties of the soil.

3. The type of rate effect depends not only on the soil properties, but also on the test procedure used to change the shear displacement rates, especially for a very low permeability clay. Therefore, the multi-stage procedure should be used to evaluate the rate dependency of the residual strength for reactivated landslides in low-permeability soil.

4. The residual interface strength and its rate dependency significantly depended on the characteristics of the contact material. The residual interface strength also shows stress-dependent behaviour. However, the effect of normal stress on the magnitude of the positive dependency of the residual interface strength also depends on the contact material.

5. The negative rate effect on the residual strength of high-plasticity, low-permeability clay can be attributed to the delayed dissipation of the shear-induced pore water pressure and to the

increase in water content within the shear zone with the increasing shear rates. On the other hand, the positive rate effect can be attributed to the structural changes (from sliding to turbulent), soil extrusion through the gap (machine effect), and the shear viscosity effect.

6. The rate dependency of the shear strength is found to be dependent on the stress history (OCR). For the peak strength, the rate effect on the shear strength changes from negative to positive when the OCR changes from NC to OC conditions. As opposed to the peak strength, the positive rate effect on the residual strength is not related to the OCR. However, the magnitude of the positive rate effect coefficient tends to decrease as the OCR increases.

7. The effect of the OCR on the rate dependency of the shear strength leads to the difference in the variations in cohesion and internal friction angles of OC clay at peak and residual states. In addition, the independence of the peak friction angle with an increasing shear rate indicates that it is almost independent of the negative pore water pressure.

8. The residual strength of OC clay can be determined based on the multi-stage procedure for decreasing the normal stress in order to reduce the test duration. However, this multi-stage procedure should not be used to determine the residual strength of OC clay at shear rates above 0.5 mm/min.

9. Higher acceleration might lead to greater fluctuations in the residual strength. However, it does not seem to have an effect on the overall residual strength. This indicates that the rate effect should be considered, rather than the acceleration effect, when determining the residual strength by ring shearing. Therefore, when reactivated landslides reach the stage of tertiary creep, the residual strength of the soil mobilized on a slip surface can be influenced by the sliding velocity but not by the acceleration.

10. The rate effect on the residual strength can be used to explain and predict the behaviour of reactivated landslides. In addition, the rate dependency of the residual strength should be taken into account when using the Newmark method to estimate the earthquake-induced velocity and displacement of a sliding block.

9.2. Limitations and recommendations

a. Limitations of the research

This research has contributed to and filled in the gap in literature concerned with the rate dependency of the shear strength of high-plasticity, low-permeability clays and of OC clays in ring shearing. In addition, the rate dependency of the residual interface strength between two different soil layers has been extensively studied. The causes of the rate effect on the residual strength have been clearly interpreted based on the changes in volume, the changes in water content within the shear zone, and the changes in the void ratio after shearing. The relationships between the rate

dependency of the residual strength and the clay fraction, the plasticity index, and the OCR have been investigated and established. The acceleration effect on the residual strength has been clarified. Regarding the application of the rate effect on the residual strength, an estimation procedure of velocity and displacement for the velocity and displacement of an infinite slope at the residual state under earthquake conditions has been introduced. However, this research has the following several limitations:

1. During shearing at different shear rates, the shear-induced pore water pressure may affect the shear strength at both peak and residual states, especially for low permeability clays and at fast shearing. However, the generation and dissipation of pore water pressure were not measured during shearing.

2. The shear surface structure of OC clay can be disturbed by the dilation effect. This disturbance may affect the residual strength, especially at fast shearing. In addition, the thickness of the shear zone within the specimen can be affected by soil extrusion which, in turn, can then influence the measured strength. However, the structure and thickness of the shear zone were not observed after shearing.

3. In this research, the rate dependency of the residual strength was just applied to investigate the earthquake-induced velocity and displacement of a block sliding on a kaolin clay infinite slope. In addition, some assumptions have been used and some factors affecting the critical acceleration were ignored in order to simplify the model when using the Newmark method to estimate the earthquake-induced displacement. Moreover, the estimation results were not compared to the results of an actual case. However, this research also provides a means of evaluating the application of the rate effect to estimate earthquake-induced landslides.

b. Recommendations for future research

Based on the limitations of this research, some suggestions for the future research are proposed as follows:

1. The shear-induced pore water pressure should be measured to examine its effect on the shear strength in ring shearing in more detail.

2. The shear surface structure of OC clays can be disturbed during shearing due to the dilation process. The disturbance of the shear zone is different at different OCRs and different shear rates, especially at fast shear rates. Therefore, it would be better if scanning electron microscopy (SEM) were employed to observe the shear surface microstructure after shearing. In addition, the thickness of the shear zone within the specimen after shearing should be measured.

3. The rate dependency of the residual strength was applied to estimate the earthquake-induced displacement of an infinite slope with a pre-existing shear surface. However, more

research should be conducted on a slope with a circular sliding shear surface. In addition, the effect of the dynamic pore water pressure should be considered in the analysis. Moreover, the estimation of the earthquake-induced velocity and displacement of a sliding block with regard to the rate dependency of the residual strength should be conducted and compared to the results of an actual case.

REFERENCES

Anayi, J. T., Boyce, J. R., Rogers, C. D., 1988. Comparison of alternative methods of measuring residual strength of a clay. Transportation Research Record 1192, 16–26.

Anderson, W. F., Hammoud, F., 1988. Effective of testing procedure in ring shear tests. Geotech. Test. J. 11(3), 204–207.

Asaoka, A., Nakano, M., Noda, T., 1994. Soil-water coupled behaviour of saturated clay near/at critical state. Soils and Founds. 34(1), 91–105.

Asaoka, A., Noda, T., Nakano, M., Kaneda, K., 1998. Undrained creep rupture of normally consolidated clay due to bifurcation mode switching during pore water migration. Proc. 4th. European Conf. on Numerical Methods in Geotech. Eng – NUMGE98, 243–252.

Askarani, K. K., Pakbaz, M. S., 2016. Drained shear strength of over-consolidated compacted soil-cement. Journal of Material in Civil Engineering, ASCE 25, No 5.

ASTM D6467–99. Standard test method for Torsional ring shear test to determine drained residual shear strength of cohesive soils

Augustesen, A., Liingaard, M., Lade, P. V., 2004. Evaluation of time-dependent behavior of soils. International Journal of Geomechanics 4(3), 137–156.

Berg, G. V., Housner, G. W., 1961. Integrated velocity and displacement of strong earthquake ground motion. Bulletin of the Seismological Society of America, 51 (2), 175–189.

Bhandary, N. P., Yatabe, R., Takata, S., 2005. Chapter 27. Clay mineral contributing to creep displacement of fracture zone landslides in Japan. In Proceedings of Landslides: Risk analysis and sustainable disaster management, 219–223.

Bhat, D. R., 2013. Effect of shearing rate on residual strength of Kaolin clay. Electronic Journal of Geotechnical Engineering (EJGE) 18, 1387–1396.

Bhat, D. R., Bhandery, N. P., Yatabe, R., Tiwari, R. C., 2011. Residual state-creep test in modified torsional ring shear machine methods and implications. Int. J. of GEOMATE 1 (1), 39–43.

Bhat, D. R., Yatabe, R., 2015. Effect of shearing rate on residual strength of landslide soils. Engineering Geology for Society and Territory 2, 1211–1215.

Bhat, D. R., Yatabe, R., Bhandary, N. P., 2013. Study of preexisting shear surfaces of reactivated landslides from a strength recovery perspective. J. of Asian Earth Sciences 77, 243–253.

Bishop, A. W., Green, G. E., Garga, V. K., Anderson, A., Brown, J. D., 1971. A new ring shear test apparatus and its application to the measurement of residual strength. Géotechnique 21(4), 273–328.

Bromhead, E. N., 1979. A simple ring shear apparatus. Ground Engineering 12(5), 40–44

Bromhead, E. N., 2004. Landslide slip surfaces: their origins, behavior, and geometry. Landslides: Evaluation and Stabilization 1, 3–22.

Bromhead, E. N., 2013. Reflections on the residual strength of clay soils, with special reference to bedding-controlled landslides. Quarterly J. of Eng. Geol. and Hydrogeo. 46, 132–155.

Bromhead, E. N., Ibsen, M, L., 2004. Bedding-controlled coastal landslides in Southeast Britan between Axmouth and the Thames Estuary. Landslides 1, 131–141.

Carlà, T., Intrieri, E., Farina, P., Casagli, N., 2017. A new approach to assess the stability of rock slopes and identify impending failure conditions. Advancing culture of living with landslides, volume 2 – Advances in Landslide Science (4th World Landslide Forum), 733–748.

Carrubba, P., Colonna, P., 2006. Monotonic fast residual strength of clay soils. Italian Geotechnical Journal 3, 32–51.

Cassgrande, A., Wilson, S. D., 1951. Effect of rate of loading on the strength of clays and shales at constant water content. Géotechnique 2(3), 251–263.

Chen, X. P., Liu, D., 2013. Residual strength of slip zone soils. Landslides 11, 305–314.

Chigara, M., Yagi, H., 2006. Geological and geomorphological characteristics of landslides triggered by the 2000 Mid Niigata prefecture earthquake in Japan. Eng. Geol 82, 202–221.

Chowdhury, R. N., Bertoldi, C., 1977. Residual shear tests on soil from two natural slopes. Australian Geomechanics Journal, 1–9.

Cruden, D. M., Varnes, D. J., 1996. Landslide types and processes. In Landslides: Investigation and Mitigation. Transportation Research Board, Special report 246, National Research Council, National Academy Press, Washington D.C., 36–75.

Dai, F. C., Lee, C. F., Ngai, Y. Y., 2002. Landslide risk assessment and management: an overview. Eng. Geol. 64, 65-87.

Diaz-Rodriguez J. A., Martinez-Vasquez, J. J., Santamarina, J. C., 2009. Strain-rate effects in Mexico City soil. J. Geotech. Geoenviron. Eng. (ASCE) 135(2), 300–305.

Fanyu, Z., Gonghui, W., Toshitka, K., Wnewu, C., Dexuan, Z., Jun, Y., 2013. Undrained shear behavior of loess saturated with different concentrations of sodium chlorite solution. Engineering Geology 155, 69–-79.

Fredlund, D. G., Xing, A., Fredlund, M. D., Barbour, S. L., 1995. The relationship of the unsaturated soil shear strength function to the soil-water characteristic curve. Can. Geotech. J. 32, 440–448.

Fukuoka, H., Sassa, K., 1991. High-speed high-stress ring shear tests on granular soils and clayey soils. The XIX World Congress of the International Union of Forestry Research Organizations, Canada, 33–41.

Gibo, S., Egashira, K., Ohtsubo, M., 1987. Residual strength of smectite-dominated soils from the Kamenose landslide in Japan. Can. Geotech. J. 24, 456–462.

Glastonbury, J., Fell, R., 2008. Geotechnical characteristics of large slow, very slow, and extremely slow landslides. Can. Geotech. J. 45, 984–1005.

Graham, J., Crooks, J. H. A., Bell, A. L., 1983. Time effects on the stress-strain behavior of natural soft clays. Géotechnique 33(3), 327–340.

Gratchev, I., Sassa, K., 2015. Shear strength of clay at different shear rates. J. Geotech. Geoenviron. Eng. (ASCE) 141(5), 1–3.

Gratchev, I., Sassa, K., Fukuoka, H., 2005. The shear strength of clayey soils from reactivated landslides. Annual of Disaster Prevention Research Institute, Kyoto, No 48, 431–438.

Gylland, A. S., Jostad, H. P., Nordal, S., 2014. Experimental study of strain localization in sensitive clays. Acta Geotechnica, 9, 227–240.

Han, J., Dano, C., Hicher, P.Y., Yin, Z.Y., 2014. Strain-rate dependency of shear strength for a highly overconsolidated clay. Geo-Shanghai, Soil Behavior and Geomechanics, 343–352

Hanzawa, H., Adachi, K., 1983. Overconsolidation of alluvial clays. Soils and Founds 23(4), 106–118.

Has, B., Nozaki, T., 2014. Role of geological structure in the occurrence of earthquake-induced landslides, the case of the 2007 Mid-Niigata Offshore Earthquake, Japan. Eng. Geol. 182, 25–36.

Hattab, M., Hammad, T., Fleireau, J, M., 2015. Internal friction angle variation in a kaolin/montmorillonite clay mix and microstructural identification. Géotechnique 65 (1), 1–11.

Hong, Y., Yu, G., Wu, Y., Zheng, X., 2011. Effect of cyclic loading on the residual strength of over-consolidated silty clay in a ring shear test. Landslides 8, 233–240.

Hungr, O., Morgenstern, N. R., 1984. High velocity ring shear tests on sand, Géotechnique 34(3), 415–421

Iannicelli, J., Millman, N., 1966. Relation of viscosity of kaolin-water suspensions to montmorillonite content of certain Georgia clays. Clays and Clay Minerals: Proceedings of the Fourteenth National Conference, Berkeley, California, 347–354.

Japanese Geotechnical Society, JGS 0411–2009. Test method for one-dimensional consolidation properties of soils using incremental loading.

Japanese Geotechnical Society, JGS 0560–2009. Method for consolidated constant-volume direct box shear test on soils.

Jostad, H. P., Andresen, L., Thakur, V., 2006. Calculation of shear band thickness in sensitive clays. Proc. of the 6th European Conference on Numerical Methods in Geotechnical Engineering, Austria, 27–32.

Kenny, T. C., 1967. The influence of mineral composition on the residual strength of natural soils. Proceeding of Norwegian Geotechnical Institute 1, 123–129.

Khosravi, M., Meehan, C. L., Cacciola, D. V., Khosravi, A., 2013. Effect of fast shearing on the residual shear strengths measured along pre-existing shear surfaces in Kaolinite. Geotechnical Special Publication No. 231, 245–254.

Kimura, S., Nakamura, S., Vithana, S. B., Sakai, K., 2013. Shearing rate effect on residual strength of landslide soils in the slow rate range. Landslides 11(6), 969–979.

La Gatta D. P., 1970. Residual strength of clay and clay-shales by rotation shear tests. Harvard Soil Mechanics Series No. 86, Harvard University, Cambridge, Massachusetts.

Lee, E.M., Jones, D. K. C., 2004. Landslide risk assessment. Thomas Telford, London, 462p.

Lefebvre, G., LeBoeuf, D., 1987. Rate effects and cyclic loading of sensitive clays. J. Geotech. Engrg (ASCE) 113(5), 476–489.

Lemos, L. J. L. J., Coelho, P. A. L. F., 1991. Displacements of slopes under earthquake-loading. Proceedings of 2nd International Conference on Recent Advances in Geotechnical Earthquake Engineering and Soil Dynamics, Rolla, MO. Balkema, Rotterdam, 1–6.

Lemos, L. J. L., 2003. Shear behaviour of pre-existing shear zones under fast loading - insights on the landslide motion. In Proceedings International Workshop on Occurrence and Mechanisms of Flow-like Landslides in Natural Slopes and Earth Fills, 229–236.

Lemos, L. J. L., Vaughan, P. R., 2000. Clay-interface shear resistance. Géotechnique 50(1), 55–64.

Lemos, L. J. L., Vaughan, P. R., 2004. Shear behaviour of pre-existing shear zones under fast loading. Advances in Geotechnical Engineering: The Skempton Conference, Volume 1, 510–521.

Lemos, L., Skempton, A. W., Vaughan, P. R., 1985. Earthquake loading on shear surfaces in slopes. Proceedings of the Eleventh International Conference on Soil Mechanics and Foundation Engineering, San Francisco, 1955–1958.

Leroueli, S., 2001. Natural slopes and cuts: movement and failure mechanisms. Géotechnique 51 (3), 197–243.

Leshchinsky, D., 2001. Design dilemma: use peak or residual strength of soil. Geotextiles and Geomembranes 19, 111–125.

Li, D., Yin, K., Glade, T., Leo, C., 2017. Effect of over-consolidation and shear rate on the residual strength of soils of silty sand in the Three Gorges Reservoir. Scientific Reports 7, 1–11.

Li, Y. R., Aydin, A., 2013. Shear zone structure and stress fluctuations in large ring shear tests. Eng. Geol 167, 6–13.

Li, Y. R., Wen, B. P., Aydin, A., Ju, N. P., 2013a. Ring shear tests on slip zone soils of three giant landslides in the three gorges project area. Eng. Geol. 154, 106–115.

Li, Y. R., Chan, L. S., Yeung, A. T., Xiang, X. Q, 2013b. Effects of test conditions on shear behaviour of composite soil. Proceedings of ICE – Geotechnical Engineering, 1–11.

Locat, A., Leroueil, S., Bernander, S., Demers, D., Jostad, H. P., Ouehb, L., 2011. Progressive failure in eastern Canadian and Scandinavian sensitive clays. Can. Geotech. J 48, 1696–1712.

Lupini, J. F., Skinner, A. E., Vaughan, P. G., 1981. The drained residual strength of cohesive soils, Géotechnique 31(2), 181–213.

Mahajan, S. P., Budhu, M., 2008. Shear viscosity of clays to compute viscous resistance. Proc. 12th Int. Conf. of International Association for Computer Methods and Advances in Geomechanics (IACMAG), 1516–1523.

Marui, H., Tiwari, B., 2004. Relationship between clay mineralogy and residual strength through the model based on shearing mechanism of soil. Advances in Geotechnical Engineering: The Skempton Conference, Volume 1, 522–534.

Massey, C. I., Petley, D. N., McSaveney, M. J., 2013. Patterns of movement in reactivated landslides. Engineering Geology 159, 1–19.

Mazzanti, P., Bozzano, F., Cipriani, I., Prestininzi. A., 2015. New insights into the temporal prediction of landslides by a terrestrial SAR interferometry monitoring case study. Landslides 12, 55–68.

Meehan, C. L., Brandon, T. L., Duncan, J. M. 2007. Measuring drained residual strengths in the Bromhead ring shear. Geotech. Test. J. 30(6), 466–473.

Meehan, C. L., Brandon, T. L., Duncan, J. M. 2008. Measuring fast shear strengths along slickensided surfaces in the Bromhead ring shear. Geotech. Test. J. 31(3), 239–242.

Merchan, V., Romero, E., Vaunat, J., 2011. An adapted ring shear apparatus for testing partly saturated soils in the high suction range. Geotech. Test. J. 34(5), 433–444.

Mesri, G., Shahien, M., 2003. Residual shear strength mobilized in first-time slope failures. J. Geotech. Geoenviron. Eng. (ASCE) 129(1), 12–31.

Mesri, G., Huvaj-Sarihan, N., 2012. Residual shear strength measured by laboratory tests and mobilized in landslides. J. Geotech. Geoenviron. Eng. (ASCE) 138(5), 585–593.

Mitchell, J. K., Soga, K., 2005. Fundamentals of soil behaviour. The 3rd Edition, Wiley, New York.

Moayed, R. Z., Alibolandi, M., Alizadeh, A., 2017. Specimen size effects on direct shear test of silty sands. Int. J. Geotech. Eng. 11(2), 1–17.

Mun, W., Teixeira, T., Balci, M. C., Svoboda, J., McCartney, J. S., 2016. Rate effects on the undrained shear strength of compacted clay. Soils and Founds 56(4), 719–731.

Nakamura, H., Shimizu, K., 1978. Soil tests for the determination of shear strength along the sliding surface. Landslides 15 (2), 25–32 (in Japanese).

Newmark, N.M., 1965. Effects of earthquakes on dams and embankments. Géotechnique 15(2), 139–159.

Nishimura, T., Fredlund, D. G., 2000. Relationship between shear strength and matric suction in an unsaturated silty soil. Proceedings of the Asian Conference on Unsaturated Soils, 563–568.

Parathias, A. N., 1995a. Displacement rate and shear direction effects on the residual strength of plastic soils. Proc 7th Int. Conference on Soil Dynamics and Earthquake Engineering, 67–72.

Parathiras, A. N., 1995b. Effects of Earthquake induced rates of shearing on residual soil strength. Proceedings of 3rd International Conference on Recent Advances in Geotechnical Earthquake Engineering and Soils Dynamics, 1057–1060.

Peterson, R. W., 1990. The influence of soil suction on the shear strength of unsaturated soil. PhD thesis, Texas A&M University, USA. 307p.

Petley, D. J., Taylor, P., 1999. Modelling rapid shearing of cohesive soils along undulating shear surfaces. Proc. 7th Int. Symp. Slope Stability Engineering. Shikoku, Japan, 754–750.

Picarelli, L. 2000. Mechanisms and rates of slope movements in fine grained soils. Geotechnical and Geological Engineering, GEOENG 2000, Melbourne, 1618–1670.

Quinn, T.A.C., Brown, M. J., 2011. Effect of strain rate on isotropically consolidated kaolin over a wide range of strain rates in the triaxial apparatus. Proc. Int. Symp. on Deformation Characteristics of Geomaterials, Seoul, 607–613.

Ramiah, B. K., Dayalu, N. K., Purushothmarai, P., 1970. Influence of chemicals on residual strength of silty clay. Soils and Founds. 10 (1), 25–36.

Richardson, A. M., Whitman, R. V., 1963. Effect of strain rate upon undrained shear resistance of a saturated remoulded fat clay. Géotechnique 13(4), 310–324.

Robinson, S., Brown. M. J., 2013. Rate effects at varying strain levels in fine grained soils. Proceedings of the 18th International Conference on Soil Mechanics and Geotechnical Engineering, ICSMGE, Paris, 263–266.

Sadrekarimi, A., Olson, S. M., 2008. Shear band formation observed in ring shear tests on sandy soils. J. Geo. Geoenvir. Eng. (ASCE), 136(2), 366–375.

Sadrekarimi, A., Olson, S. M., 2009. A new ring shear device to measure the large displacement shearing behavior of sands. Geotech. Test. J. 32(3), 1–12.

Saito, R., Fukuoka, H., Sassa, K., 2006. Experimental study on the rate effect on the shear strength. Disaster Mitigation of Debris Flows, Slope Failures and Landslides, 421–427.

Saito, R., Sassa, K., Fukuoka, H., 2007. Effect of shear rate on the internal friction angle of silica sand and bentonite mixture samples. Landslides – J. Jpn. Landslide Society 44 (1), 33–38.

Sassa, K. 1984. The mechanism staring liquefied landslides and debris flows. Proceedings of 4th International Symposium on Landslides, Toronto, 349–354.

Scaringi, G., Di Maio, C., 2016. Influence of displacement rate on residual shear strength of clays. The 4th Italian Workshop on Landslides. Procedia Earth and Planetary Science 16, 137–145.

Scaringi, G., Hu, W., Xu, Q., Huang, R., 2018. Shear-rate-dependent behavior of clayey bi-material interfaces at landslide stress levels. Geophysical Research Letters 44(23).

Sedano, J. A. I., Vanapalli, S. K., Garga, V. K., 2007. Modified ring shear apparatus for unsaturated soils testing. Geotech. Test. J. 30(1), 39–47.

Sheahan, T. C., Ladd, C. C., Germaine, J. T., 1996. Rate-dependent undrained shear behaviour of saturated clay. J. Geotech. Engrg (ASCE) 122(2), 99–108.

Skempton, A. W., 1970. First-time slides in over-consolidated clays. Géotechnique 20(3), 320–324.

Skempton, A. W., Hutchinson, J. N., 1969. Stability of natural slopes. Proc. 7th Int. Conf. Soil Mech. Found. Eng, Mexico City, State of the art volume, 291–340.

Skempton, A. W., Leadbeater, A. D., Chandler, R. J., 1989. The Mam Tor landslide, North Derbyshire. Philosophical Transactions of the Royal Society of London A 329, 503–547.

Skempton, A.W., 1964. Long term stability of clay slopes. Géotechnique 14(2), 77–102.

Skempton, A.W., 1985. Residual strength of clays in landslides, folded strata and the laboratory. Géotechnique 35(1), 3–18.

Stark, T. D., 1995. Measurement of drained residual strength of overconsolidated clays. Transportation Research Record 1479, 26–34.

Stark, T. D., Choi, H., McCone, S., 2005. Drained shear strength parameters for analysis of landslides. J. Geotech. Geoenviron. Eng. (ASCE) 131(5), 575–588.

Stark, T. D., Contreras, I. A., 1996. Constant volume ring shear apparatus. Geotech. Test. J. 19(1), 3–11.

Stark, T. D., Eid, H. T., 1993. Modified Bromhead ring shear apparatus. Geotech. Test. J. 16 No 1, 100–107. Transportation Research Record 1479, 26–34.

Stark, T. D., Eid, H. T., 1994. Drained residual strength of cohesive soils. J. Geotech. Eng. Div. (ASCE) 120(1), 856–871.

Stark, T. D., Eid, H. T., 1997. Slope stability analyses in stiff fissured clays. J. Geotech. Geoenviron. Eng. (ASCE) 123(4), 335–343.

Stark, T. D., Hussain, M. 2010. Drained residual strength for landslides. GeoFlorida Conference, Orlando, Florida, United States, 3217–3226.

Stark, T. D., Poeppel, A. R., 1994. Landfill liner interface strengths from torsional-ring-shear tests. J. Geotech. Eng. Div. (ASCE) 120(3), 597–615

Suzuiki, M., Sasanishi, T., Yamamoto, T., Sugawara, M., 2003. Influence of salinity on residual strength of clays. Proc. 38th Jpn National Conf. Geotech. Eng., 207–208 (in Japanese).

Suzuiki, M., Umezaki, T., Kawakami, H., 1997. Relation between residual strength and shear displacement of clay in ring shear test. J. Jpn. Soc. Civ. Eng. 575 (III-40), 141–158 (in Japanese).

Suzuki, M., 2008. 1.2. Shear strength of sands subjected to a large deformation in an earthquake and its rate effect, 17–46. Earthquake-induced Landslide Disasters in Middle Mountains-Study Report on the 2004 Mid-Niigata Earthquake Part II – Geotechnical Engineering (in Japanese).

Suzuki, M., Hai, N. V., Yamamoto, T., 2017. Ring shear characteristics of discontinuous plane. Soils and Founds. 57 (1), 1–22.

Suzuki, M., Tanikawa, K., Fukuda, J., Hisanaga, K., 2001. Variation in residual strength of clay with shearing speed. Memoir of the Faculty of Engineering of Yamaguchi Univ. 52 (1), 45–49.

Suzuki, M., Tsuzuki, S., Yamamoto, T., 2007. Residual strength characteristics of naturally and artificially cemented clays in reversal direct box shear test. Soils and Founds. 47 (6), 1029–1044.

Suzuki, M., Umezaki, T., Kawakami, H., 1997. Relation between residual strength and shear displacement of clay in ring shear test. J. Jpn. Soc. Civ. Eng. 575 (III-40), 141–158 (in Japanese).

Suzuki, M., Umezaki, T., Takahaza, H. 2012. Fast and cyclic shearing of cemented sand in Earthquake induced landslide. Proceedings of 15th World Conference of Earthquake Engineering, Lisbon.

Suzuki, M., Yamamoto, T., Kai, Y., 2009. Rate effect on residual state strength of clay related with fast landslide. Proc. Int. Symposium on Prediction and Simulation Methods for Geohazard Mitigation, 347–352.

Thermann, K., Gau, C., Tiedemann, J., 2006. Shear strength parameters from direct shear tests-influencing factors and their significance. The Geological Soc. of London, IAEG2006, 1–12.

Tika, T. E., Hutchison, J. N., 1999. Ring shear tests on soil from the Vaiont landslide slip surface. Géotechnique 49 (1), 59–74.

Tika, T. E., Vaughan, P. R., Lemos, L. J. L., 1996. Fast shearing of pre-existing shear zones in soils. Géotechnique 46(2), 197–233.

Tiwari, B., Marui, H., 2005. A new method for the correlation of residual shear strength of the soil with mineralogy composition. J. Geotech. Geoenviron. Eng. (ASCE) 131(9), 1139–1150

Tiwari, B., 2007. Chapter 9. Residual shear strength of Tertiary mudstone and influencing factors. In Proceedings of Progress in Landslide Sciences, 135–145.

Tiwari, B., Marui, H., 2002. Influence of clay mineralogy in residual shear strength of soil. Annual Report of Research Institute for Hazards in Snowy Areas, Niigata University, No 24, 37–56.

Tiwari, B., Marui, H., 2003. Estimation of residual shear strength for bentonite-kaolin-Toyoura sand mixture. Landslides – J. Jpn. Landslide Society 40 (2), 124–133.

Tiwari, B., Marui, H., 2004. Objective oriented multistage ring shear test for shear strength of landslide soil. J. Geotech. Geoenviron. Eng. (ASCE) 130(2), 217–222.

Townsend, F. C., Gilbert, P. A., 1976. Effects of specimen type on the residual strength of clays and clay shales, in Soil Specimen Preparation for Laboratory Testing, ASTM special technical publication 599, American Society for Testing and Materials, 43–65.

Toyota, H., Nakamura, K., Sugimoto, M., Sakai, N., 2009. Ring shear tests to evaluate strength parameter in various remolded soils. Géotechnique 59 (8), 649–659.

Vaid, Y. P., Campanella, R. G., 1977. Time-dependent behavior of undisturbed clay. J. Geotech. Engrg. Div. (ASCE) 103(7), 693–709.

Van Asch, Th. W. J., Van Beek, L. P. H., Bogaard, T. A., 2007. Problems in predicting the mobility of slow-moving landslides. Eng. Geol. 91, 46–55.

Varnes, D. J., 1978. Slope movement types and process. In Landslides, Analysis and Control. Special report 176, chapter 2: Transportation research board, National Academy of Sciences, Washington, D.C., 11–33.

Vithana, S. B., Nakamura, S., Kimura, S., Gibo, S., 2012. Effects of overconsolidation ratios on the shear strength of remoulded slip surface soils in ring shear. Eng. Geol. 131–132, 29–36.

Walker, L. K., 1969. Undrained creep in a sensitive clay. Géotechnique 19(4), 515–529.

Wang, H.B., Sassa, K., Xu, W. Y. 2007. Analysis of a spatial distribution of landslides triggered by the 2004 Chuetsu Earthquakes of Niigata Prefecture Japan. Natural Hazards 41, 43–60.

Xu, C., Wang, X., Lu, X., Dai, F., Jiao, S., 2018. Experimental study of residual strength and the index of shear characteristics of clay soil. Eng. Geol. 233, 183–190.

Xu, Q., Yuan, Y, Zeng, Y., Hack, R., 2011. Some new pre-warning criteria for creep slope failure. Science China Technological Sciences 52(1), 210–220.

Yatabe, R., Yagi, N., Enoki, M., 1991. Ring shear characteristics of clays in fractured-zone-landslide. Journal of Geotechnical Engineering, Japan Society of Civil Engineers, No 436/III-16, 93–101 (in Japanese).

Zhu, J. G., Yin, J. H., Luk, S. T., 1999. Time-dependent stress-strain behavior of soft Hong Kong marine deposits. Geo. Tech. J. 22(2), 118–126.

Zhu, J. G., Yin, J. H., 2000. Strain-rate-dependent stress-strain behavior of overconsolidated Hong Kong marine clay. Can. Geotech. J. 37, 1272–1282.